PL-TR-
97-1185

ELECTRON BEAM MANUFACTURABLE COMPOSITES FOR SPACE APPLICATIONS

Dr. Larry A. Harrah, Dr. Andrea E. Hoyt, and Dr. Ronald E. Allred

Adherent Technologies, Inc.
9621 Camino del Sol NE
Albuquerque, NM 87111

March 1998

Final Report

AIR FORCE RESEARCH LABORATORY
Space Vehicles Directorate
3550 Aberdeen Ave SE
AIR FORCE MATERIEL COMMAND
KIRTLAND AIR FORCE BASE, NM 87117-5776

Using Government drawings, specifications, or other data included in this document for any purpose other than Government procurement does not in any way obligate the U.S. Government. The fact that the Government formulated or supplied the drawings, specifications, or other data, does not license the holder or any other person or corporation; or convey any rights or permission to manufacture, use, or sell any patented invention that may relate to them.

This report has been reviewed by the Public Affairs Office and is releasable to the National Technical Information Service (NTIS). At NTIS, it will be available to the general public, including foreign nationals.

If you change your address, wish to be removed from this mailing list, or your organization no longer employs the addressee, please notify AFRL/VS, 3550 Aberdeen Ave SE, Kirtland AFB, NM 87117-5776.

Do not return copies of this report unless contractual obligations or notice on a specific document requires its return.

This report has been approved for publication.

ROBERT N. PITTMAN, Capt, USAF
Project Manager
Vehicle Technologies Branch

FOR THE COMMANDER

ERIC J. HERUP, Maj, USAF
Chief, Vehicle Technologies Branch

BRUCE A. THIEMAN, Col, USAF
Deputy Director, Space Vehicles

REPORT DOCUMENTATION PAGE

Form Approved
OMB No. 074-0188

1. AGENCY USE ONLY (Leave blank)	2. REPORT DATE	3. REPORT TYPE AND DATES COVERED
	March 1998	Final Report May 96 - Mar 98

4. TITLE AND SUBTITLE

Electron Beam Manufacturable Composites for Space Applications

5. FUNDING NUMBERS

C: F29601-95-C-0184
PE: 063401F
PR: NASA
TA: TX
WU: AE

6. AUTHOR(S)

Dr. Larry A. Harrah, Dr. Andrea E. Hoyt,
and Dr. Ronald E. Allred

7. PERFORMING ORGANIZATION NAME(S) AND ADDRESS(ES)

Adherent Technologies, Inc.
9621 Camino del Sol NE
Albuquerque, NM 87111

8. PERFORMING ORGANIZATION REPORT NUMBER

ATI97-5159-FR001

9. SPONSORING / MONITORING AGENCY NAME(S) AND ADDRESS(ES)

Air Force Research
Laboratory/VSDV
3550 Aberdeen Avenue SE
Kirtland AFB, NM 87117-5776

10. SPONSORING / MONITORING AGENCY REPORT NUMBER

PL-TR-97-1185

11. SUPPLEMENTARY NOTES

12a. DISTRIBUTION / AVAILABILITY STATEMENT

Approved for public release; distribution is unlimited

12b. DISTRIBUTION CODE

13. ABSTRACT ***(Maximum 200 Words)***

This program investigated electron beam curing with three types of composite matrix resins for use in space applications. Cyanate ester and propargyl terminated resins were shown to undergo radiation-induced rearrangements and did not polymerize. Recommendations are included for chemical structures containing cyanates and acetylene groups that should not undergo rearrangement and thus should produce high molecular weight polymers. Cationic-initiated epoxy resins polymerized to high glass transition polymers were selected for fabrication of composites reinforced with an intermediate modulus carbon fiber. Those systems displayed mechanical and thermal properties equivalent to those of thermally cured composites with similar matrix resins even when electron beam cured at temperatures below -30°C. When optimized, electron beam curing at subambient temperatures will result in high performance composite structures for space applications with low, stress-free temperatures and improved dimensional stability.

14. SUBJECT TERMS

electron beam curing, radiation curing, cationic polymerization

15. NUMBER OF PAGES

122

16. PRICE CODE

17. SECURITY CLASSIFICATION OF REPORT	18. SECURITY CLASSIFICATION OF THIS PAGE	19. SECURITY CLASSIFICATION OF ABSTRACT	20. LIMITATION OF ABSTRACT
U	U	U	Unlimited

EXECUTIVE SUMMARY

Electron-beam (e-beam) curing has the potential to significantly reduce the overall cost of manufacturing polymer matrix composite parts for use in aerospace applications. E-beam cure is extremely fast; cycle times of several minutes to several hours are possible, in contrast to currently used thermal technologies that may require several days for full cure. Additionally, part sizes and shapes are virtually unlimited. Tooling costs are also significantly reduced since common materials such as wood may be used in part fabrication. E-beam curing technology could greatly benefit numerous Air Force applications such as composite cryogenic tanks, rocket motor cases, and precision optics.

Currently, there are very few resin systems available that are amenable to e-beam curing and none are qualified to the stringent requirements for space applications. The best currently available e-beam curing materials are cationic cure epoxies, which have a service temperature limited by the glass transition temperature (T_g), typically around 200°C. It is desirable to have e-beam curing compatible resin systems based on currently space qualified resin systems such as cyanate esters or the closely related propargyl systems. The overall goal of this program was to investigate those resin systems with the specific goals of meeting the requirements for space applications while being e-beam processable.

To accomplish these goals, cyanate ester and propargyl ether resin formulations were modified with appropriate sensitizers designed to transfer e-beam energy to the resins to initiate polymerization. The chosen sensitizers functioned as planned, however, deleterious photochemical rearrangements occurred in both the cyanate ester and propargyl ether resins that did not lead to polymerization. Alternate resin structures that should not undergo photochemical rearrangements are proposed for future examination.

Once the cyanate and propargyl resins were eliminated from consideration as matrices for space composite applications, three epoxy resins were investigated in this study for their radiation curing effectiveness using two different cationic initiators. The epoxy functionality undergoes homopolymerization when initiated with a strong acid cation. The chain extension reaction is very rapid and leads to polymer with relatively high T_g even when the resin is kept at ambient temperature during cure. The resulting cured epoxy has no volatile components except for those small quantities of impurities in the starting system and a small amount of initiator by-product.

Two initiator structures were examined: triaryl sulfonium hexafluoroantimonate and diaryl iodonium hexafluoroantimonate. Our work indicates that the sulfonium salts are the preferred initiators for e-beam cure. They provide faster cure, lower dose for effective cure and the by-product of cation formation acts as a radiation

stabilizer for benzene ring containing resins. We noted that the strength of the cured resins developed a maximum at cure doses of about 7-10 MRad and dropped below that maximum for higher initiation dose. Samples of resins initiated with the iodonium salt showed more strength reduction at the highest doses than did those initiated with sulfonium salt. Sulfonium salt initiation also gave more complete cure at lower dose. These are the results expected from the spectral data obtained in this study; the spectral properties of the initiator and resin allow their e-beam performance to be predicted.

Unidirectional and quasi-isotropic composites incorporating an intermediate modulus carbon fiber (IM7) were fabricated with the most promising system, EPON® 828 epoxy/Cyracure™ 6974 triaryl sulfonium hexafluoroantimonate (2%). The e-beam cured composites showed mechanical properties equivalent to those of thermally cured composite systems, even when cured at reduced temperatures. All the composites displayed 100% cure and T_gs around 190°C for e-beam cures between 23°C and near -30°C. This shows that high performance composite space structures can be fabricated with stress-free temperatures near -30°C, which should improve dimensional stability in the space environment. This epoxy matrix system appears to be a viable e-beam curing system for space applications. A cure dose of 5-7 MRad was sufficient to afford good product. A somewhat lower dose may be useful during manufacture to cause part hardening.

Difficulties encountered with pressure application during this program should be alieviated by the use of stiffer pressure plates, possibly using honeycomb composite materials. Additional work is needed in optimizing matrix cure chemistry versus radiation dose, improving bonding at the fiber-matrix interface, producing well consolidated, low void composites at subambient temperatures, and controlling temperature during subambient cure. Finally, additional effort should be expended examining e-beam curing of modified cyanate and propargyl-like resins with structures that cannot undergo deleterious photochemical rearrangements.

CONTENTS

CONTENTS (concluded)

LIST OF FIGURES

LIST OF FIGURES (continued)

LIST OF FIGURES (continued)

LIST OF FIGURES (concluded)

LIST OF TABLES

PREFACE

This report summarizes the results of the program entitled "Electron Beam Manufacturable Lightweight Composite Space Structures." The purpose of this program was twofold: (1) to investigate the e-beam initiated cure of space-qualifiable resins using triplet energy transfer, cationic initiation or other methods of catalysis; and (2) to prepare and characterize e-beam cured composites suitable for use in space applications (*e.g.*, launch vehicles, cryotanks, space structures).

Significant efforts were undertaken in materials synthesis and characterization, calculation of dose magnitude and uniformity based on selected beam parameters, composites preparation, and mechanical testing. We would like to thank Capt Robert Pittman at the Air Force Research Laboratory for his technical guidance throughout the program. We would like to acknowledge the following people for their contributions to these efforts.

Adherent Technologies, Inc., Albuquerque, NM

Mr. Andy Coons for mold design and mechanical testing.
Mr. Brent Gordon for gas chromatography, mechanical testing, electronics support.
Mr. Jack Greiner for resin sample preparation, spectroscopic analysis.
Mr. Richard Jensen for materials synthesis, resin sample preparation, composites layup.
Ms. Nicole King for resin sample preparation, thermal analysis.

Applied Poleramic, Benicia, CA

Mr. Richard Moulton for the survey of state-of-the-art in e-beam cure and general consulting.

Tetra Corporation, Albuquerque, NM

Mr. Ray Cravey for calculation of e-beam dose and dose uniformity.

Titan AIT, Albuquerque, NM

Mr. Jerry Clifford and Mr. Kerry Habiger for e-beam irradiation experiments.

INTRODUCTION

Performance requirements for polymer matrix composites (PMCs) in space applications are generally quite stringent. Depending upon the specific application, these requirements may include excellent thermal stability, high strength, high toughness, low porosity, low hydrogen permeability, low outgassing, radiation and atomic oxygen stability, and the ability to withstand long-term thermal cycling with retention of properties. Easy processing is also desirable. Matrix materials currently in use such as toughened epoxies and cyanate esters are often deficient in one or more of these areas. Elevated temperatures and high pressures are required, leading to significant costs in equipment and energy-related expenses. Additionally, the part sizes and shapes that can be manufactured are severely limited by the currently available thermal cure technology.

Electron-beam (e-beam) curing has the potential to significantly reduce the overall cost of manufacturing PMC parts for use in aerospace as well as in other applications. E-beam cure is extremely fast; cycle times of several minutes to several hours are possible, in contrast to currently used thermal technologies that may require several days for full cure. Additionally, part sizes and shapes are virtually unlimited. Tooling costs are also significantly reduced since common materials such as wood may be used in parts fabrication. The use of e-beam curing technology could greatly benefit numerous Air Force applications such as composite cryogenic tanks, rocket motor cases, and precision optics.

However, there are very few resin systems available that are amenable to e-beam curing. The best currently available materials are cationic cure epoxies, which have a service temperature limited by the glass transition temperature (T_g), typically around 200°C. It is desirable to have e-beam curing compatible resin systems based on currently space qualified resin systems such as cyanate esters or the closely related propargyl systems. The overall goal of this program was to investigate those resin systems designed with the specific goals of meeting the aforementioned requirements for space applications while being e-beam processable. To accomplish these goals, the following general tasks were undertaken:

- assessment of the state-of-the-art in nonthermal cure
- development of new e-beam processable formulations for composite structures with processability and properties equivalent to or better than current systems
- demonstration of prototype composite panels using a low-cost e-beam fabrication process.

Qualified resin materials and resins modified for the purpose of promoting e-beam curability were investigated. These resins were blended with additives to enhance

e-beam energy transfer during composite manufacture. Unidirectional panels were then fabricated using the e-beam cure method and subjected to mechanical testing. Thermally processed composites were fabricated and tested as a baseline control.

BACKGROUND

Radiation Chemistry of Polymeric Systems

The radiation chemistry of polymeric systems has been under intense study by many investigators since the early days of the nuclear weapons program. Bovey [1] published a book on ionizing radiation effects in natural and synthetic high polymers in 1958. This work was followed by many similar study compilations on these subjects: Charlesby [2] in 1960, Chapiro [3] in 1962, Gould [4] in 1967, and Dole [5] in 1972.

The book edited by Gould [4], an ACS symposium compilation (Advances in Chemistry Series, #66), contains papers on the nature of the reactive species produced in polymeric systems by both ionizing radiation and UV excitation. In this time period, the major success for radiation treatment of polymers was the radiation crosslinking (vulcanization) of polyethylene and other hydrocarbon-like polymers. It was recognized that the degree of crystallinity of the material before radiation treatment, strongly influenced the cross-link yield and structure of the resulting system. Compared to chain polymerization, the radiation intensity necessary for development of crosslinks is much higher. Mechanical properties such as tensile strength are improved by irradiation at doses of 10-25 MRad (1-2.5 x 10^9 erg/g deposited dose).

In the aliphatic hydrocarbon-like systems, the radiation exposure ultimately produces bond cleavage in the initial radiation chemical event, followed by coupling of the resulting free radicals to form new bonds in a random manner. In those polymers containing vinyl or vinylene moieties as defects in the initial structure, free radical addition to these moieties causes higher crosslink yield. For systems with little or no unsaturation, yield is lower and results primarily from C-H bond cleavage to form H-H molecules and C-C bonds.

Although a variety of reactive species were recognized to be formed by the ionizing radiation (ions, free radicals, excited states), the most active species in producing end product chemistry are the free radicals resulting from random chemical bond rupture. Other intermediates were postulated to occur and contribute substantially to the chemistry in the initial phases. Discussions of these processes and their role in the product chemistry are given in the papers by Charlesby, Chapiro, and Dole *et al.* in Refs. 2-5.

Electron Beam Curing

In France, Aerospatiale has developed a nonthermal curing process that can meet most of the requirements for rocket motor cases [7]. Their process reduced the cure time of large structures from days to hours and eliminated the curing oven or autoclave. Aerospatiale has demonstrated that a combination of electron-beam and X-rays is the best and lowest cost approach for their composite motor cases. However, the resins used exhibit low glass transition temperature (T_g), their process results in high void content (10-20%), and their product does not meet most high-performance matrix materials requirements.

In addition to the Aerospatiale work, the best composites database available to industry comes from Atomic Energy of Canada, Ltd. (AECL) in Manitoba, Canada. In 1992 AECL cured a variety of free radical initiated matrix candidates and FW-3 (a proprietary multifunctional epoxy/vinyl ester formulated by Applied Poleramic in Benecia, CA) [8]. FW-3 was judged to be significantly superior to other free radical cured resins. Subsequent work with sized and unsized graphite, each with and without an added coupling agent, has added to the composite database. In addition, e-beam cured bismaleimide (BMI) base filament winding and resin transfer molding (RTM) matrix formulations prepared by Applied Poleramic have been exposed to various doses and characterized with dynamic mechanical analysis.

Epoxy formulations containing precursors to cationic initiators have also been examined for e-beam cure [9]. These materials are formulated to be sensitive in the ultraviolet region of the electromagnetic spectrum, and are activated by ionizing radiation as well. Precursors to cationic initiators commonly used are aryl sulfonium or iodonium salts of large, highly ionic anions, typically hexafluorophosphates of Group V atoms. Upon irradiation with either UV or ionizing radiation, they dissociate to the aryl sulfides or iodides and a strongly acidic cation. The iodonium salts absorb farther in the UV than the sulfonium salts and should be less efficient in energy harvesting from ionizing radiation than the sulfonium salts. Prior results [10] have shown that the sulfonium salts give the expected higher yield and reactivity. However, the mechanical properties of epoxies cured with sulfonium salts are reportedly inferior [10].

Resins currently in development or use by US industry for e-beam cure are modified epoxies and BMIs.

APPROACH

As mentioned in the introductory section, composites to be used in the space environment have additional requirements over the high strength, high toughness and good thermal stability characteristic of most aerospace composites. Depending on the specific applications, these additional requirements may include low

porosity, low permeability, retention of properties with thermal cycling, low moisture absorption, low outgassing, and high dimensional stability. Our approach was designed in a specific attempt to address these needs.

E-Beam Energy Channeling and Concentration

In order for the energy deposited in the resin system by the electron beam or molecular excitations caused by light absorption to effect the desired chemical reaction, this energy must be localized in a material or molecular fragment that leads to the desired reaction. To ensure the energy is harvested efficiently, rapid energy transfer must occur between the bulk material's molecular species and from these species to the sensitizer molecules that produce the active electronic state or initiator product.

In this work we have used electronic excitations to harvest the excitation produced by the energy source, either e-beam or ultraviolet light. The following terminology is more fully described in Appendix A and is briefly summarized here:

Energy transfer is the non-radiative migration of electronic excitation of molecular species from one molecular entity to another. This is also called Förster transfer or *long-range resonant transfer.*

Intersystem crossing is the intramolecular conversion from one type of electronic excitation to another, usually from the singlet manifold of states to the triplet states.

Internal conversion is the intramolecular conversion of electronic excitation from one level to another with the production of thermal energy. This usually involves a loss of excitation and a return to the unexcited ground electronic state with the production of thermal energy as molecular vibrations.

A singlet state is a molecular electronic configuration in which all the electrons of the molecule are paired; a state with no spin angular momentum. This is the normal state of most stabile molecules.

A triplet state is a molecular electronic configuration in which a pair of electrons have parallel spin vectors and give a resultant spin angular momentum of one. Generally, this is an excited state of the molecule.

Sensitizers are materials that can harvest electronic excitations by energy transfer and channel them into desired results.

Stabilizers are materials that can harvest electronic excitations by energy transfer and deplete the energy by non-chemical pathways (fluorescence or heat).

Initiators are molecules that initiate chemical reaction and generally form a propagating specie with similar reaction activity to the initiator itself. We have also applied this terminology to precursors to the initiator specie that form the reactant by electronic excitation, more properly called initiator precursor.

Catalysts are molecules that accelerate chemical reactions by participating in the reaction but are not themselves changed by the reaction. It is possible to use an inactive material that produces a catalyst under electronic excitation.

Initially, we attempted to initiate either cyclotrimerization or linear polymerization of triply bonded compounds by using triplet electronic excitations. These excitations are produced by intersystem crossing from an excited singled state to the triplet electronic manifold in certain molecular structures, the sensitizers. By selecting molecular structures that have low lying singlet excitations and that undergo facile singlet-triplet intersystem crossing, we hoped to sensitize the desired reactions and efficiently harvest the deposited energy.

Several conditions must be satisfied for these energy transfer processes to be effective: (1) the energy levels of the bulk material's molecular structure must be of nearly the same energy for each distinct moiety (nearly degenerate from molecule to molecule); (2) the excited state produced by radiation must be long-lived; (3) the sensitizer must efficiently harvest the excitations from the bulk material; and (4) the decay from this collected excitation to the effective product must be rapid. The UV and fluorescence spectra of these materials contain the information needed for calculating the effectiveness of the required processes as well as information that allows estimation of the influence of concentration and density on the requisite reactions. A detailed discussion of excitation and energy transfer and associated terminology can be found in Appendix A.

In this report, we often refer to the energy of excitations in discussing energy transfer and localization processes. The electronic spectra are shown as spectral intensity versus wavelength of light rather than energy since our spectrometer scans the spectrum in equal wavelength intervals. These data are interpreted in terms of the energy of the observed transitions and the absorbing wavelength is related to energy by:

$$E=1/\lambda\ ,$$

where E is the energy in units of 1/cm (cm^{-1}) and λ is the wavelength of the absorbing transition in centimeters.

Initial Polymer Systems of Choice for this Effort

Two basic polymer systems were chosen to formulate the resins for this work: an aromatic bis(propargyl ether) of Bisphenol-A and a dicyanate ester of Bisphenol-A

(commercially available as AroCy B-30, Rhône-Poulenc). Thermally, both of these materials cure by the cyclotrimerization of the endgroups to give an aromatic nucleus. The trimerization reaction for the bis(propargyl ether) system is shown in Figure 1. Similar structures are obtained when cyanate esters are used.

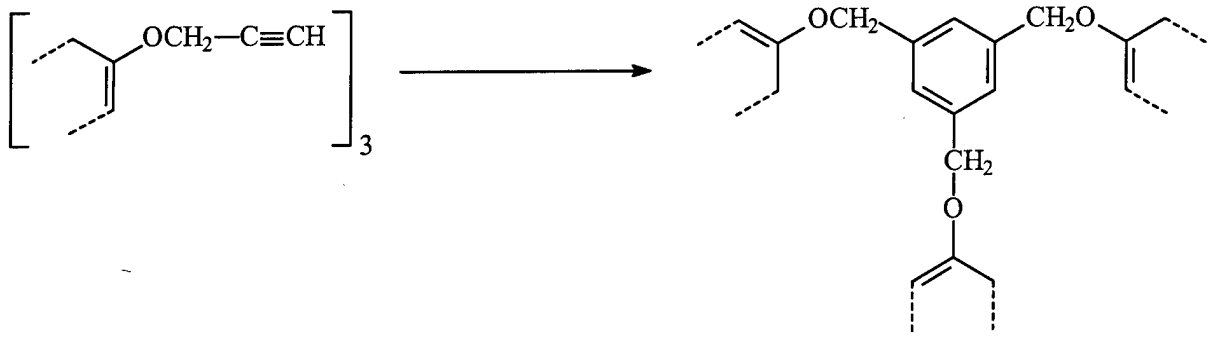

Figure 1. Trimerization of a propargyl-functionalized resin material. Similar structures are obtained for cyanate ester-functionalized resins.

These materials do have other cure reaction routes that are analogous to the chain extension of vinyl groups. These additional curing reactions, shown for the propargyl system in Figure 2, provide the possibility of higher yield than trimerization alone due to the chain nature possible with linear polymerization.

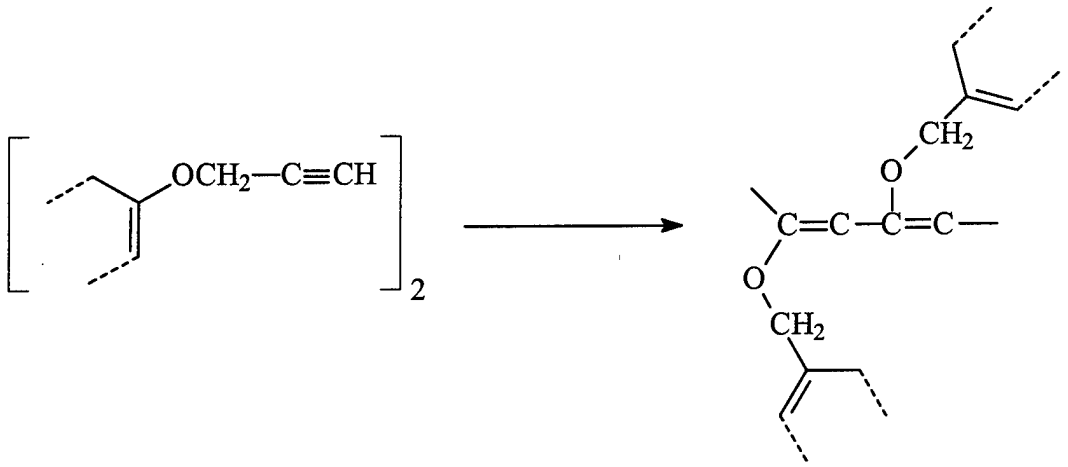

Figure 2. Linear polymerization of a propargyl-functionalized resin. Similar structures are obtained for linear polymerization of cyanate ester-functionalized resins.

Trimerizing resin systems such as these propargyl- or cyanate-functionalized resins offer several potential advantages with respect to space requirements. No volatiles are released during cure, the resins are inherently hydrophobic, and the resins expand during cure [11,12]. Thermally initiated cure of the dicyanate ester of Bisphenol-A is well-known [11-17], and this resin has been shown to exhibit many

of the properties required for space applications [12-14,16,17]. Similar results are expected for the propargyl system. Radiation-induced cure of these systems has not been investigated.

Both systems yield tightly crosslinked systems; there have been several investigations of toughening for cyanate ester resins. The tightly crosslinked system obtained from the propargyl ether resin may also require additional components to ensure toughness, although the additional CH_2 linkage may make the cured system tougher than that of the cyanate ester, and should facilitate cure at low temperature.

The bis(propargyl ether) was the first target of our investigation. This system affords the aromaticity to allow rapid energy transfer and little opportunity for adverse radiation chemical damage to the basic structure. The trimerization reaction yields an aromatic structure, as indicated above, but may require relatively high dose to cure; radiation initiation of this reaction has not been studied. The additional possibility for chain polymerization should result in lower cure dose over cyclotrimerization alone.

Sensitizers were added to both formulations for the purpose of enhancing cure and for protecting the system from unwanted radiation damage.

Initiators for Polymerization Reactions

Two types of reactive sensitizers/initiators were contemplated for use in these resins. The first type is a functionalized derivative of benzophenone, a known triplet state sensitizer. The benzophenone structure has a lower energy first excited singlet state than those of the resin structures proposed in this effort and thus will efficiently harvest migrating excitations from the host. Furthermore, this ketone undergoes a rapid intersystem crossing to the lowest triplet excited state in high yield. This triplet state is chemically reactive but is lower in energy than that of the acetylene group (24,000 cm^{-1} *vs.* about 30,000 cm^{-1}). It may initiate the trimerization of the acetylenes as well as promoting addition polymerization of these groups by temporary addition to the reactive group (exciplex formation) followed by further addition of reactive groups to the activated moiety. This process would serve to lower the triplet state energy of the sensitizer, and to reduce the electron spin coupling in the resulting complex (an exciplex) as well. By the series of additions of the reactive functionality from the resin to this complex, the path to the ground state is facilitated and, upon reaching this state, the complex dissociates leaving the resin functionality coupled. No such process has been reported but may exist; it is this process that we hoped to use.

We used this material to determine if the initiation of the reaction could be accomplished by proximity of the high spin state and to determine if linear and/or cyclic polymerization is initiated in high yield through indirect triplet excitation of

the resin molecules. The triplet excited state of the sensitizer is much lower in energy than the triplet of acetylenes and direct transfer cannot occur.

We have synthesized initiators from 2,4'-dihydroxybenzophenone and 4,4'-dihydroxybenzophenone by the Williamson synthesis; the general synthetic scheme is shown in Figure 3, below. These initiators have a similar structure to the monomer used to formulate the resin:

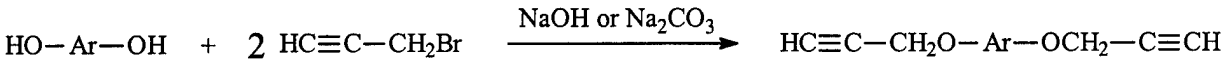

Figure 3. Williamson synthetic method used for production of resin and sensitizer molecules. Ar can be any aromatic containing moiety (e.g., benzophenone).

The direct bromination of the resin component, Bisphenol-A, before forming the propargyl ether (or cyanate ester) was also investigated. A system composed of brominated resin precursor should have given even higher triplet yield than a sensitized system.

After synthesis of the several initiators, their UV and fluorescence spectra were examined and compared with the spectra of the resin major component. These spectra allowed estimation of energy transfer effectiveness [18] and assisted in choosing the initiators to best match the monomers being used.

EXPERIMENTAL PROCEDURES

E-Beam Exposure Experimental Plan

Mold Design for Fabrication of Resin Plaques and Composite Panels

Initially, resin samples were placed into 5 cm x 5 cm x 3 mm deep wells machined into a 1-cm polyethylene block. A drawing of the mold design is shown in Figure 4. Resin samples were heated as necessary to facilitate pouring from bottles into the mold. The mold containing unexposed resin samples was then covered with a sheet of Kapton® polyimide film to prevent UV-induced reactions in the samples.

In the first experiment, it was observed that e-beam exposure resulted in significant warping of the polyethylene mold used for the resin samples. Therefore, the mold was redesigned before additional e-beam exposure experiments. The major redesign element was an aluminum support frame. This supporting frame, in conjunction with wood blocks used to lift the mold off the graphite beam stop, successfully prevented mold warpage due to heating during the course of the exposure. The new mold also had slightly deeper sample wells, 5 mm depth as opposed to the original 3 mm depth, which were filled with approximately 7 cc of resin material.

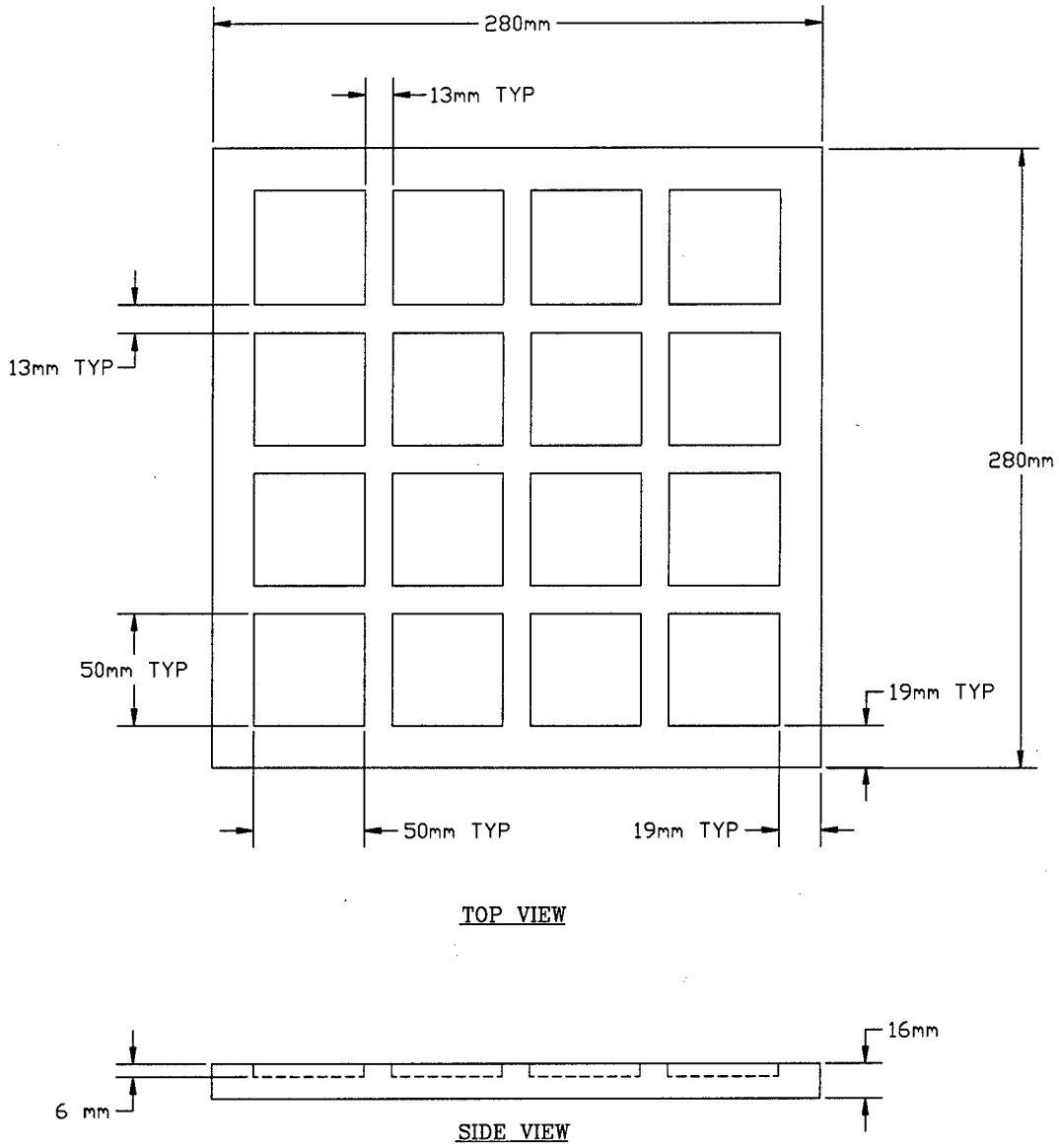

Figure 4. Design of polyethylene mold used for resin plaque exposure

Electron Beam Exposures

Electron beam (e-beam) exposures were conducted at the Titan AIT facility. A photograph of the experimental setup is shown in Figure 5.

Basic beam parameters for all experiments are given in *Table I.* Parameters varied slightly between experiments; every attempt was made to match the beam parameters as closely as possible to those listed in *Table I.* The dose per pass was calculated using a spreadsheet created by Ray Cravey of Tetra Corporation. A discussion of the spreadsheet program can be found in Appendix B. The normal distance between the sample and the e-beam exit window (9.5 cm) was chosen to give an absorbed dose of 5 Mrad per pass. No attempt was made to maintain a constant low temperature in the resins. The desired dose was achieved by exposing the sample to the number of beam passes appropriate for delivery of the desired dose. Promising resins identified in the early exposures were then subjected to several different doses for the purpose of determining the optimum dose for completeness of cure and mechanical properties.

Figure 5. Experimental setup for e-beam exposure of resin plaques and composite samples

Table I. Target Beam Parameters Used in all E-Beam Exposure Experiments

Parameter	Value
Beam Energy	12 MeV
Total Beam Current	0.192 A
Pulse Repetition Rate	35 Hz
Pulse Width	5.8 μs
Beam speed	0.83 cm/s
Distance to Sample	9.5 cm

The deposited dose from the e-beam was determined experimentally using radiochromic nylon film dosimeters supplied by Far West Technology of Goleta, CA. The electron density of these films closely approximate that of the target resin and the measured dose to these films was assumed to apply to the resins as well. These films were also used to map the beam profile of the 12 MeV beam and to construct scan parameters required for uniform exposure.

Calculations of the current density profile were done initially based on an expected 2.5 cm diameter beam. Assuming a one-inch beam diameter, the necessary translation spacing would be 4.45 cm to achieve the desired dose over the sample. This is shown in Figure 6.

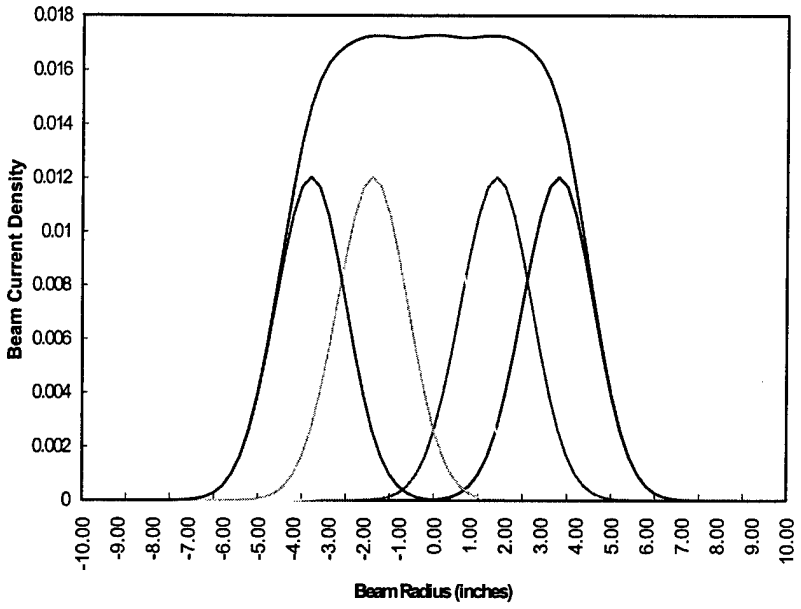

Figure 6. Current density profile calculated based on 4.45 cm spacing between passes assuming 2.54 cm beam diameter

After three passes, it was apparent from the radiochromic film that the beam width was much lower than 2.5 cm. Figure 7 shows what the total current density profile would look like if the spacing was kept at 4.45 cm between passes but with a beam diameter of 1.27 cm. This is similar to what was seen on the film.

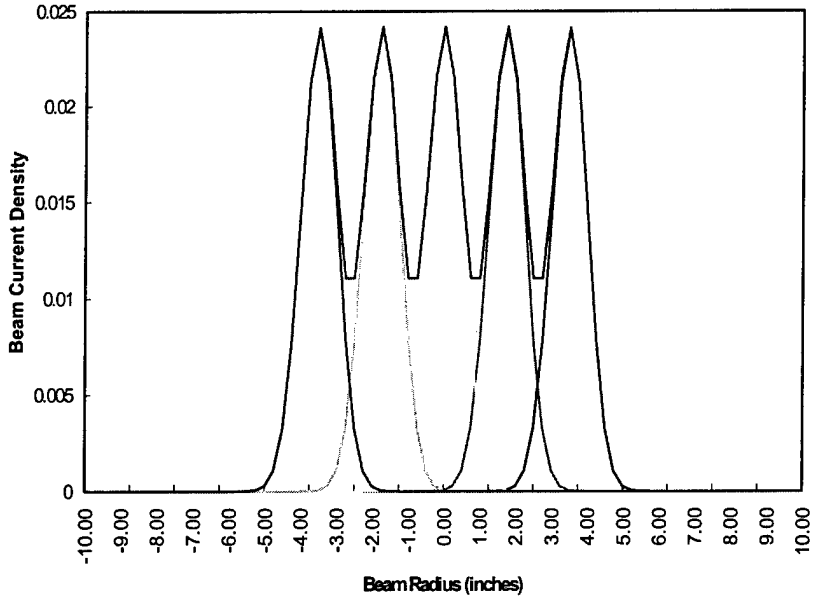

Figure 7. Current density profile calculated based on 4.45 cm spacing between passes and 1.27 cm beam diameter

Based on these observations, the distance between passes was reduced to 2.2 cm. The resulting calculation of current density profile is shown in Figure 8.

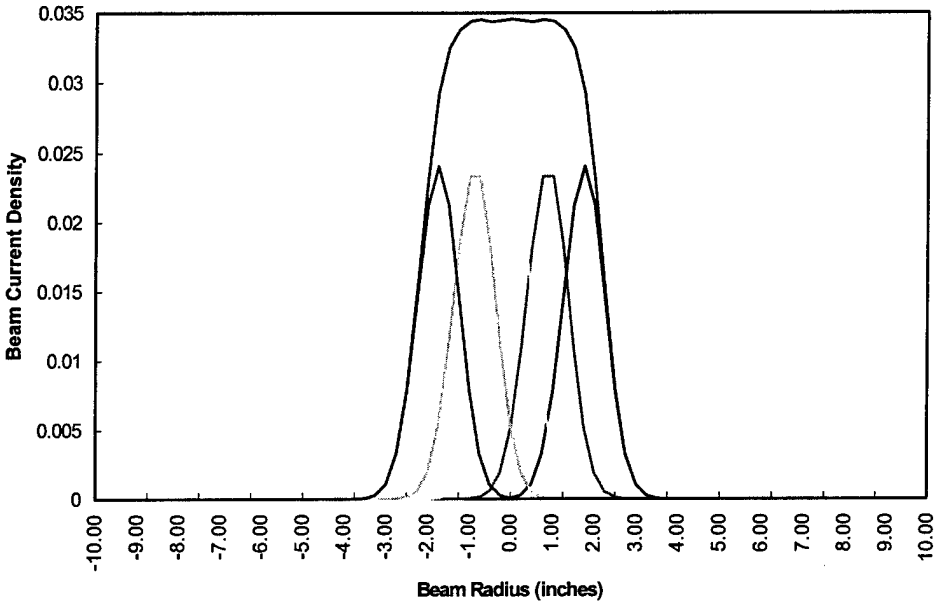

Figure 8. Current density profile based on 2.22 cm spacing between passes and 1.27 cm beam diameter

Nevertheless, the dosage received by the samples remained quite nonuniform as observed on the dosimetry film. When the spacing was recalculated, it was found that a relatively uniform dose would be obtained only if a translation distance of 0.9 cm or less was used. The consequences of the translation distance can be clearly seen in Figure 9; smaller translation distances give more uniform doses over the sample area.

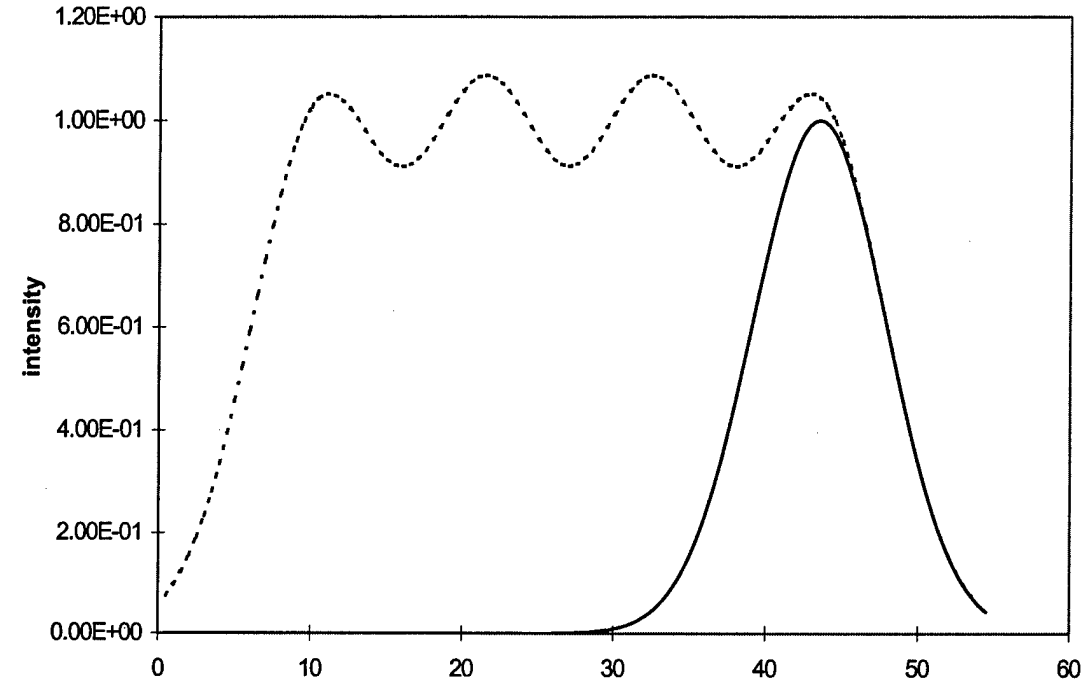

(a)

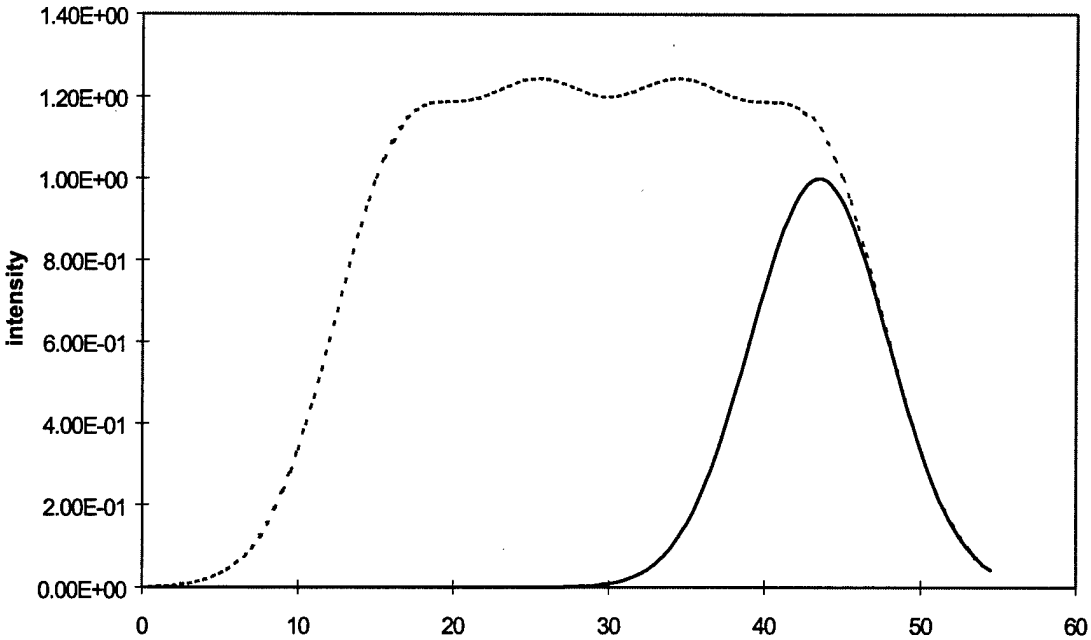

(b)

Figure 9. Sample dosing profiles (intensity vs mm distance) obtained employing (a) 1.1 cm translation distance and (b) 0.9 cm translation distance. Solid-line curves correspond to the beam profile of a single pass, used in the calculation of translation distance for four overlapping profiles (dashed-line curves).

A more uniform dose over the sample can be obtained using even smaller translation distances. However, this becomes impractical from an experimental standpoint. Therefore, the remaining exposures were run using a translation distance of 0.9 cm to provide a fairly uniform radiation dosage over the entire sample surface. This uniformity can be clearly seen in Figure 10.

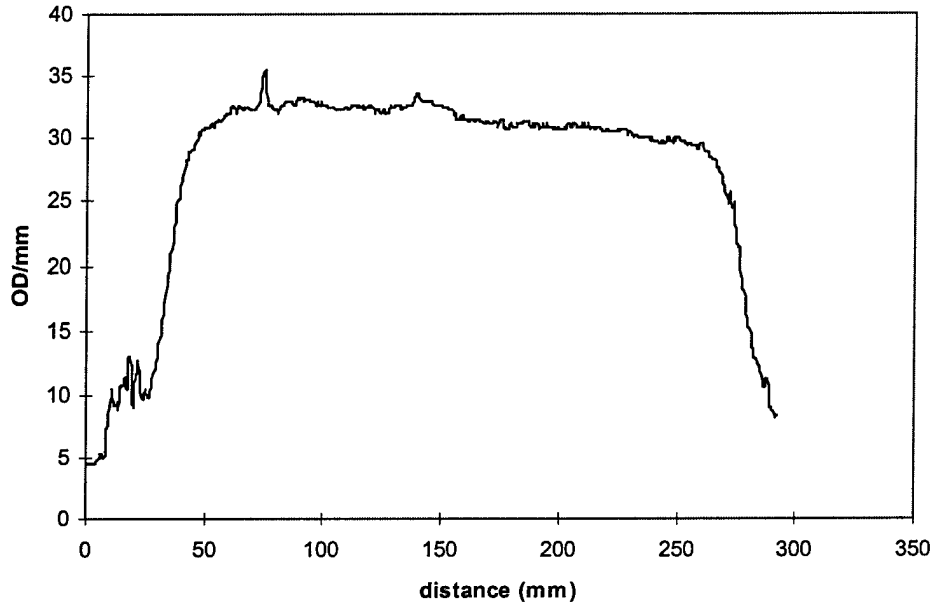

Figure 10. Actual measurement of dose uniformity achieved at 0.9 cm translation distance

Resin/Sensitizer Synthesis and Characterization

For the sake of convenience, several abbreviations are often used for compounds used during the course of this work. Table II summarizes these abbreviations.

Table II. Abbreviations for Compounds Used During the Course of this Work

Abbreviation	Compound
Bis-A	Bisphenol-A
Bis-A-P	Bisphenol-A bis(propargyl ether)
Bis-A-C	Bisphenol-A dicyanate ester
AT-S-24P	2,4'-bis(propargyloxy)benzophenone
AT-S-44P	4,4'-bis(propargyloxy)benzophenone
AT-S-4P	4-propargyloxybenzophenone
AT-S-4AP	4-propargyloxyacetophenone
PY-1a	2,3-dihydroxypyridine
PZ-1a	3,6-dihydroxypyridazine
AT-4BrA-P	propargyl-functionalized 4-bromoaniline
AT-4Br26DM	propargyl-functionalized 4-bromo-2,6-dimethylaniline
AT-9304	Adherent Technologies' proprietary initiator
AT-9307	Adherent Technologies' proprietary initiator
AT-9305	Adherent Technologies' proprietary fiber finish

The Bisphenol-A dicyanate ester is available commercially as AroCy B-30 from Rhône-Poulenc. This resin was used as obtained for these studies.

A complete discussion of methods used in the synthesis and characterization of resin and sensitizer systems is provided in Appendix C. Resins and sensitizers with propargyl endgroups were prepared using variations on the standard Williamson ether synthesis, shown schematically in Figure 3, above. The standard Williamson method involves the reaction of a metal alkoxide (*e.g.*, the sodium salt of Bisphenol-A) with an alkyl halide (*e.g.*, propargyl bromide). While this is a common and relatively inexpensive synthetic method, difficulties in isolating intermediates and incomplete reactions made this reaction method unrealistic for the preparation of these resin and sensitizer systems. Therefore, several totally organic variations on

the Williamson ether synthesis were attempted. Details of all variations attempted are provided in Appendix C.

The reaction of hydroxyl compounds such as Bisphenol-A and the sensitizer precursors with propargyl bromide in N,N-dimethylacetamide at 90°C in the presence of potassium carbonate was found to be the best method for preparation of resins and sensitizers. In this method, the potassium salt of the starting material is generated *in situ* and immediately reacts with propargyl bromide to yield the final propargyl derivatized product. Solubility of the reactants and products was not an issue and the reaction could be conducted in a relatively short time, 4 hours as opposed to the overnight reactions required for several of the other methods evaluated. Isolation of the product by precipitation in water was simple and provided high yields of pure product.

Figure 11 shows the infrared spectrum of the product obtained from the organic Williamson reaction to yield the Bisphenol-A bis(propargyl ether) monomer.

Absorbance bands at 2120 cm^{-1} and at 3289 cm^{-1}, corresponding to the acetylene C≡C and C—H stretching vibrations, respectively, clearly indicate the presence of the propargyl endgroups in the reaction product.

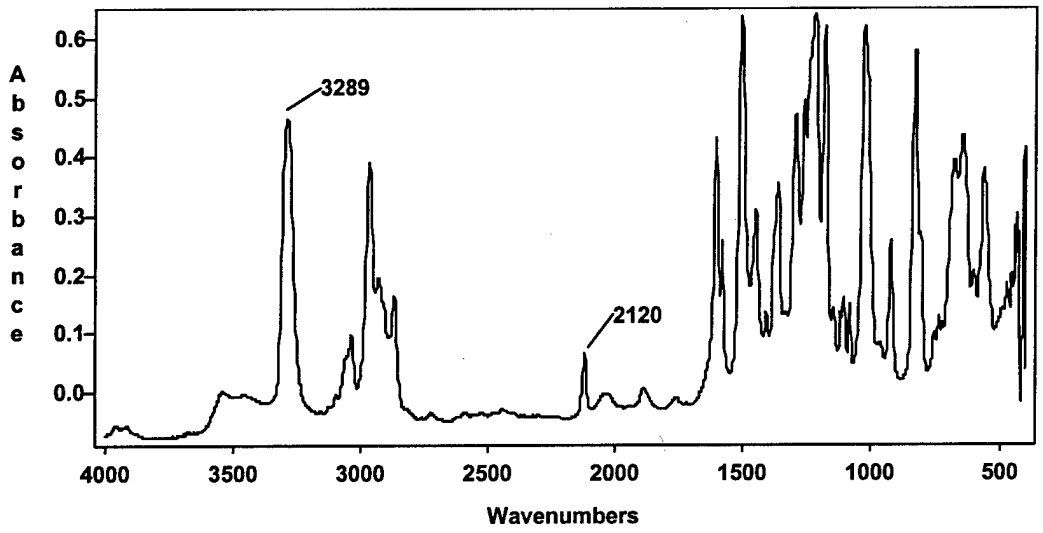

Figure 11. Infrared spectrum of Bisphenol-A bis(propargyl ether) resin as synthesized in DMAc

RESULTS AND DISCUSSION

UV and Fluorescence Spectroscopy

The spectra of Bisphenol-A, its bis(propargyl) ether, its dicyanate ester and various sensitizers were examined to estimate the lowest energy levels of these compounds and to determine the nature of possible energy transfer processes. Spectra were produced in 2-propanol, a moderately polar compound, to simulate the expected dielectric properties of the neat polymer. Using this solvent, the dilute solution spectra of these two materials were obtained. Solutions in methylcyclohexane, a nonpolar solvent, were also obtained to allow an examination of the effects of dielectric constant and hydrogen bonding and to allow for proper band assignments for these compounds.

Bisphenol-A

Bisphenol-A is the starting material for both the propargyl ether resin and the dicyanate ester resin studied in this program. Two distinct transitions, shown in the spectrum in Figure 12 are apparent: a relatively weak band between 250 nm and 300 nm and a band of approximately 4 times the intensity at shorter wavelengths. Only the long wavelength band is of interest in this study. It is from this excitation that we will estimate the energy transfer parameters and excited state lifetimes. In 2-propanol, that transition has an energy of approximately 34000 cm^{-1} estimated from the point where the band intensity falls to 1/10th of its maximum. The 1/10th intensity point will be used for the estimates in this report. The spectrum taken in methylcyclohexane is not appreciably different from that in 2-propanol, indicating that the band is primarily π-π^* (that is, little difference in the polarity of ground and excited states is expected or shown). For this reason, it is not likely to change appreciably for either of the two resin structures of this study.

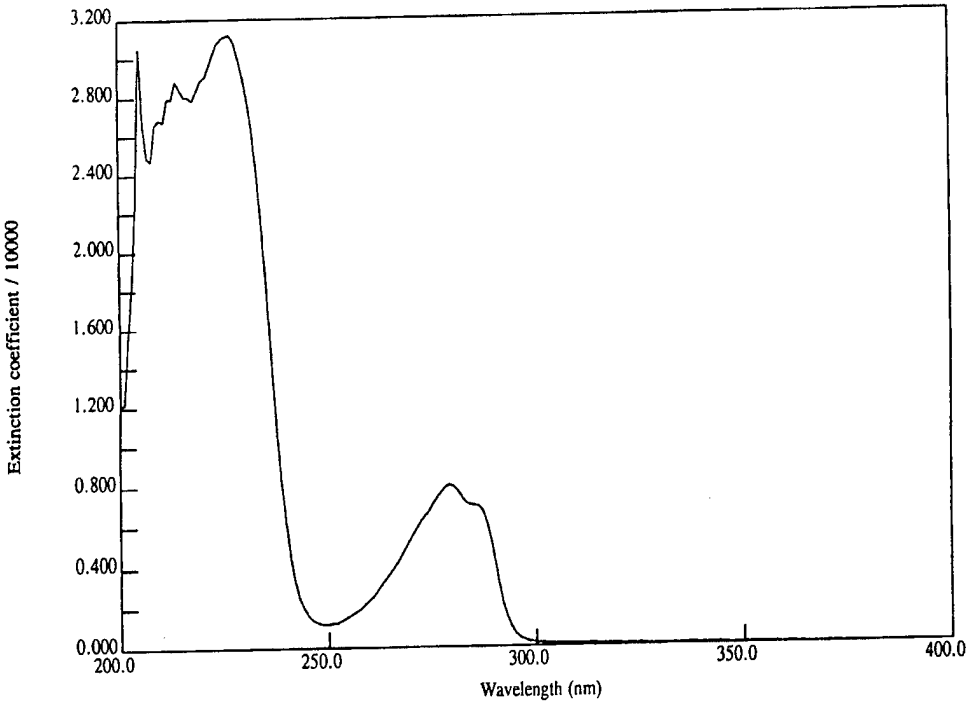

Figure 12. UV absorption spectrum of Bisphenol-A in 2-propanol

Bisphenol-A Bis(propargyl ether)

The spectra of the bis(propargyl) ether of Bisphenol-A in 2-propanol and in methylcyclohexane are shown in Figure 13.

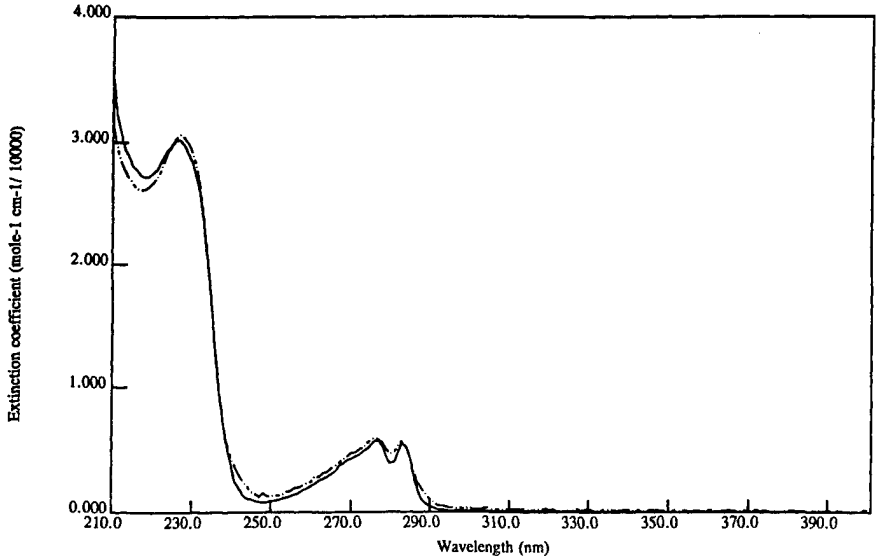

Figure 13. Spectrum of Bisphenol-A bis(propargyl) ether in 2-propanol (solid line) and in methylcyclohexane (dashed line)

These spectra show only a small shift from that of Bisphenol-A with energies of 34500 and 34600 cm^{-1} respectively. This is the expected result and indicates that there is little contribution from n-π^* in this excitation. n-π^* transitions involve substantial charge displacement in the excited state and would be stabilized by a polar solvent giving a bathochromic (red) shift relative to non polar solvents. It is likely that these results will pertain to the dicyanate ester structure as well.

Figure 14 shows the fluorescence observed from this compound in 2-propanol. Here, we have estimated the fluorescence quantum efficiency to be about 10% from comparison with similar compounds in the literature and the concentration at which fluorescence and energy transfer have equal probability (C0) was calculated to be 0.17 molar directly from the observed overlap between the absorption and fluorescence spectra of the bispropargyl ether in 2-propanol. (Note: In bulk, this figure gives a mean number of 840 transfers for an equal probability of fluorescence.

Here we have assumed a bulk density of 1.5 in the polymerizing system, and the bulk concentration of 4.9 molar. If we examine the case where the density is lowest [at the start of polymerization, about 0.9], we get 300 transfers per fluorescence, still a significantly high number.)

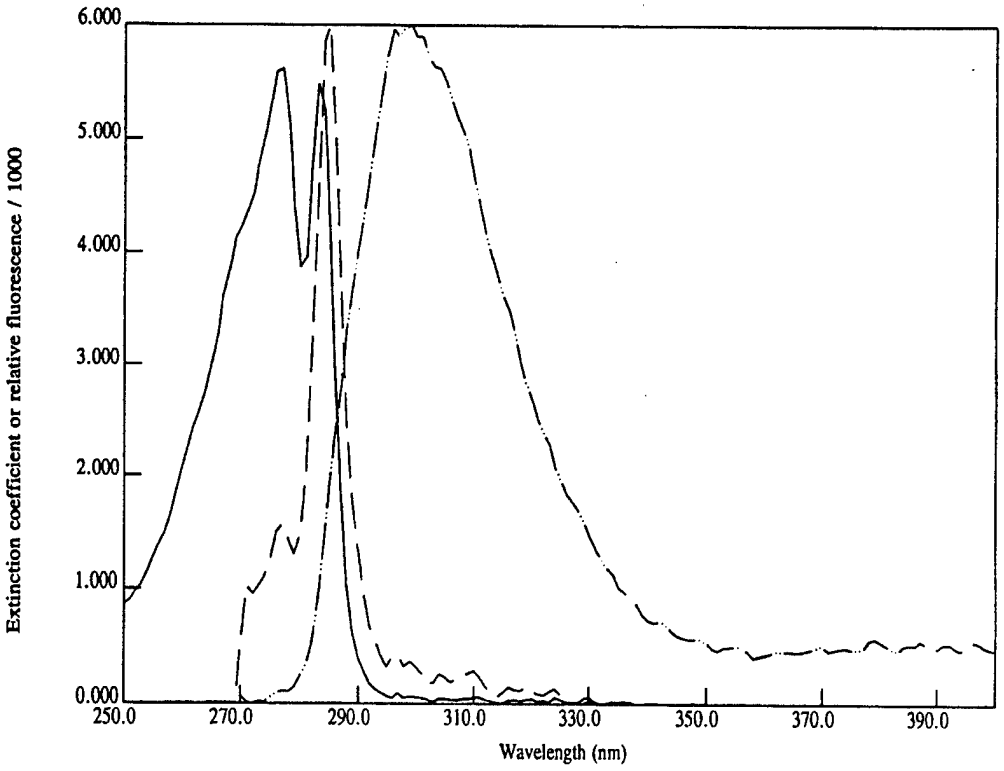

Figure 14. Absorption (solid line), fluorescence (long dash-dot line), and their overlap (dashed line) for Bisphenol-A bis(propargyl) ether in 2-propanol

If we assume that the transfer to the sensitizer is at least as fast as that between monomers, we would need one sensitizer molecule in a sphere with a radius of about 13-15 monomer dimensions to harvest ½ of the singlets. At the start of polymerization, we would need approximately a concentration of 1/300 of the monomer, about 0.33% for sensitizers of similar molecular weight. Our formulations will contain somewhat greater concentrations to ensure more efficient harvest. At 1% sensitizer, we expect to gather about 75% of the migrating singlet [19,]. Clearly, as the polymerization proceeds, the harvesting efficiency increases with density.

These data show that energy transfer between the monomers, Bisphenol-A bis(propargyl) ether (and most probably the dicyanate ester) is sufficiently rapid to make the proposed harvesting scheme viable.

Bisphenol-A Dicyanate Ester

As expected, results from this spectroscopic examination show that the band assignment proposed for the bispropargyl ether applies to the dicyanate esters as well; the lowest (and longest lived) singlet excited state is the π-π^* state of the benzene ring modified by the attached groups.

In the case of the dicyanate ester, it was not possible to derive an accurate value for the band intensity since the material was very insoluble in the chosen spectroscopic solvents. However, based on concentrations estimated by weighing residue left after evaporation of solvent from the sample, band intensities for the Bisphenol-A dicyanate ester are estimated to differ no more than 10-15% from those observed for the Bisphenol-A bispropargyl ether. This is not an unexpected result, since the ether differs only slightly from Bisphenol-A itself, having approximately 24% lower intensity. Differing substitution at the pendant oxygens should not alter the intensity greatly. What was unexpected was the blue shift of the spectrum relative to Bisphenol-A and its bispropargyl ether. The π-π^* ring excitation in the dicyanate ester has shifted 1530 cm^{-1} to the blue relative to Bisphenol-A, as a result of the cyanate substitution; the shift upon etherification was only 350 cm^{-1}.

The spectrum of Bisphenol-A dicyanate ester is compared with that of Bisphenol-A bispropargyl ether in Figure 15.

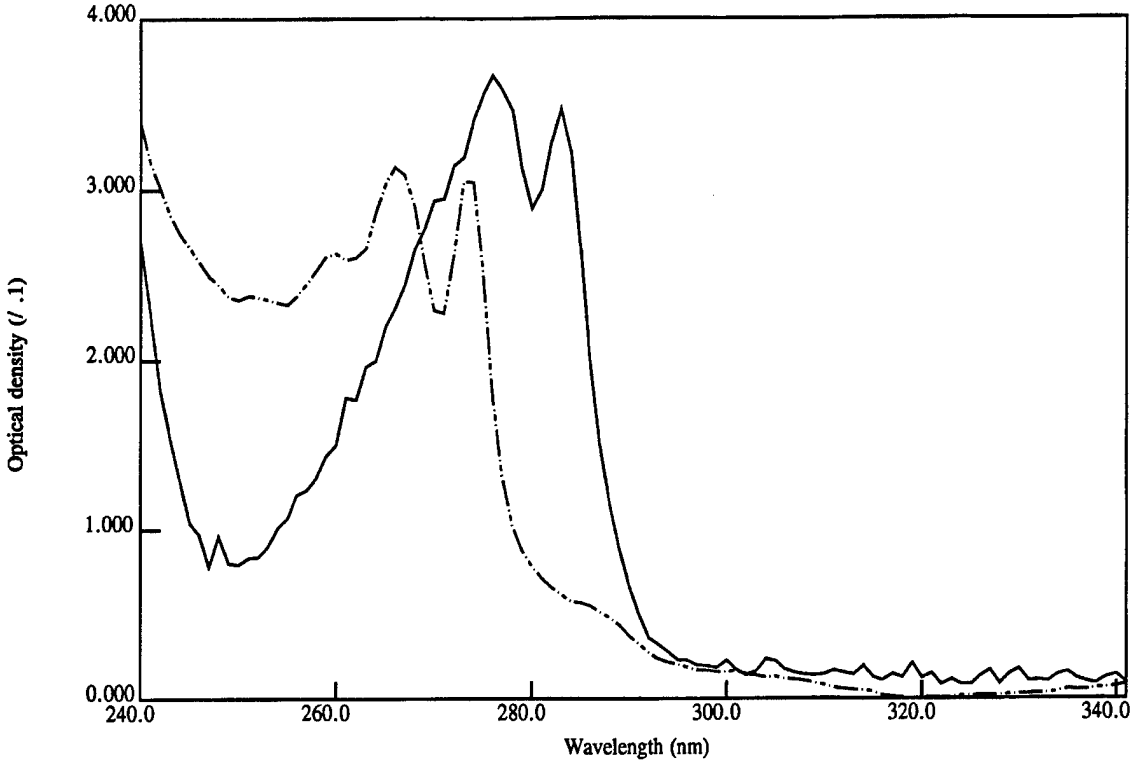

Figure 15. Bisphenol-A bispropargyl ether (solid line); Bisphenol-A dicyanate ester (dashed line), in 2-propanol

The blue shift in the Bisphenol-A dicyanate ester spectrum has much the same origin as the much lower solubility of this material in the chosen spectroscopic solvents. The cyanate moiety is linear and of relatively small size compared with the propargyl moiety. Thus, it is possible for the cyanate group to reside in the same plane as that of the attached aromatic ring, giving the system more symmetry and a more stable solid phase. The high electron density associated with the C≡≡N linkage, when the cyanate moiety lies in the plane of the ring, raises the energy for exciting the ring electrons by confining them to a more compact space. The C≡≡C bond in the bispropargyl ether is farther removed from the ring, and is not confined to planarity, thus it has a smaller influence on ring electron excitation.

This energy change in the Bisphenol-A dicyanate ester is advantageous in that it allows a greater range of sensitizers to be utilized for this material than are viable for the bispropargyl ether. Furthermore, the presence of the coplanar cyanate should not influence the active triplet state as much as the observed singlet perturbation. A small band near 288 nm, apparent in the isocyanate spectrum, is not expected and may arise from an impurity or may be associated with a nearly forbidden charge transfer transition (π_1-π_2^*) from the cyanate π orbitals to the ring. The fluorescence spectrum (Figure 16) suggests the impurity explanation.

Figure 16 shows the absorption and fluorescence spectra of the dicyanate ester. The data imply that the energy transfer rate for this species is comparable to that of the bispropargyl ether and transfer to each of the sensitizers should be nearly the same as observed for propargyl substitution.

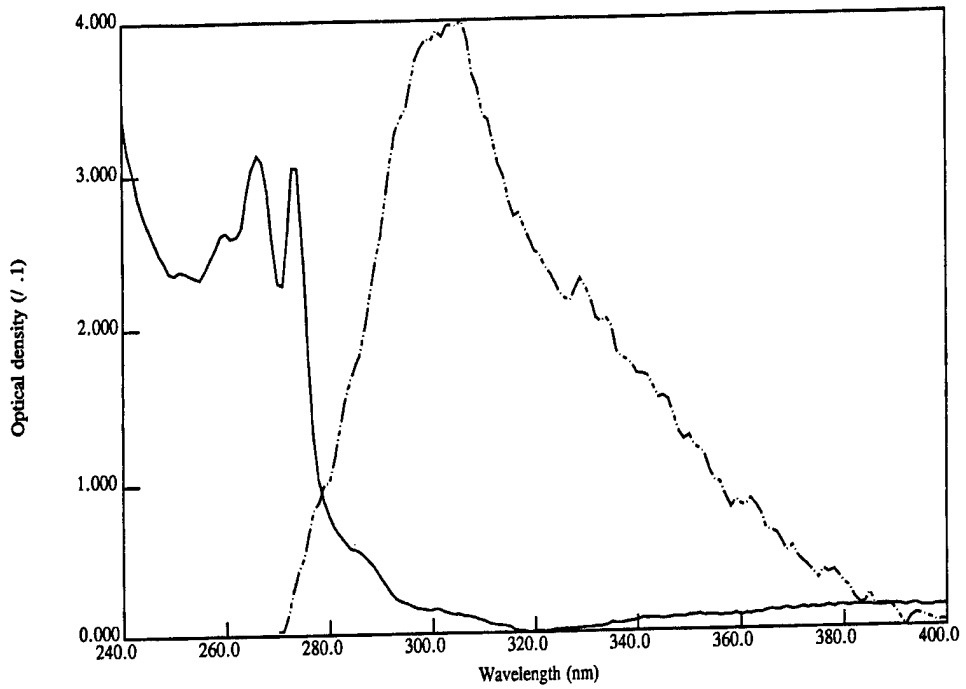

Figure 16. Bisphenol-A dicyanate ester absorption (solid line) and fluorescence (dashed line) spectra in 2-propanol

Sensitizers

Several sensitizer candidates were evaluated. These materials include aryl ketones and aryl nitrogen heteroatom ring structures and are expected to offer high intersystem crossing yields and compatibility with the dicyanate esters and propargyl ethers. They also provide a great range of energy level and chemical structure tailoring.

Benzophenone-derived sensitizers

Compounds AT-S-4P and AT-S-24P were examined for their utility as sensitizers for the electron beam polymerization of Bisphenol-A derivatives. These compounds were examined for lower transition energy (*vs.* Bisphenol-A derivatives) to allow energy localization, the nature of the lowest excited state, and spectral overlap with Bisphenol-A derivatives.

The UV absorption spectra of sensitizer AT-S-4P are shown in Figure 17.

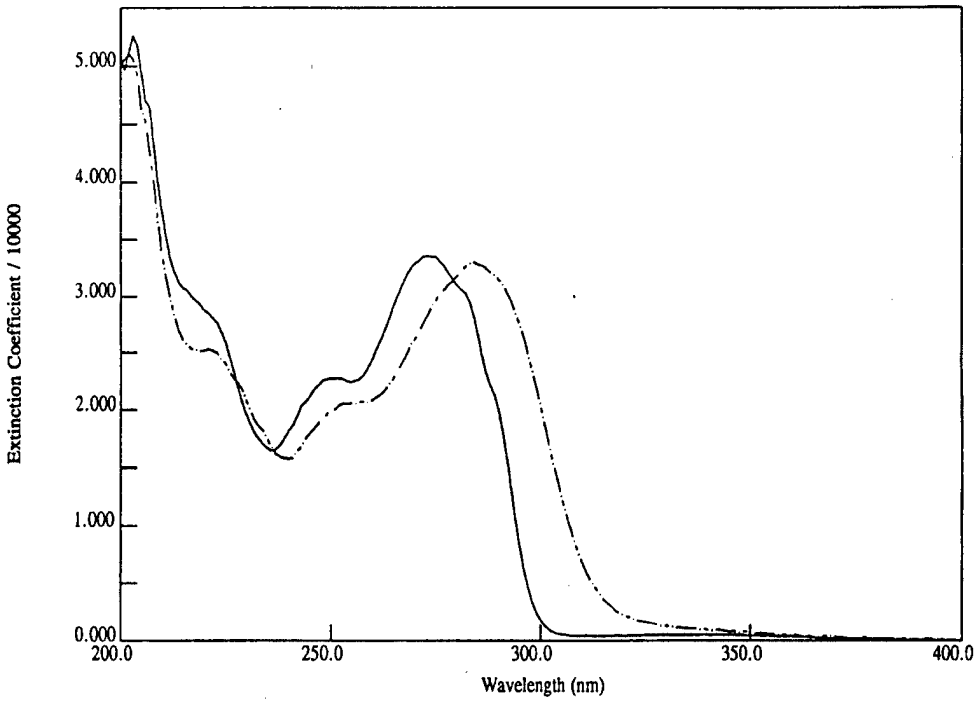

Figure 17. UV Absorption spectra of sensitizer AT-S-4P in methylcyclohexane (solid line) and 2-propanol (long dash-dot line)

The transition energies for these compounds are 33700 and 32000 cm^{-1} respectively, both sufficiently below the transition of Bisphenol-A derivatives (>34000 cm^{-1}) for rapid localization. They have significant overlap with Bisphenol-A fluorescence and a critical concentration of 0.018 M, nearly 1/10 lower than the self-overlap between the fluorescence and absorption of Bisphenol-A. The overlap between AT-S-4P absorption and Bisphenol-A bis(propargyl ether) fluorescence is shown in Figure 18.

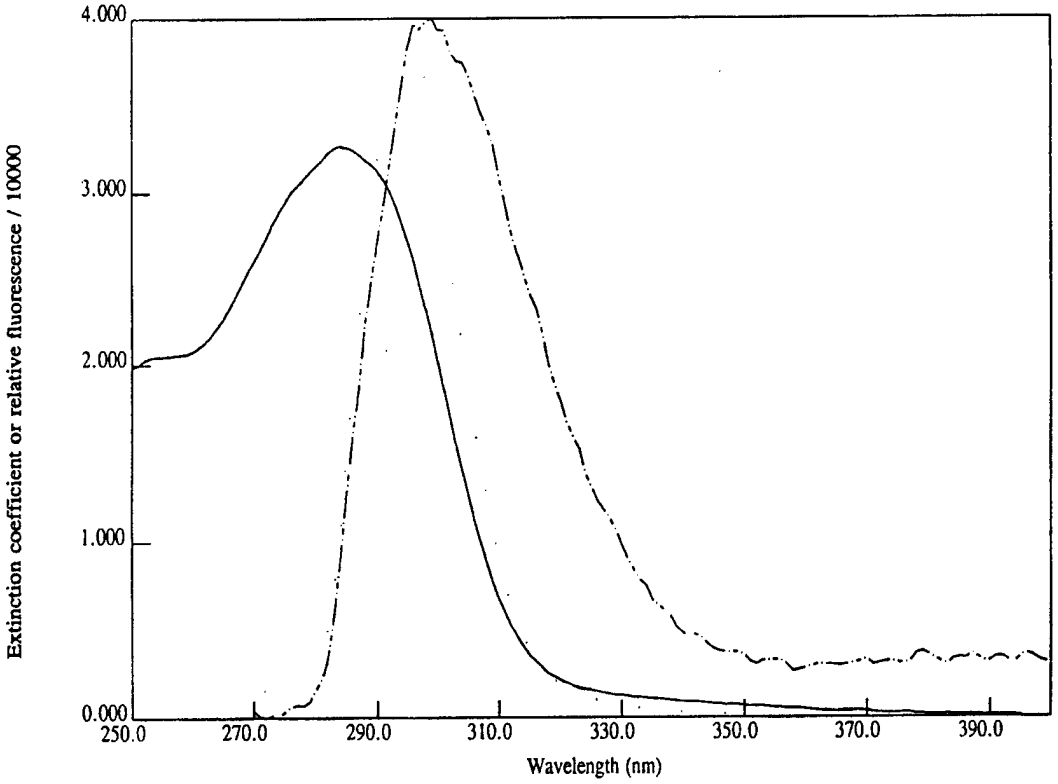

Figure 18. UV absorption of AT-S-4P with Bisphenol-A bis(propargyl) ether fluorescence

This material should be a successful sensitizer. The lowest excited state appears to be n-π^* as expected, but the proximity to the π-π^* (a few hundred wavenumbers, from slight structure apparent in the methylcyclohexane solution) may reduce the intersystem crossing rate.

Compound AT-S-24P was also examined for sensitizer application. The UV spectra obtained for the parent compound are shown in Figure 19.

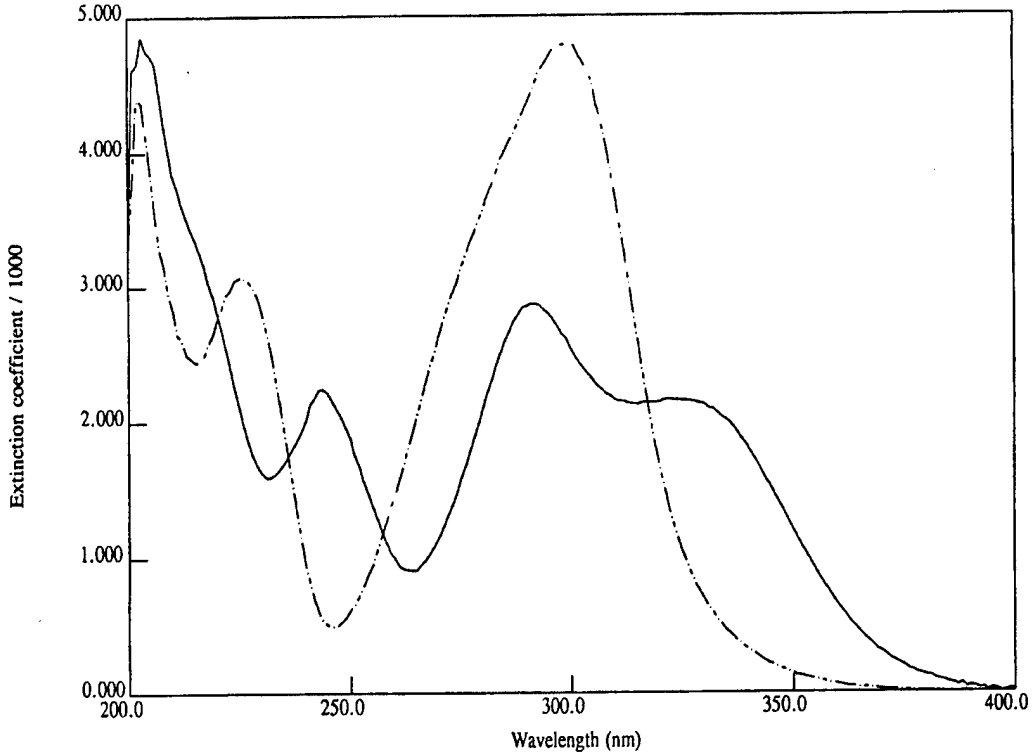

Figure 19. UV Absorption spectra of AT-S-24P parent compoundin 2-propanol (solid line) and in methylcyclohexane (dash-dot line)

The marked change between these two solvents clearly demonstrates that the lowest excitation is n-π^* with a band origin near 26300 cm^{-1}. A second transition near 300 nm is apparent in 2-propanol, which is apparently masked in methylcyclohexane. This transition does not appear to shift between these two solvents and is assumed to be the first π-π^*. The single band in methylcyclohexane does appear to have a short wavelength shoulder, probably the poorly resolved transition seen clearly in 2-propanol.

The spectra for the AT-S-24P itself are shown in Figure 20, again taken in 2-propanol and methylcyclohexane.

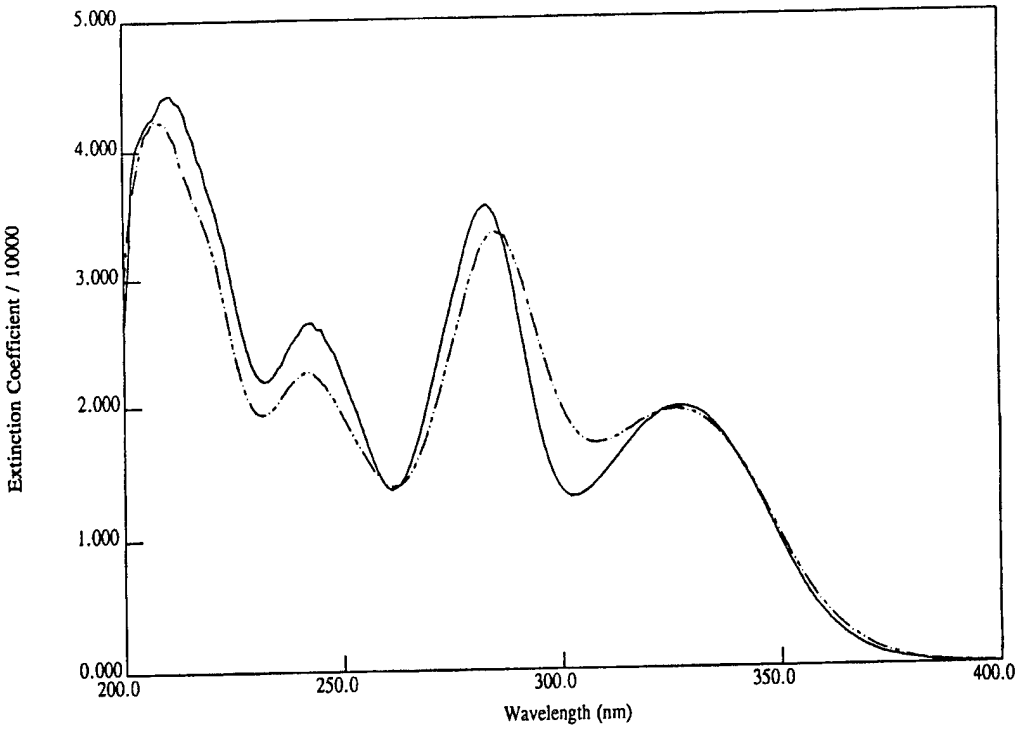

Figure 20. UV absorption spectra of AT-S-24P (solid line) in methylcyclohexane and (dash-dot line) 2-propanol

These spectra are quite surprising in that there does not appear to be a noticeable shift between solvents. The lowest band does seem to be nearly identical to that from the parent compound in 2-propanol and must be the n-π^* transition. We interpret this behavior to indicate that the propargyloxy moiety located at the 2 position on the ring adjacent to the carbonyl group, is bound to the carbonyl oxygen by some secondary valence force comparable to solvation strength. This may arise from the acidity of the acetylenic hydrogen on propargyl, and if so, places this moiety in an advantageous position for the triplet activation process. The overlap between this absorption and the Bisphenol-A ether is very strong, again giving a small C_0 (0.013 M, Figure 21).

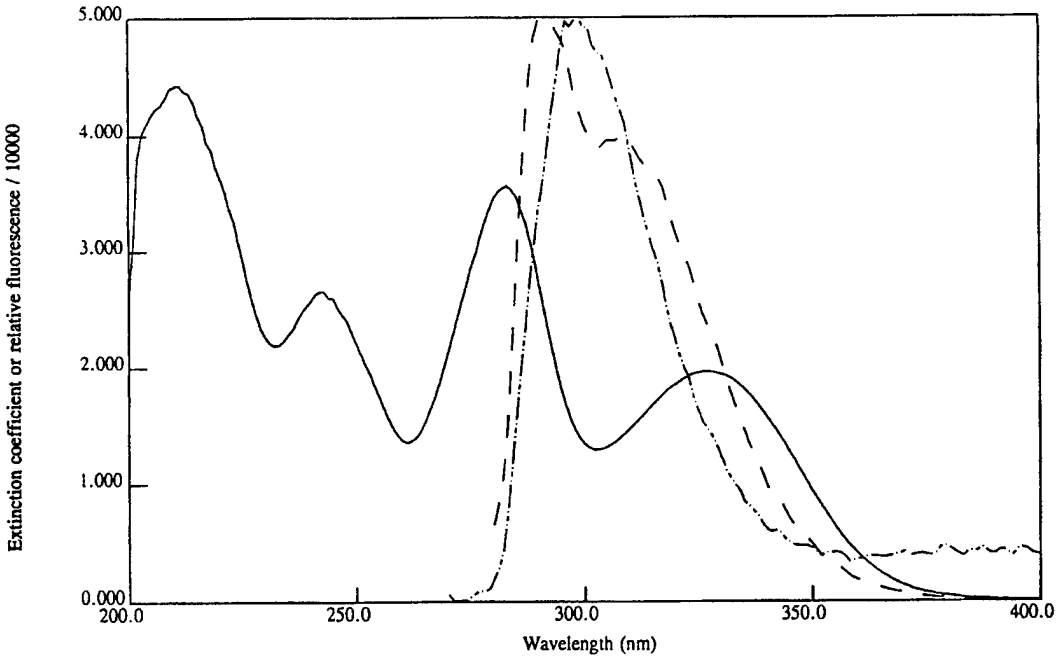

Figure 21. UV absorption of AT-S-24P (solid line) and overlap with Bisphenol-A bis(propargyl) ether fluorescence (dash-dot line)

This material should provide an excellent sensitizer for triplet reactive systems. The peculiarity of the solvent effects shown in Figure 19 does call some doubt on our interpretation of its origin. If our interpretation is correct, this should the most effective material. However, the other possible sensitizer materials were not discounted.

We have demonstrated thus far that the systems proposed have the proper ordering of electronic energy levels to assure efficient energy harvesting. Indeed, these activators did demonstrate efficient energy harvesting in the resin systems under study. However, they did not induce polymerization but instead led to resin rearrangements, discussed in detail in the section entitled Series 2.

Pyridine-derived sensitizers

Two pyridine-derived sensitizers were also screened as they could prove more effective in complexation with the cyanate ester resin. With this in mind, two such materials, identified as PY-1a and PZ-1a, based on pyridine and pyradazine, respectively, were examined. A large degree of overlap between sensitizer absorption and the fluorescence of the Bisphenol-A dicyanate ester resin was noted, demonstrating their applicability for energy harvesting.

However, when the absorption spectra of these materials were compared with their own fluorescence, it was found that the fluorescence intensity was surprisingly

high. This would imply that the formation rate of triplet is slow compared with excited state deactivation by fluorescence. To verify the strong fluorescence of PY-1a and PZ-1a, the fluorescence quantum yields of these and the other sensitizer candidates and resins were estimated by comparing the integrated fluorescence with that of *p*-terphenyl in the same cell. *p*-Terphenyl is an aromatic hydrocarbon whose quantum yield has been accurately measured to be 0.93 [20]. Fluorescence quantum yields and other spectral data for Bisphenol-A-derived resins, benzophenone-derived sensitizers, and pyridine-derived sensitizers are summarized in Table III. The data in this table use the crossover between the absorption spectrum and the fluorescence spectrum when plotted on the same scale relative to their maxima. This technique gives a more accurate estimation of transition energy threshold.

Note that the fluorescence quantum yields of PY-1a (3.3%) and PZ-1a (12%) were extremely high relative to that observed for the benzophenone-derived sensitizers (<1%). These relatively high yields from these sensitizers indicate that they would be inferior to the benzophenone-derived sensitizers. It was thus concluded that these two candidates were not suitable.

Table III. Summary of Resin and Sensitizer Spectroscopic Data

Compound	Solvent	First Excited State (cm^{-1})	Band Intensity (cm^{-1}/Mol)	Fluorescence Quantum Yield
Bis-A propargyl	2-propanol	34722	5910	0.004
Bis-A propargyl	methylcyclohexane	34904	5688	0.001
Bis-A cyanate	2-propanol	35778	5700	0.005
Bis-A cyanate	methylcyclohexane	36101	5500	0.006
AT-S-24P	2-propanol	27778	2163	0.003
AT-S-24P	methylcyclohexane	28248	1961	0.0006
AT-S-44P	2-propanol	31846	22370	0.0006
AT-S-44P	methylcyclohexane	32300	32207	0.0006
AT-S-4AP	2-propanol	28090	733	0.008
AT-S-4AP	methylcyclohexane	27790	768	0.004
PY-1a	2-propanol	30460	38765	0.033
PZ-1a	2-propanol	28653	4795	0.12

Aniline-derived sensitizers

Two aniline derivatives were also investigated as possible sensitizer candidates. These nitrogen-containing derivatives were tested as possible alternatives to the oxygen-containing sensitizers. Like the oxygen-containing sensitizer candidates, the lone pair of electrons present on the nitrogen in these materials is expected to catalyze the intersystem crossing from the excited singlet state to the triplet state desired for reaction to occur. However, unlike the oxygen-containing sensitizers, the nitrogen-containing candidates are not subject to Norrish type dissociation reactions that can interfere with the desired polymerization reactions through sensitizer degradation.

Ultraviolet absorption and fluorescence spectra were collected as described in the previous section. The overlap of the donor (resin) and acceptor (sensitizer) spectra was excellent, indicating high potential for the desired energy transfer reactions. The absorption spectra of one sensitizer precursor in methylcyclohexane and 2-propanol are shown in Figure 22. The fluorescence spectra in these solvents were also run (not shown) and indicated a very low quantum yield. This result suggests that this material structure would be ideal for triplet sensitization. Functionalized sensitizers were synthesized from the aniline precursors and applied in UV screening and e-beam exposures.

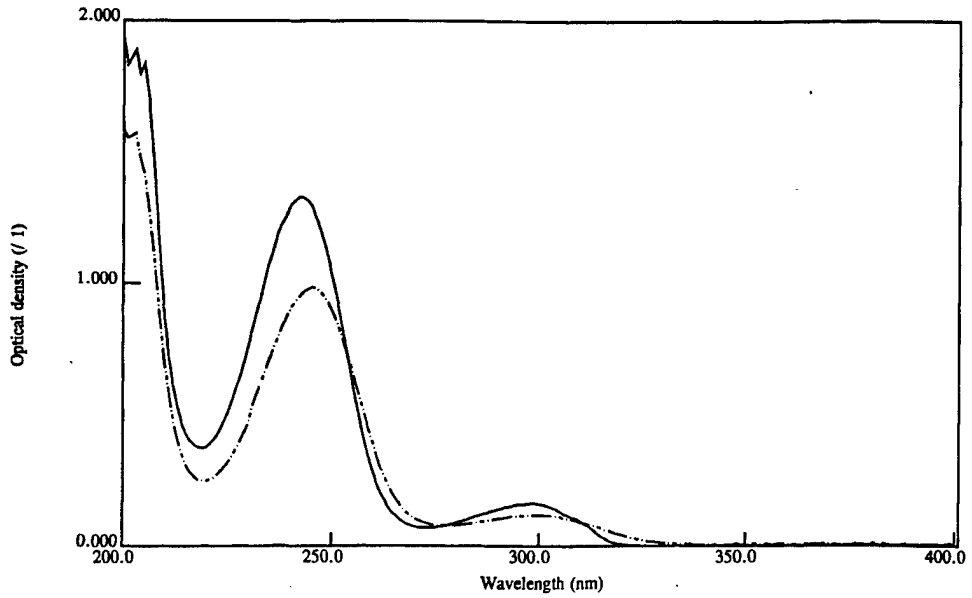

Figure 22. Spectra of aniline based sensitizer precursor in methylcyclohexane (solid line) and in 2-propanol (dashed line)

UV screening tests and initial e-beam exposures indicated that triplet sensitization, while effective, gave rise to resin rearrangement in both propargyl ether and cyanate ester resins as discussed later in this report. Therefore, extensive testing

with these triplet sensitizers was not undertaken. The rearrangement reaction subverts polymerization and provides a route for energy dissipation that does not lead to productive reaction. As such, excitation polymerization of these structures was not studied extensively.

UV and E-beam Cure Experiments

Series 1

UV cure experiments were used to identify the sensitizers most likely to provide effective cure when e-beam processing is used. Before the first e-beam exposure experiment, two series of UV screening tests were conducted.

In the first test, only propargyl resin systems were evaluated. The resin samples consisted of the Bisphenol-A bispropargyl resin with 3% (w/w) sensitizer. Four resin/sensitizer combinations were investigated: Bis-A-P/AT-S-44P, Bis-A-P/AT-S-4P, Bis-A-P/AT-S-4AP, and Bis-A-P/AT-S-24P. Small amounts of the resin/sensitizer mixtures were placed into aluminum weighing dishes, which were then placed inside plastic bags that were purged with nitrogen and then sealed. The samples were irradiated for 20 minutes using a 3 kW mercury arc lamp in an aluminized box.

In the second test, both propargyl and cyanate systems were tested. Four sensitizers were evaluated with the bispropargyl ether resin: Cyracure 6990 (Union Carbide) (6% [w/w]) of solution in propylene carbonate), 4-bromoaniline (10% [w/w]), 4-bromo-2,6-dimethyl aniline (10% [w/w]), and AT-4-BrA-P (10% [w/w]). Four sensitizers were also investigated for the dicyanate resin: Cyracure 6990 (6% [w/w]) of solution in propylene carbonate), AT-S-24P (3% [w/w]), Cyracure 6990 (3% [w/w]) of solution in propylene carbonate) + AT-S-24P (1.5% [w/w]), and AT-S-44P (3% [w/w]). Sample preparation and irradiation conditions were as described above.

Methylene chloride solutions of the resin/sensitizer mixtures both before and after UV exposure were prepared and analyzed using Fourier transform infrared spectroscopy. Solution experiments were chosen here for the purpose of avoiding complications in data analysis that might arise as a result of resin crystallization. The following spectral regions were integrated as appropriate: 3334-3201 cm^{-1} (acetylenic C—H stretch), 3018-2777 cm^{-1} (aliphatic C—H stretch), 2333-2200 cm^{-1} (C≡≡N stretch), 2150-2092 cm^{-1} (acetylenic) C≡≡C stretch), 1536-1467 cm^{-1} or 1529-1452 cm^{-1} (aromatic C==C stretch), and 1068-981 cm^{-1} (C—O stretch).

During polymerization, the intensities of the bands associated with the propargyl functionality (~3300 cm^{-1} and ~2120 cm^{-1}) or with the cyanate functionality (2333-2200 cm^{-1}) are expected to decrease relative to the other bands analyzed. Thus, by comparing the propargyl or cyanate bands with these other "internal standard"

bands, it can be determined whether or not reaction is occurring as a result of UV exposure.

Propargyl Resin UV Screening

Sensitizer AT-S-44P showed the most promise, giving about an overall 4% reduction of the acetylenic hydrogen and triple bond stretching bands (~3300 and 2120 cm^{-1}), with respect to the aliphatic C—H stretch or aromatic in-plane ring stretching (~1508 cm^{-1}). Sensitizer AT-S-4AP was about half as effective, while sensitizer AT-S-24P acted to protect the system from damage. Sensitizer AT-S-4P seemed to have little or no effect.

The process of sensitization in the attempted systems is closely related to the normal method used to protect polymers and other organic compounds from photodegradation. Sensitization or protection is a consequence of the relative placement of the energy levels of the solvent (resin) and the solute. Where the solute (here, the sensitizer) excitations are lower in energy that those of the solvent (resin), energy deposited in the solvent will be transferred to the solute. The fraction transferred to the solute is then not available for inducing chemical reactions directly in the solvent. Where the solute is a sensitizer, its excitations serve to induce chemical reactions in the solvent. If the solute is used to protect the solvent, its excited states decay without persistent chemical reaction. Appendix A outlines the various processes involved in the energy transfer and subsequent decay of excitation in the sensitizers and stabilizers.

The spectroscopy of the components, conducted in dilute solution in inert solvents, can be used to estimate these pertinent levels, but direct evaluation is needed to confirm the spectroscopic conclusions. For the practical system, the solvent is the resin itself, and interactions between the resin and the sensitizer can alter the energy levels in ways not apparent from the dilute solution spectra.

The observed changes (from IR spectra) after UV exposure suggested that, even in the effective sensitizer, reactions other than the desired addition between acetylenic groups were occurring. Consequently, the fluorescence spectra of the effective compounds, sensitizers AT-S-44P and AT-S-4AP, were reexamined. Both of these fluoresced in methylcyclohexane in two distinct bands. These dual fluorescences were initially thought to arise either from an impurity in the freshly prepared sensitizers, or from fast phosphorescence (unlikely). Because the ratio of these two emissions did not materially change on dilution, and since the ratio did change on going to the more polar 2-propanol solvent, it is clear that both emissions are fluorescences of the parent specie.

Dual fluorescence is known to occur when the excited state of the parent molecule can have more than a single structure, and when the two (or more) possible structures can interchange on the time scale of excited state lifetime. Here, rotation

of the propargyl end groups into or out of the aromatic plane most probably accounts for these observations. The absence of dual fluorescence in the related AT-S-24P sensitizer serves as confirmation; this material is sterically prevented from attaining a coplanar conformation. For the structures of AT-S-44P, AT-S-4P, and AT-S-4AP, the existence of two types of excited states *is* possible and these states may give rise to different photo- or radiation chemistry. To optimize our system, a sensitizer that cannot exhibit this structural isomerism and that meets the energy level requirements must be identified. Candidates were available that meet these additional (unexpected) requirements; these will be discussed in the following sections.

Cyracure 6990 is a commercially available cationic initiator commonly used in UV-cured epoxy systems. It was tested here to investigate the possibility of curing propargyl and/or cyanate resins by a cationic mechanism rather than by a triplet transfer mechanism. Analysis of the propargyl bands (3334-3201 cm^{-1} and 2150-2092 cm^{-1}) relative to the internal standard bands (3018-2777 cm^{-1} and 1536-1467 cm^{-1}) indicated that no significant reaction of propargyl groups occurred during a 20 minute UV exposure. This initiator was also examined in an e-beam experiment to assure that mechanism differences did not exist.

Using 4-bromoaniline and 4-bromo-2,6-dimethylaniline also proved inadequate for initiating significant UV initiated reaction of propargyl groups in the resins. Increases in propargyl band intensities relative to aliphatic C—H stretch bands were noted, but decreases in propargyl band intensities relative to the aromatic C=C stretch band were also noted. There was also a significant darkening of the resin that occurred during exposure. It is well known that amine compounds with electron-withdrawing substituents are prone to fast oxidation. While such oxidation would be unlikely in a well-purged system, the bags used here to contain the inert nitrogen atmosphere may not have been totally sealed and thus oxidation could have occured. Based on this observation, a propargyl derivative of 4-bromoaniline was prepared as described in Appendix C. Derivatization of the $-NH_2$ groups on these compounds serves to inhibit oxidation of the nitrogen-containing compounds as well as allowing the material to be polymerized into the propargyl resin system, thus minimizing the potential for outgassing.

A sample containing the propargyl resin and 10% (w/w) of this sensitizer was then subjected to UV irradiation as described above. For this sample, propargyl bands were integrated over the ranges 3359-3226 cm^{-1} and 2150-2092 cm^{-1}. Comparison of propargyl bands with "internal standard" bands for this system indicated a 15-20% decrease in propargyl intensity relative to the aliphatic C—H stretch band. This sensitizer is clearly superior for these resins but did not result in polymer!

Cyanate Resin Screening

The Bisphenol-A dicyanate resin was tested for UV curing with several different initiators: Cyracure 6990, AT-S-24P, Cyracure 6990 + AT-S-24P and AT-S-44P. The cyanate C≡≡N stretch band, in the range 2333-2200 cm^{-1}, was compared with aliphatic C—H stretch (3018-2848 cm^{-1}) and aromatic C=C stretch (1529-1452 cm^{-1}) bands to monitor reaction of the cyanate endgroups. The sample containing Cyracure 6990 alone showed a decrease in C≡≡N intensity relative to all "internal standard" bands. The results from the other systems were inconclusive, a decrease in C≡≡N intensity was noted relative to some "internal standard" bands whereas an increase in C≡≡N intensity was noted relative to other bands in the same sample.

The tests on cyanate resin systems containing AT-S-24P were conducted before analysis of propargyl resin systems containing AT-S-24P. It was reported above that AT-S-24P appeared to *stabilize* the propargyl resin system rather than catalyzing the desired reaction of propargyl endgroups. It might reasonably be expected that the same phenomenon could occur in a cyanate resin system, thus affording the results described above. Consequently, the AT-S-44P sensitizer was also tested with the cyanate resin system. AT-S-44P was shown previously to initiate reaction of propargyl groups when subjected to UV irradiation. As in the case of the propargyl resin system, AT-S-44P was considerably more effective at initiating reaction of the cyanate groups than was AT-S-24P. A 4-6% decrease in C≡≡N band intensity relative to both aliphatic C—H stretch and aromatic C=C stretch bands was noted.

Electron Beam Curing Experiments

Based on the UV screening experiments described above, several resin/sensitizer formulations were selected for initial testing in the electron beam. These formulations were as follows:

- Bisphenol-A bis(propargyl) ether (propargyl resin) without additives (1 sample)
- Bisphenol-A dicyanate (cyanate resin) without additives (1 sample)
- Propargyl resin + 3% (w/w) AT-S-44P (2 samples)
- Propargyl resin + 3% (w/w) AT-S-4AP (2 samples)
- Propargyl resin + 10% (w/w) AT-4BrA-P (2 samples)
- Cyanate resin + 10% (w/w) AT-9307 (1 sample)
- Cyanate resin + 10% (w/w) AT-9304 (2 samples)
- Cyanate resin + 3% (w/w) AT-S-44P (1 sample)
- "Cat-B" cationic epoxy (1 sample)

- "Cat-M" cationic epoxy (1 sample)
- "RA-1" cationic epoxy (1 sample)
- EPON®-826 + 3% (w/w) malachite green methoxide (anionic epoxy, 1 sample).

The propargyl resin was prepared at Adherent Technologies as described in Appendix B. The commercially available dicyanate resin (AroCy B-30) was obtained from Rhône-Poulenc. Resins were heated as necessary to melt or induce flow after which the initiators were added and further heated as required for complete dissolution of the initiators in the resin. Cationic epoxy systems, used as control samples, were obtained from Applied Poleramic and used as received.

The only samples that exhibited complete or near-complete curing from this initial electron beam exposure were the cationic epoxy systems. The propargyl resin formulations were waxy in texture whereas the cyanate resin formulations remained as high viscosity liquids. However, FTIR spectroscopic analysis of these samples indicated that some reaction had indeed occurred in these samples as a result of e-beam exposure.

All propargyl resin formulations except that containing AT-4BrA-P exhibited a decrease in propargyl C—H stretch intensity relative to both aliphatic C—H stretch bands and aromatic C=C stretch bands. This change ranged from 17% for the propargyl resin samples with AT-S-44P or AT-S-4AP to 30% for the propargyl resin alone. An increase in aromatic C—H stretch (3099-3018 cm^{-1}) intensity relative to aliphatic C—H stretch was also noted for these samples. This change in aromatic C—H stretch intensity would be expected if the resins are reacting to form ring structures as anticipated. The changes in relative intensities of the propargyl C—H stretch and aromatic C—H stretch bands can be seen for the propargyl resin with AT-S-44P additive in Figure 23. Similar results are observed for the other propargyl resin samples. Analysis of the propargyl C≡≡C stretch band at ~2120 cm^{-1} was not attempted.

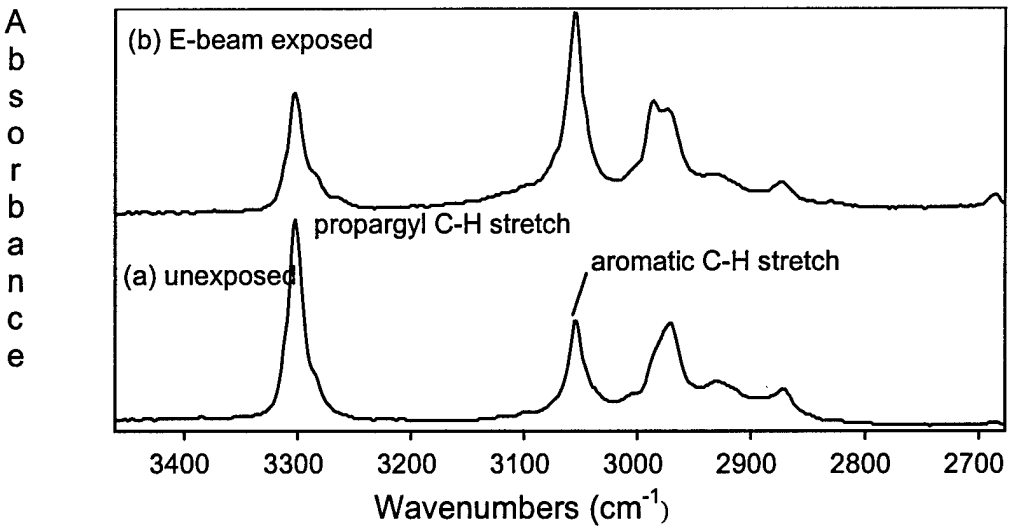

Figure 23. FTIR spectra of the C—H stretch region for (a) unexposed and (b) e-beam exposed propargyl resin with AT-S-44P additive. (Changes in the relative intensities of propargyl and aromatic C—H stretch bands are indicative of reaction of the propargyl endgroups on the resin.)

Interference from carbon dioxide (CO_2) bands in the infrared spectra was a problem for the cyanate resin analyses. Since the only diagnostic bands for the cyanate group are in the range 2333-2200 cm^{-1}, integration was performed over a more limited range (2316-2200 cm^{-1}) to minimize the effects of the CO_2 bands on the reaction calculations. All cyanate resin spectra indicated decreasing cyanate C≡≡N intensity relative to the aliphatic C—H stretch bands. The decrease in band intensities were: 7.8% for the formulation containing AT-S-44P, 19-21% for the formulation containing AT-9307, and 17% for the formulation containing AT-9304. Accompanying increases in aromatic C—H intensities were also noted for those formulations containing AT-9307 and AT-9304. While the change in C≡≡N band intensity is difficult to see in the spectra, other qualitative changes were noted. Of particular interest is the appearance of a band ~1422 cm^{-1}, which is likely due to C=N bonds that are formed as a result of cyanate reaction. Figure 24 shows the spectra of unexposed and exposed cyanate resin with AT-9304 additive. The presence of the band at ~1422 cm^{-1} is noted on the spectrum of the exposed sample.

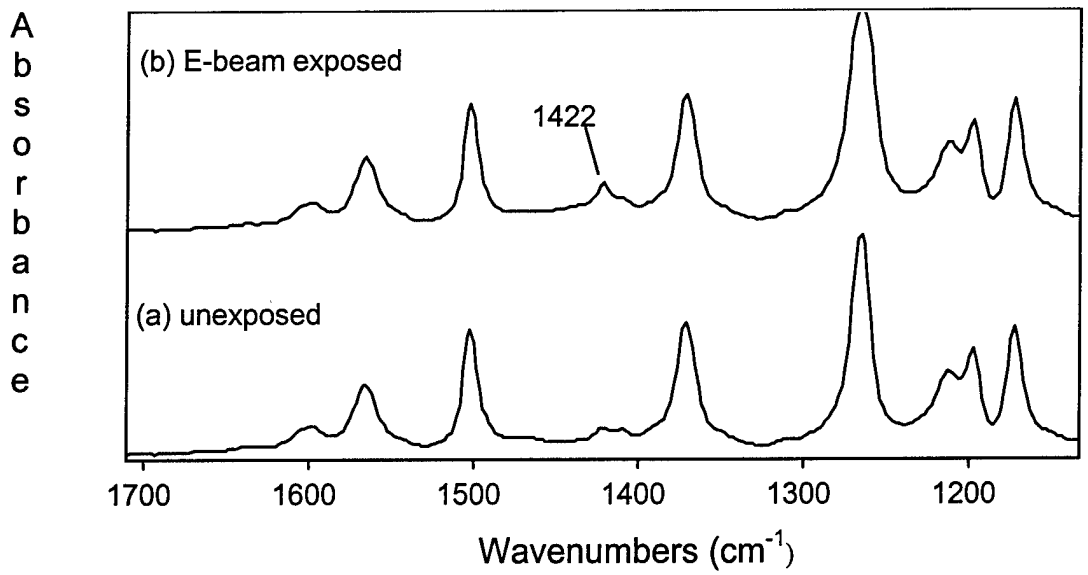

Figure 24. FTIR spectra of (a) unexposed and (b) e-beam exposed cyanate resin with AT-9304 additive. (The increase in band intensity at 1422 cm^{-1} is indicative of reaction of the cyanate endgroups on the resin.)

Series 2

Ultraviolet (UV) Screening of Propargyl and Cyanate Resins

The following resin/sensitizer combinations were chosen for UV cure screening before scheduled e-beam exposures:

- propargyl resin + iodinated (self-sensitized) propargyl resin (50/50 mixture)
- propargyl resin + 10% (w/w) AT-4Br26DM
- propargyl resin + 10% (w/w) AT-9307
- propargyl resin + 10% (w/w) AT-9304
- cyanate resin + 10% (w/w) AT-9307.

Small amounts of preheated (75°C) resins were placed into aluminum weighing dishes. The dishes were placed into plastic bags that were purged with nitrogen. The samples were then exposed to UV radiation generated by a 3 kW mercury arc lamp for 5 minutes at a time. All analyses were qualitative only, spectroscopic analyses of these samples were not performed.

Visual inspection of the samples exposed to UV irradiation indicated no significant changes to most samples, even after 20 minutes exposure. The only samples that indicated any changes (increase in viscosity) were the propargyl resin/AT-9307 and

the cyanate resin/AT-9307. Based on these results, some UV-staged samples of these formulations were prepared for the scheduled e-beam exposure experiment.

Electron Beam Curing Experiment #2

The following resin formulations were used in the electron beam exposure experiment:

- "CAT-B" cationic cure epoxy (1 sample)
- "CAT-M" cationic cure epoxy (1 sample)
- Propargyl resin + iodinated propargyl material (50/50 mixture)
- Propargyl resin + 10% (w/w) AT-4B26DM
- Cyanate resin + 3% (w/w) AT-S-44P (1 sample)
- Cyanate resin + 10% (w/w) AT-9307 (1 sample)
- Cyanate resin + 10% (w/w) AT-9304 (1 sample)
- Propargyl resin + 10% (w/w) AT-9307 (1 sample)
- Propargyl resin + 10% (w/w) AT-9304 (1 sample)
- Cyanate resin + AT-9307, UV staged
- Propargyl resin + AT-9307, UV staged.

Samples were prepared for e-beam exposures in the same manner as described for the section entitled Series 1. The target dose was 10 MRad. The sample tray was placed into a polyethylene bag that was sealed and purged with nitrogen.

Dose Evaluation

Based on the beam parameters, the dose was calculated at approximately 4.9 MRad per pass. Therefore, to achieve the target dose of 10 MRad, two passes would be required. Squares of nylon-based dosimetry film were used to monitor the actual dose received by the samples. Assuming the same film thickness for all films tested, a wide range of doses, 6.8 MRad to 12.5 MRad, was observed. In addition, there was not any pattern to the distribution of doses. This is shown in Figure 25. The doses for Samples 1 and 2 are not reported; the film associated with Sample 1 appeared contaminated with adhesive from the tape used to attach it to the Kapton sheet and that associated with Sample 2 stuck to the Kapton sheet and could not be recovered for analysis.

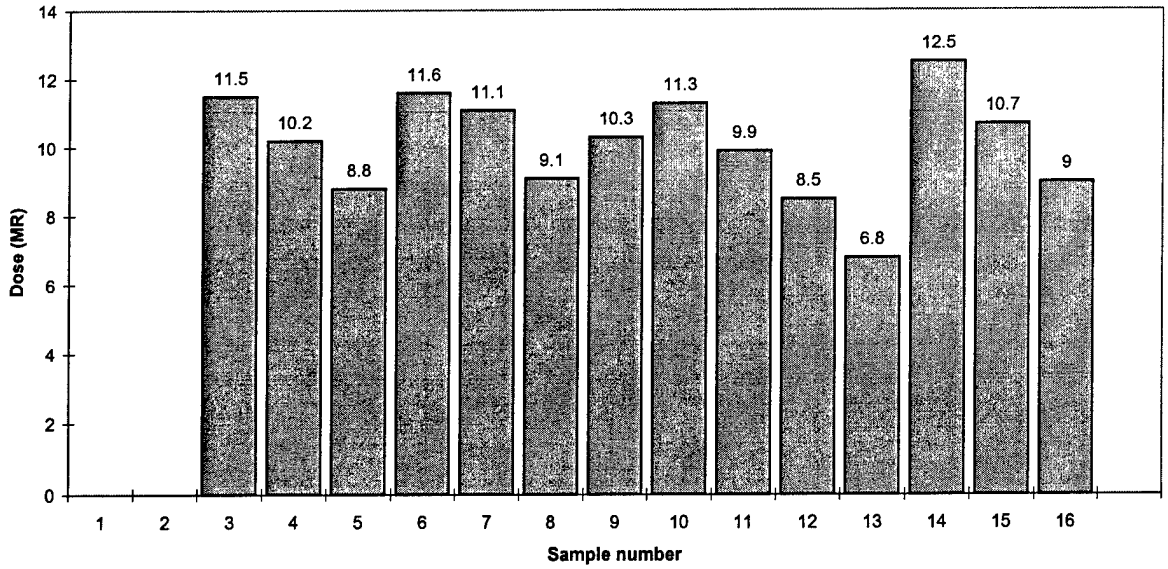

Figure 25. Radiation dose received. Samples 1,5,9, and 13 all lie along the same edge of the mold (left side of Fig. 4). Samples 4,8,12, and 16 lie along the opposite edge.

Taking film thicknesses into account did not have any effect on the measured uniformity of dosage. The radiation dose remained quite inconsistent over the range of samples. As can be seen in Figure 25, above, it appears that the samples on the edges of the mold received lower radiation dosages than those at the center, perhaps related to the presence of the polyethylene outer bag used in this experiment.

Resin FTIR Analyses

The only samples that exhibited complete or near-complete curing as a result of e-beam exposure were the cationic epoxy systems. Again, the propargyl resin formulations were waxy in texture whereas the cyanate resin formulations remained as high viscosity liquids. As before, FTIR spectroscopic analysis of these samples indicated that some reaction had occurred as a result of electron beam exposure. However, the extents of reaction were not as great as those observed in the first e-beam exposure experiment. It is believed that the most likely reason for the lower extents of reaction was the lower radiation dose used for the second e-beam exposure experiment (avg. 10.1 MRad) relative to the first experiment (14.5 MRad).

Propargyl Resins: All propargyl resin formulations exhibited a decrease in propargyl C—H stretch intensity relative to both aliphatic C—H stretch bands and aromatic C=C stretch bands. The decrease in propargyl intensity relative to aliphatic C—H stretch was most noticeable for the formulations containing AT-9304 (~ 5.1%) and AT-9307 (7.1 - 7.7%). The change for the system containing AT-

4Br26DM was more modest, a decrease in propargyl C—H stretch intensity of around 2% relative to aliphatic C—H intensity was noted for this formulation.

The system containing iodinated material also showed a decrease of approximately 3% in propargyl C—H stretch intensity after e-beam exposure. However, the iodinated material added to the propargyl resin was not really the desired derivative of the propargyl resin. In fact, it appears that the procedure used in an attempt to iodinate the propargyl resin actually resulted in several reactions, including cleavage of the material and complete iodination of the propargyl group. Figure 26 shows the infrared spectrum of the iodinated material as compared with the propargyl parent compound.

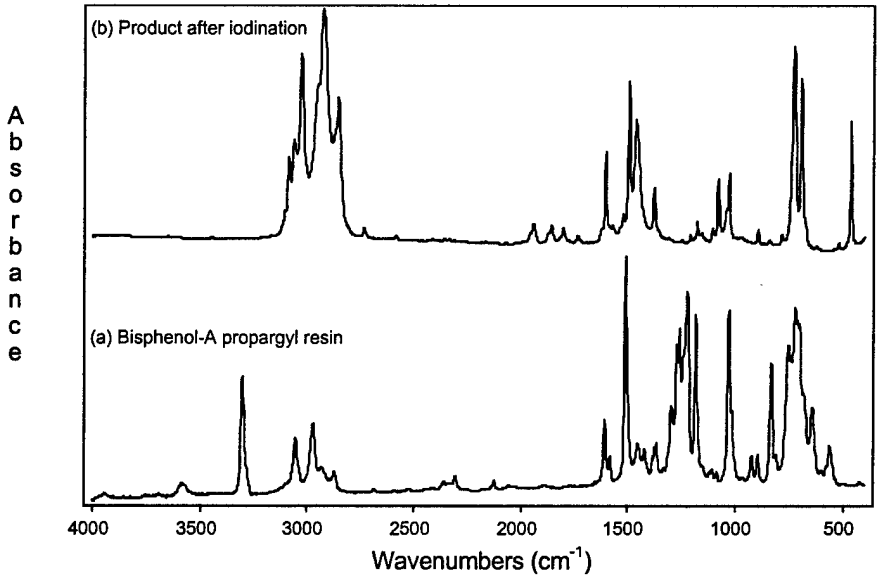

Figure 26. FTIR spectra of (a) Bisphenol-A propargyl resin and (b) the reaction product from iodination. Note the absence of the propargyl C—H stretch band (~3300 cm^{-1}) in the iodinated material.

The infrared spectrum of the iodinated material is far more consistent with the structure of iodobenzene than with the structure of the propargyl resin, leading to the conclusion that the material was in fact cleaved during the iodination process. Additionally, the complete loss of propargyl C—H stretch indicates a loss of the reactive functionality in the system, rendering it inappropriate for use as a large component (50%) in any resin formulation.

Cyanate Resins: Infrared spectra of the cyanate resin formulations containing AT-S-44P or AT-9304 indicated decreasing cyanate C≡≡N intensity relative to the aliphatic C—H stretch bands. The decrease in band intensities were 5.9% for the formulation containing AT-S-44P, and 7.2% for the formulation containing AT-9304. The results for the UV-staged formulation containing AT-9307 were inconclusive.

Table IV summarizes the results of spectroscopic analyses of cyanate ester formulations from both e-beam exposure experiments.

Table IV. Comparison of Cyanate Band Decrease for Two Different E-Beam Doses

	Decrease in C≡N stretch relative to aliphatic C—H stretch	
Additive	**Exposure 1 (14.5 MRad)**	**Exposure 2 (10.1 MRad)**
AT-S-44P	7.8%	5.9%
AT-9304	17.4%	7.2%
AT-9307	19.4%	inconclusive

The cyanate ester/AT-S-44P formulation shows only a very small difference in the extent of reaction for the two different radiation doses. However, the cyanate ester/ AT-9304 formulation shows a much more significant difference in reaction for the two different dosages. While the data for the formulation containing AT-9307 was inconclusive, behavior similar to that of AT-9304 is expected since the overall system chemistry is the same. From these data, it is implied that the AT-S-44P sensitizer is not particularly effective for this system at these dosage levels. The extents of reaction are low, regardless of dose and there does not appear to be a significant enhancement of reaction by increasing the dose. In contrast, both AT-9304 and AT-9307 appear to be much more active in initiating the reaction of the cyanate functionalities, especially at higher radiation dosages.

In-Depth Analysis of Propargyl and Cyanate Systems

NMR Analysis of Propargyl Resins

Due to the inherent ability of NMR to provide detailed structural information, it was believed that a good deal of useful information would become available using this technique. Two propargyl resin formulations, those with AT-4Br26DM and AT-S-44P additives, were analyzed using both proton (^{1}H) and carbon-13 (^{13}C) NMR.

Integration of peaks in proton NMR spectra provides a count of how many protons (H atoms) are present in a given type of chemical environment. For the unreacted propargyl resin, one would expect to see eight protons attributable to the aromatic rings in the structure, six protons attributable to methyl groups, four protons attributable to methylene groups, and two protons attributable to the acetylenic group in the propargyl structure. In the unexposed resin samples analyzed here, there appears to be a significant deficiency of acetylenic protons. The numbers of

aromatic, methyl, and methylene protons, appear to be twice what they should be, based on reaction stoichiometry, leading to the conclusion that there are fewer propargyl functional groups present than expected. In fact, it appears that there are only half as many propargyl groups as there should be.

Given the ability to deduce chemical structure from NMR spectra, one would expect that the identification of contaminants or undesirable functional groups should be fairly straightforward. Incomplete reaction of Bisphenol-A during synthesis was ruled out since infrared spectra showed no evidence of –OH groups that would be characteristic of incomplete reaction. However, the NMR spectra did not show any significant peaks other than those expected based on the resin and sensitizer chemical structures. The use of NMR structure correlation charts [21] proved useful in identifying potential problems. It was suspected that there are a significant number of allyl groups present in the resins. If allyl groups are present, the protons associated with the methylene groups attached to the C=C structure have a resonance frequency virtually identical to that of methylene protons attached to the carbon adjacent to the C≡≡C structure of the propargyl group. The allyl protons also have a high probability of being obscured by other resonances.

Carbon-13 NMR can shed some additional light on structures present in the propargyl resin system. The major advantage of ^{13}C NMR in this case is that a different resonance frequency is observed for each carbon with different chemical linkages.

Figure 27 shows the ^{13}C NMR spectrum of an unexposed sample of the propargyl resin with AT-4BrA-P sensitizer added.

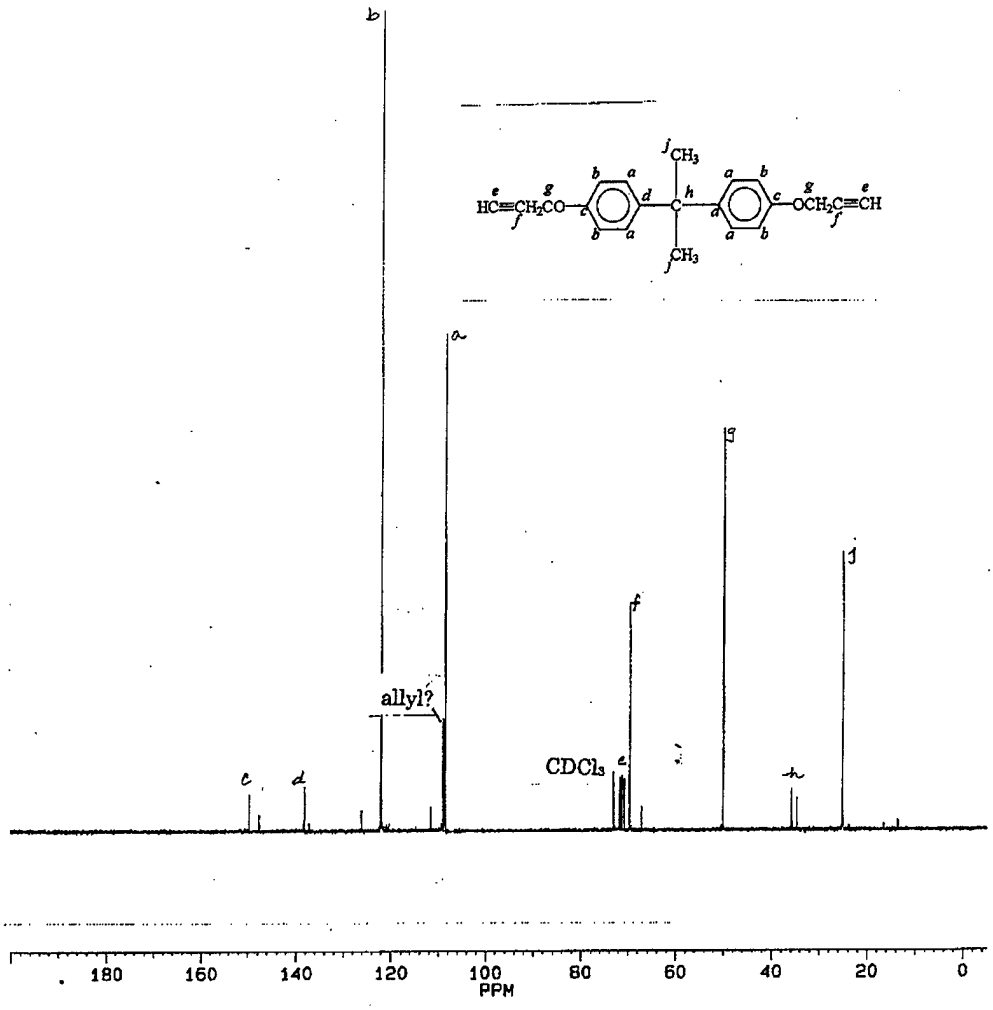

Figure 27. ^{13}C NMR spectrum of propargyl resin with AT-4BrA-P additive. Lettered peak assignments correlate with chemical structure as noted.

There are several small peaks for which assignments were not made. Some of these peaks are associated with the additive. However, there are other, larger peaks that cannot be easily associated with the additive structure. One of these peaks, at approximately 77 ppm, is associated with the deuterated chloroform solvent. Another, at approximately 112 ppm, might possibly be attributed to a carbon associated with an allyl structure.

Whether or not allyl groups were present in the resin samples investigated thus far was extremely important. Allyl groups present as a synthetic impurity would absorb the energy imparted by UV or e-beam irradiation, but would not participate in the energy transfer processes, which we were attempting to exploit to initiate trimerization of the propargyl group. Therefore, the presence of even a small amount of allyl "contamination" would significantly affect propargyl resin cure.

At this point, it was suspected that the propargyl bromide used in synthesizing the resin could be contaminated with a substantial fraction of allyl bromide. Gas chromatography (GC) was used to analyze the propargyl bromide used in syntheses.

GC Analysis of Propargyl Bromide and Propargyl Chloride

Based on the NMR analyses discussed above, determination of the source of double bond contamination was initially undertaken using gas chromatography (GC). GC separates different compounds in a mixture based on any of a variety of chemical properties. Examples of such properties include number of carbon atoms and polarity. Each compound will appear as a peak on a plot (chromatogram), relative amounts of each compound can be determined by integrating the area under the peak.

Propargyl bromide was obtained as a solution in toluene, thus it was expected that the chromatogram should show two peaks for the analyte (one for propargyl bromide and one for toluene) in addition to a peak for the carrier solvent, if any. Instead, approximately six peaks were observed, the identities of which were not determined.

Propargyl chloride could have been substituted for propargyl bromide in any synthetic procedures that were undertaken for this program. Since the propargyl bromide reagent showed a significant number of contaminants, the use of propargyl chloride in synthesis was warranted if the supplied reagent was less contaminated.

GC analysis indicated no apparent contamination of the propargyl chloride reagent. Thus a small amount of propargyl resin and a small amount of AT-S-44P sensitizer were prepared using propargyl chloride instead of propargyl bromide in an attempt to minimize contamination with double bond endgroups (*e.g.*, allyl) that would steal energy from the desired triplet energy transfer polymerization mechanism.

FTIR Analysis of Resin Prepared with Propargyl Chloride

The Bisphenol-A propargyl resin sample prepared with propargyl chloride was analyzed using FTIR spectroscopy as described above. The region from 2250-1950 cm^{-1} was the focus of the data analyses since the band structure can provide clues as to the chemical structures present. The FTIR spectrum of the as-prepared resin is shown in Figure 28.

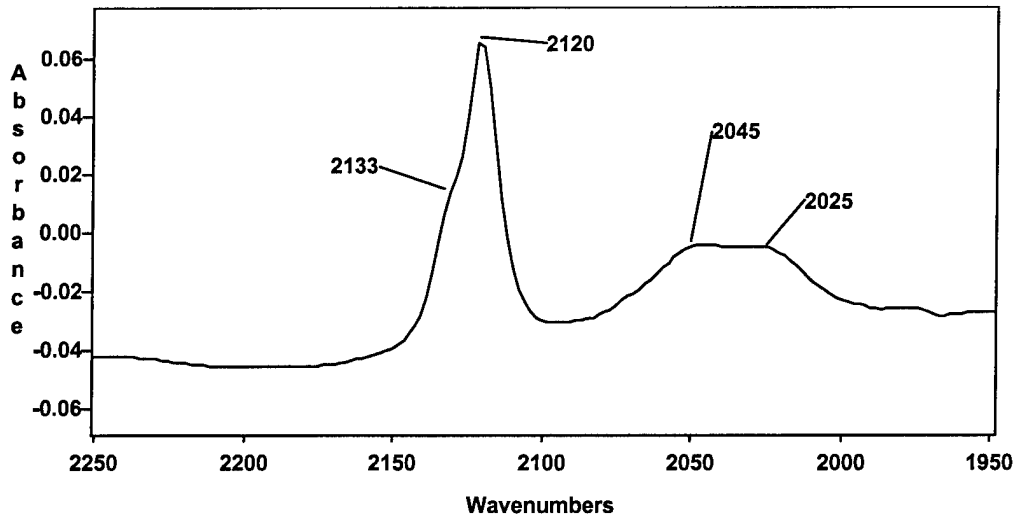

Figure 28. FTIR spectrum, in the region 2250-1950 cm^{-1}, for the Bisphenol-A propargyl resin prepared using propargyl chloride

If the resin were completely pure, two bands would be expected for the C≡≡C stretch in the propargyl endgroup (at 2120 and 2025 cm^{-1}). Instead, four bands are observed, with two of them appearing as shoulders on the other two (desired) bands. The shoulders correspond to an allene, or cumulative double bond structure, which is consistent with the NMR results reported above. Upon further analysis, it was noted that the spectrum of this material, prepared using the much purer propargyl chloride reagent, was virtually identical to that of materials previously prepared using propargyl bromide. Thus, it appears that the major source of double bonds was not from the starting reagents. In fact, we now believe that, since the synthetic reaction is ionic in nature, rearrangements can take place during the course of synthesis to yield allene, or cumulative double bond, structures.

Given this, a means of addressing the presence of double bonds (*e.g.*, removing double bonds) had to be investigated. It is well-known that double bonds are susceptible to free radical reactions; this is the basis for production of many common polymers. Triple bonds, however, are not susceptible to free-radical initiated reactions. Therefore, by adding a free radical initiator to the resin and treating at an appropriate temperature for a short period of time, all double bond structures should react, thus eliminating any interference with the desired polymerization mechanism for triple bonds.

A small amount of benzoyl peroxide (BP) was added to a solution of the Bisphenol-A propargyl resin in methylene chloride. This mixture was then deposited onto a KBr window and the solvent evaporated. The window was then placed into an oven at ~ 105°C (above the melting point of the resin and the decomposition temperature of BP) for approximately 30 min., after which the sample was analyzed using FTIR. The result was a significant reduction in the presence of double bonds. This is shown in Figure 29.

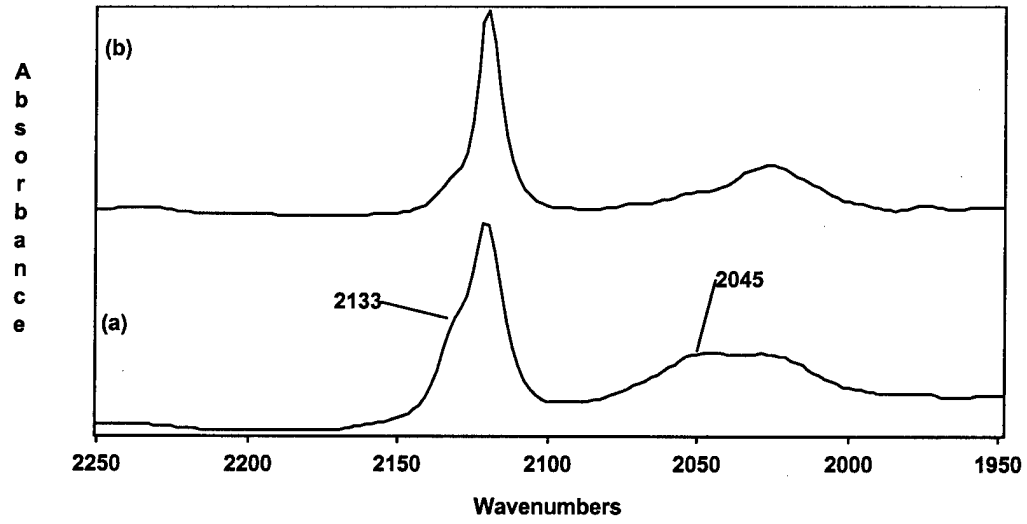

Figure 29. Infrared spectra of Bisphenol-A propargyl resin (a) before and (b) after treatment with benzoyl peroxide at 105°C. Note the significant decrease in bands associated with double bond structures (2133 cm^{-1} and 2045 cm^{-1}).

This sample, with significantly decreased double bond concentration, was then subjected to 30 min. UV irradiation with a 3 kW Hg arc lamp. Subsequent FTIR analysis showed regeneration of the double bond structures (Figure 30).

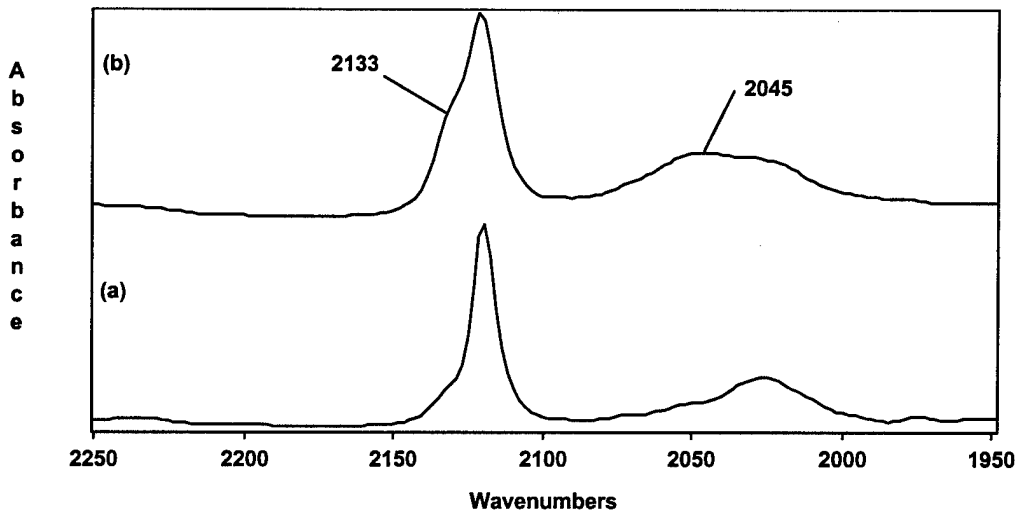

Figure 30. Infrared spectra of Bisphenol-A propargyl resin treated with benzoyl peroxide (a) before and (b) after UV irradiation. Note the regeneration of bands associated with the allene structure.

It is apparent from these data that some sort of photochemical rearrangement was occurring. Since the photochemical processes also persist in radiation chemical events, radiolysis is also expected to result in production of rearrangement structures.

Rearrangement of the propargyl end group structure can occur in the excited singlet state of the molecule, which is generated when the molecule initially absorbs UV or e-beam energy. The probable mechanism for this rearrangement, generating an allenyl (cumulative double bond) structure, is shown in Figure 31.

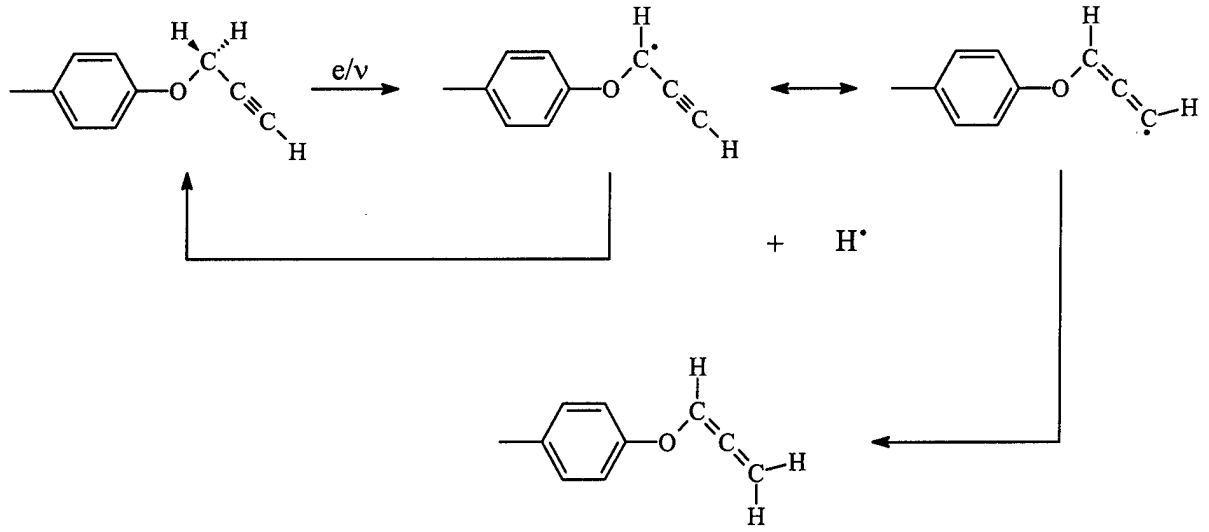

Figure 31. Photochemical rearrangement of propargyl endgroup to yield allene (cumulative double bond) structure

In an ideal situation, the lifetime of the excited singlet state before energy transfer to sensitizer or intersystem crossing to the desired triplet state would be extremely short and the rearrangement of propargyl to allene would be less likely to occur. It is possible to design chemical structures in order to minimize the singlet lifetime. An example of such structural designs is the sensitizer molecules prepared for this program. Figure 32 shows several infrared spectra of the AT-S-44P sensitizer.

Figure 32. Infrared spectra of AT-S-44-P sensitizer in the C≡C stretch region: (a) as-prepared, (b) after treatment with benzoyl peroxide at 100°C, (c) benzoyl peroxide-treated material after 30 min UV irradiation

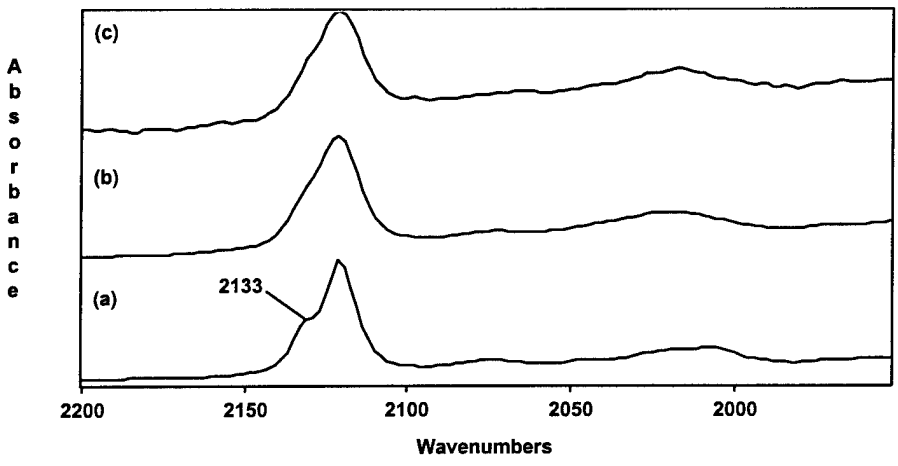

As in the case of the Bisphenol-A propargyl resin system described above, some rearrangement of propargyl endgroups to allene structures does occur during synthesis, thus the treatment with benzoyl peroxide was required to remove double bonds from the as-prepared material. However, in this case, UV irradiation did not regenerate as much allene structure in the sensitizer as was observed for the Bisphenol-A-based propargyl resin. This is because the sensitizer was designed to have a very short singlet lifetime and rearrangements occur in the singlet state.

Detailed FTIR Analysis of Cyanate Resin

After noting the regeneration of double bond structures in the propargyl resin as a result of UV irradiation, a detailed analysis of the cyanate resin was undertaken to see if similar problems could be occurring. Figure 33 shows the C≡≡N stretch region of the infrared spectra of the cyanate resin before and after UV irradiation.

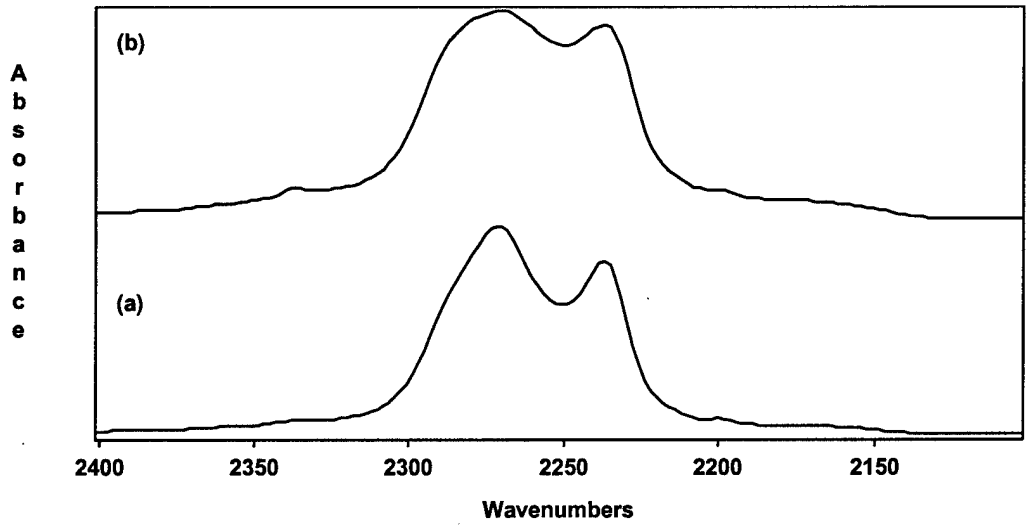

Figure 33. Infrared spectra of the C≡≡N stretch region of the cyanate resin (a) before and (b) after UV irradiation. Note the generation of additional bands as a result of UV exposure.

Again, there is evidence for photochemical rearrangement in the cyanate reactive groups of this resin material. As with the propargyl system, this rearrangement can lead to inhibition of the desired reaction mechanism, in this case the triplet energy transfer polymerization of cyanate functionalities.

Rearrangements in the cyanate case are somewhat different than for the propargyl case; rearrangements here occur from an excited vibrational level that occurs following fluorescence. The mechanism for this rearrangement is shown in Figure 34.

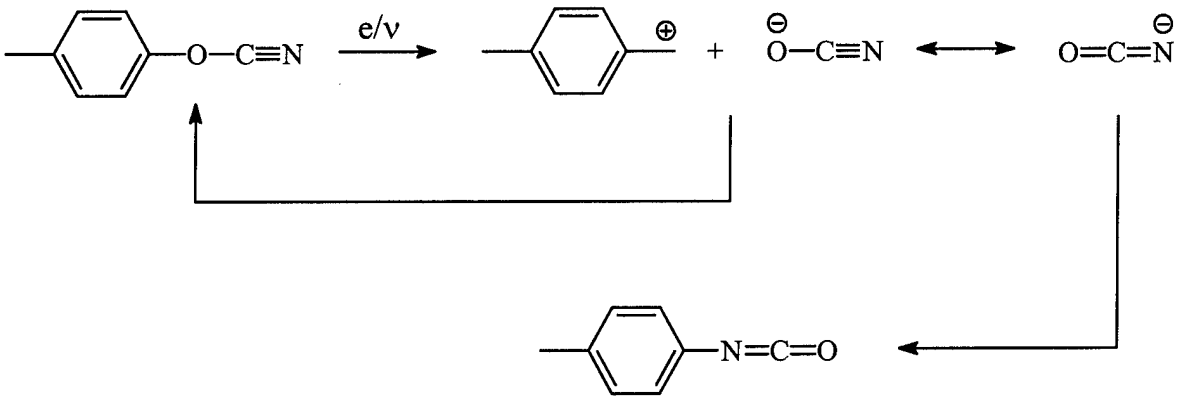

Figure 34. Rearrangement mechanism for cyanate ester endgroup to isocyanate endgroup

Rearrangement structures other than isocyanate are theoretically possible. However, infrared spectra of the cyanate resin before and after UV irradiation show an increase in bands in the 3000 - 3500 cm^{-1} region. This region is associated with O—H and N—H stretching modes; both O—H and N—H structures are consistent with the reaction between *isocyanate* and traces of water found in the resin itself or in the ambient environment. This reaction can occur following rearrangement, but does not occur with the un-rearranged cyanate moiety.

As with the propargyl system, this rearrangement can lead to inhibition of the desired reaction mechanism, in this case the triplet energy transfer polymerization of cyanate functionalities.

Alternative Resins and Model Compounds

The problem of rearrangements in propargyl and cyanate resin structures can be addressed in several different ways. Two of these methods, discussed in the following sections, are minimization of the singlet lifetime and removal of structural elements contributing to rearrangements.

Minimization of Singlet Lifetime

The basic Bisphenol-A resin structure can be modified in such a way that the excited singlet lifetime will be minimized. Shortening the excited state lifetimes may reduce the rearrangement yield and promote the polymerization in much the same way as adding a sensitizer. This can be done by adding heavy atoms, such as bromine, into the structure as shown in Figure 35. Heavy atoms increase intersystem crossing rates to the desired triplet levels in all molecular systems (see Appendix A).

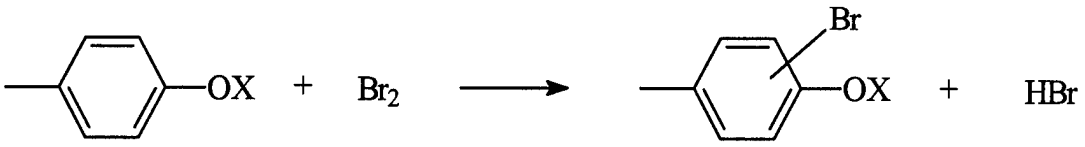

Figure 35. Preparation of resins modified by bromination in order to minimize excited singlet lifetimes, thus inhibiting rearrangements. X can be either -$CH_2C{\equiv}CH$ or $C{\equiv}N$.

The above scheme for preparing these resins is diagrammatic only; synthesis by that method directly from the resin would result in a complex mixture of components, with bromination at the reactive (triple bond) moiety dominating. The most effective method of synthesis likely involves bromination of the Bisphenol-A starting material followed by attachment of the propargyl or cyano functionalities.

The brominated propargyl resin (see Appendix C for synthetic details) was cast onto both a fused silica slide and an infrared window. These cast films were examined both before and after exposure to a 3 kW high-pressure mercury-xenon light source for various times. Infrared spectra in the range 3400 - 2000 cm^{-1} are shown in Figure 36.

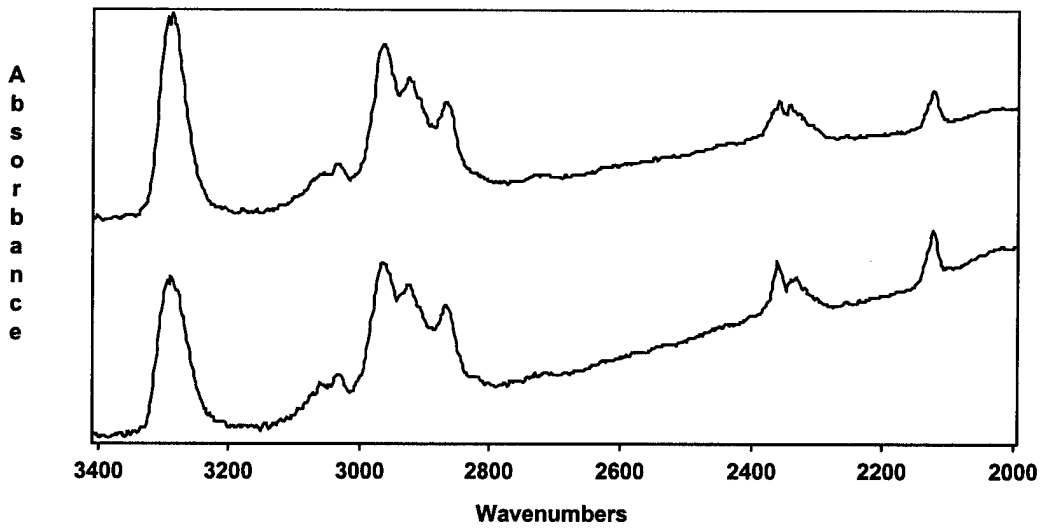

Figure 36. Infrared spectra of unirradiated (bottom) and irradiated (top) brominated Bisphenol-A bispropargyl ether

In these spectra, little change in the spectral shape is shown. It is evident that the intensity of the C—H stretch of the acetylene moiety at 3288 cm^{-1} increased relative to the C—H stretching of the aromatic Bisphenol-A residue. This was a totally unexpected result that suggests that this material is undergoing photo-reaction by a pathway not involving the propargyl acetylenic linkage.

In an attempt to reconcile these observations, the UV spectra before and after exposure were measured. In cases where the infrared spectra become quite complex due to polymerization or multiple substitution of reacting species, an examination of the UV spectral region between 250 and 400 nm can give product structural information. In this spectral region, we examined the nature of electronic transitions rather than the vibrational data from infrared. It is this region of the electromagnetic spectrum where fluorescence from the electronic states contributing to reaction occurs. Both fluorescence and absorption were examined. These spectra are shown in Figure 37.

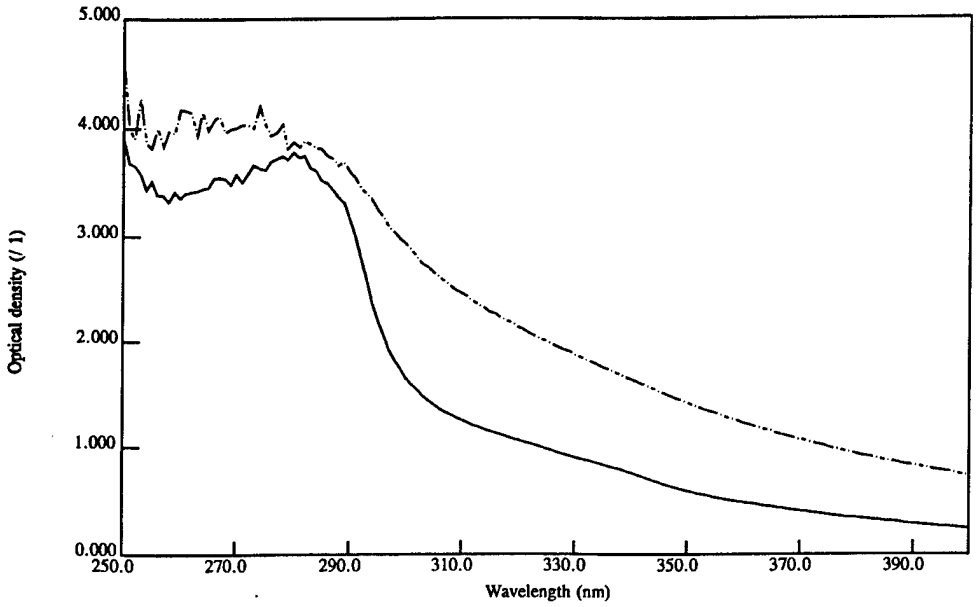

Figure 37. UV spectra of brominated Bisphenol-A before (bottom) and after UV (top) exposure

These spectra seem to confirm that photo-reaction has occurred through the aromatic ring rather than the acetylenic linkage. The reaction has formed species absorbing farther toward the visible with the sacrifice of the benzene-like nucleus (the band near 275 nm). This type of reaction can occur through photo-oxidation of the ring system and may be a result of photo-dissociation of the ring-bromine atom bond.

This method for internal sensitization of the triplet reaction at the acetylene linkage does not appear promising. We have apparently sensitized photo-oxidation rather than the desired polymerization. Photo-oxidation by the apparent route may have resulted in bromine or hydrogen bromide elimination, in either case producing a corrosive product. For these reasons, the heavy atom technique was abandoned for this program.

Nonrearranging Resin Structures

Other means of eliminating rearrangements include more significant changes in the resin structures, such as removing oxygen connecting groups and/or methylene groups connecting the propargyl or cyano functionalities to the parent Bisphenol-A moiety. Examples of structures without oxygen or methylene connecting groups are shown in Figure 38.

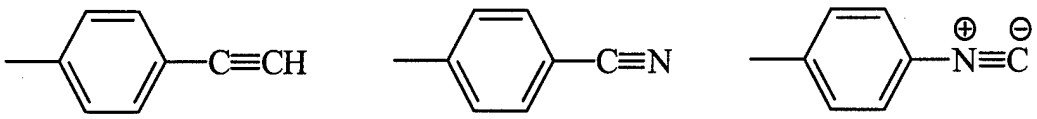

Figure 38. Alternative resin structures potentially not subject to photochemical rearrangement

Phenylacetylene and benzonitrile were chosen as model compounds for photo-polymerization experiments. Both materials are high boiling point liquids containing one of the reactive groups of the resin systems to be simulated (see Figure 38). These materials can be polymerized thermally in the presence of a suitable catalyst and similar catalysts were examined for their photo-polymerization. Resins containing these groups in place of the propargyl or cyanate ester moieties should not exhibit the competing rearrangement reactions yet would still give acceptable materials properties for space qualifiable composites.

Photopolymerization of phenylacetylene

Phenylacetylene is known to polymerize by free radical polymerization, by transition metal catalysis, or by Ziegler-Natta catalysis. Generally, this material polymerizes only to a telomer of around 3,000-10,000 molecular weight in free radical processes due to chain transfer involving the acetylenic hydrogen. Polymerization to only this low polymer would provide a suitable composite matrix in cases where the resin contains two such active functionalities.

Transition metal chelates have been used to catalyze a variety of polymerization reactions. These catalysts act in a variety of modes to effect carbon-carbon and carbon-oxygen-carbon bond formation. Iron (III) acetyl acetonate has been used to catalyze addition reactions to isocyanates and we have shown that iron (II) and manganese (II) acetyl acetonates are also effective catalysts for these types of reactions. Accordingly, we examined these materials as both radiation catalysts for acetylene and cyanate resins and as co-catalysts for epoxy polymerization.

For this study, two transition metal catalysts that have been shown to catalyze reaction of triply bonded species, iron (II) acetyl acetonate (Fe(II) AcAc) and manganese (II) acetyl acetonate (Mn(II) AcAc), were chosen for investigation of

phenylacetylene polymerization. Photochemical activation may be expected to result from the formation of a redox system in the active light (or in an e-beam). Solutions of phenylacetylene containing each of the two catalysts were exposed to the previously used 3 kW mercury-xenon source.

After 15 minutes exposure, a significant amount of polymer was formed in the solution containing Fe(II) AcAc (estimated to be on the order of 5-10% of the original solution). The infrared spectra of the irradiated sample showed definite growth of bands near 1580 and 1526 cm^{-1}, in the region where a system of conjugated double bonds would show additional structure (Figure 39). These bands are indicative of polymerization.

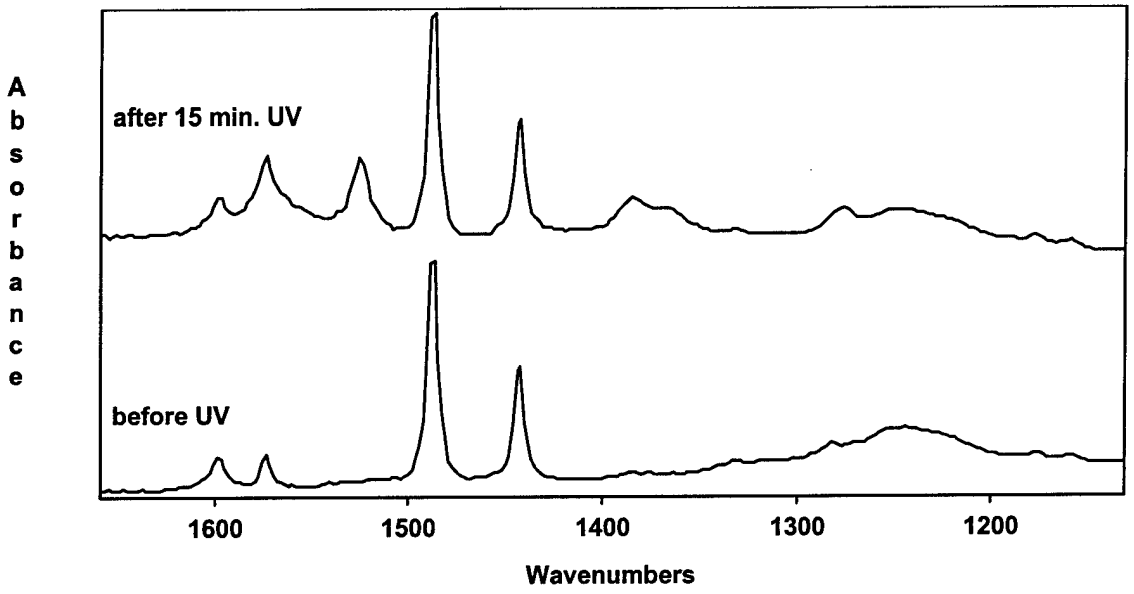

Figure 39. Infrared spectra of phenylacetylene containing Fe(II) AcAc: lower spectrum before UV exposure, upper spectrum after 15 minutes of UV irradiation

A similar solution containing Mn(II) AcAc gave entirely different results. For this catalyst, an apparent decomposition of the catalyst occurred and the spectrum showed the presence of uncomplexed carbonyl, as a strong band at 1801 cm^{-1} (Figure 40). There was no indication of polymerization in the system. Catalyst decomposition had occurred for this solution whereas the previous system showed significant polymerization.

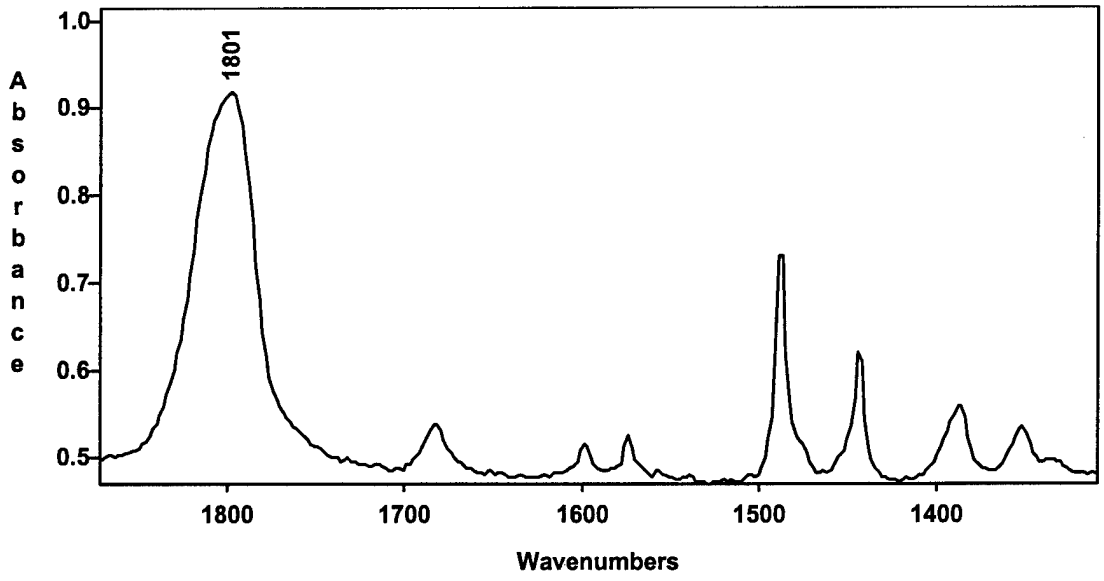

Figure 40. Phenylacetylene containing Mn(II) AcAc after 15 minutes UV irradiation

Photopolymerization of benzonitrile

Solutions of the same two catalysts in benzonitrile were also photolyzed to determine if this material undergoes polymerization. Figure 41 shows the result of photolysis of the solution of Fe(II) AcAc in benzonitrile.

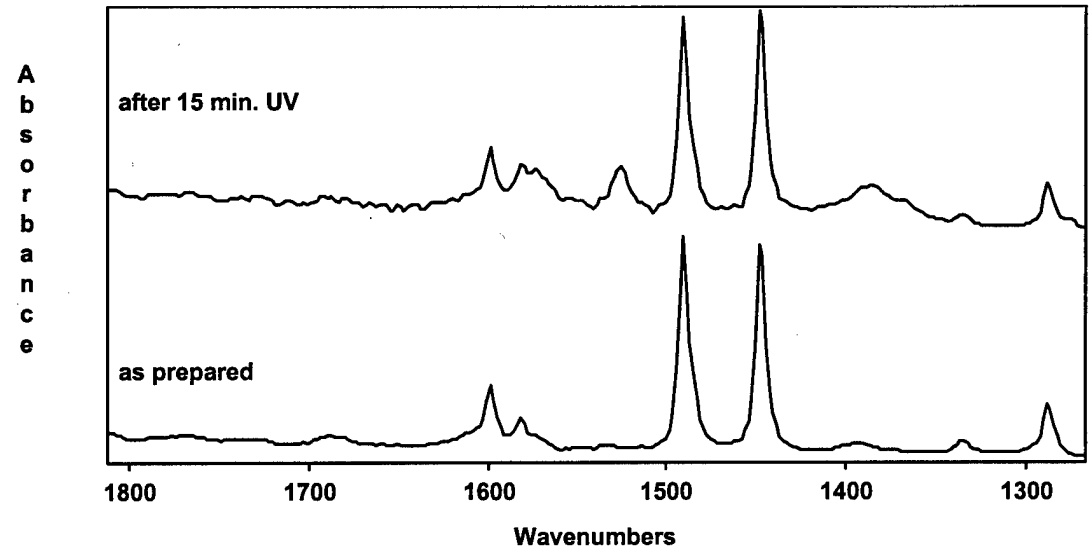

Figure 41. Infrared spectra of benzonitrile containing Fe(II) AcAc, lower curve as prepared, upper curve after 15 minute UV

As in the previous experiments with phenylacetylene, some polymerization is indicated. For the Mn(II) AcAc, less activity was shown and catalyst decomposition occurred, as before.

It appears that these catalysts can form active species upon irradiation with UV, which result in monomer polymerization. In both cases, the iron (II) catalyst is the more active.

Bis(ethynyl) endcapped resin material

Based on the results from the model compound studies, synthesis and polymerization of a bis(ethynyl) resin, bis(4-ethynylphenyl)methane, was attempted. Two synthetic procedures were attempted: a standard Friedel-Crafts alkylation in dichloromethane with aluminum chloride as the catalyst, and alkylation using a Resole phenolic resin preparation procedure.

The standard Friedel-Crafts alkylation gave a very violent reaction on adding aluminum chloride to a solution of the reactants, (dichloromethane and ethynylbenzene) even in the presence of a moderating solvent, heptane. The initial material was a dark colored precipitate suspended in the solvent. This reaction mixture was treated with 50% hydrochloric acid to dissociate the chloroaluminate complex and dissolve the inorganic product. This mixture was filtered and the water insoluble product dried and examined in the IR as a film on sodium chloride plates. This IR spectrum indicated that the acetylenic C—H bond had been completely eliminated and that a carbonyl linkage had been incorporated into the molecule. The spectrum compared well with that of cinnamaldehyde with some additional aliphatic C—H and suggests that this product has resulted from coupling of two of the ethynylbenzene moieties through the ethynyl group. This synthetic method was abandoned.

In the second synthesis, a method used for the preparation of Resole phenolic resins was used. The IR spectrum of the product material was taken and compared with that of ethynylbenzene. This material appears to have given the desired coupled ethynylbenzene product through a methylene bridge, but consists of a mixture of isomers. This product was not evaluated using UV photolysis, but was used instead in e-beam irradiation experiments.

In the e-beam experiments, some polymerization was noted using a formulation containing 2% Fe(II) AcAc in the neat resin. Only a very small amount of reaction had occurred at an exposure dose of 15 MR. While this experiment did provide guidance for future resin formulation, the yield was not sufficient to qualify the resin or sensitizer/catalyst for further study.

An attempt was made to initiate polymerization of the acetylene resin using a cationic initiator, a diaryl iodonium salt sometimes used in epoxy initiation. No polymer was formed from the bisacetylene with this initiator under e-beam irradiation. These results are summarized below.

The two bis(ethynyl) resin samples exposed in this experiment did not physically show any evidence of polymerization. The viscosity of the samples both before and

after exposure was extremely low. Infrared spectroscopic analysis of the samples also indicates that very little reaction occurred in these resins as a result of e-beam exposure. Figure 42 and Figure 43 show the infrared spectra of the two different bis(ethynyl) resin formulations both before and after irradiation. Spectral differences arising from polymerization would be expected in the acetylenic C—H stretch region (~3100 cm^{-1}) and in the acetylenic C≡≡C stretch region (~2100 cm^{-1}). These spectra indicate very little difference between the control and irradiated materials in these regions, corresponding to very little polymerization occurring in the system.

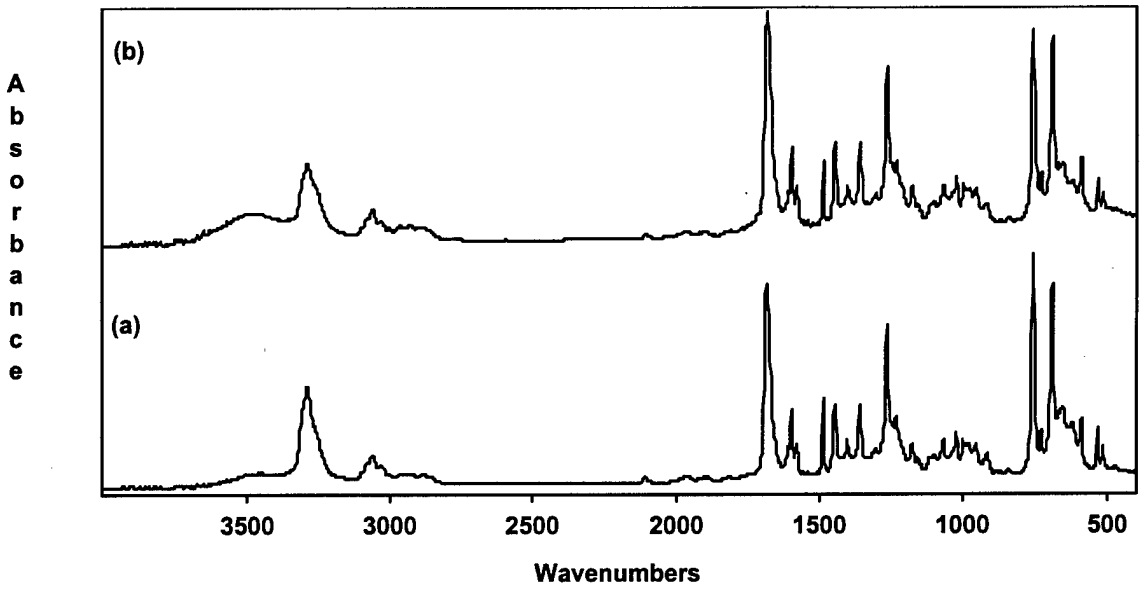

Figure 42. Infrared spectra of the bis(ethynyl) resin with Fe(II) AcAc initiator (a) before and (b) after irradiation

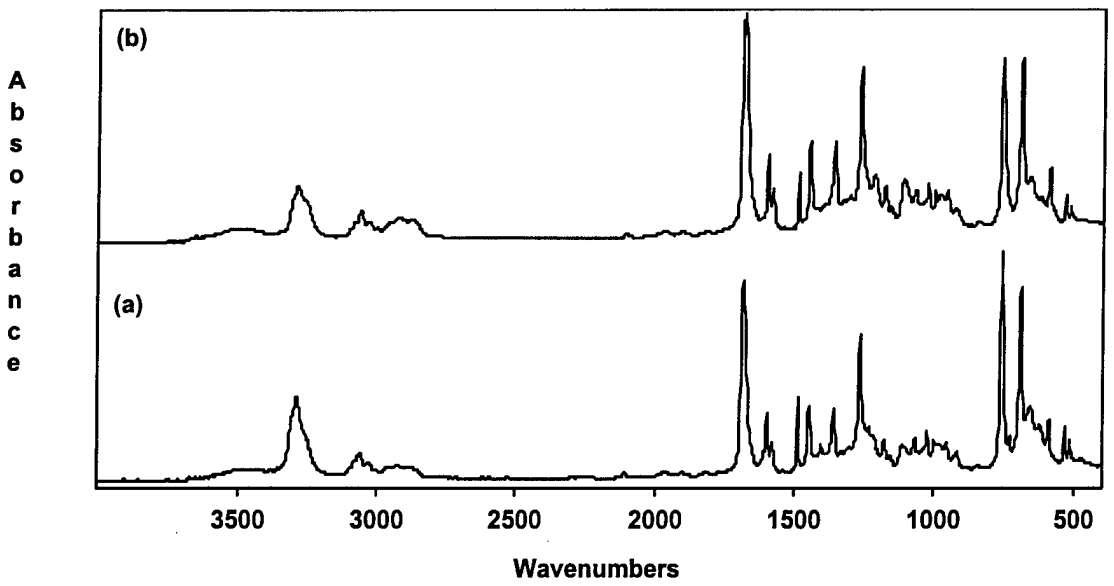

Figure 43. Infrared spectra of the bis(ethynyl) resin with DPI-1 initiator (a) before and (b) after irradiation

The absence of significant polymerization of ethynyl resins and resin precursors in these experiments indicates that these initiators are ineffective but does not eliminate similar initiators from contention. Later study of the spectra of phenylacetylene suggests that they may have partial positive charge on the acetylene moiety and thus be inactive for cationic initiation. Transition metal complex catalysis is probably possible, but the choice of metal and complex is wide and further examination was not possible. A complex that is activated by ionizing radiation may be effective for the proper choice of metal ion, oxidation state, and complexing ligand; the variations are nearly limitless and an Edisonian approach is indicated.

Cationic Epoxy Systems

With the failure to effectively polymerize acetylene or cyanate resins under low temperature photo- or radiation chemical excitation with either sensitizers, photo-catalysts or ionic initiators, cationically initiated epoxy systems were examined as possible subambient curing resins.

Initial Evaluation

Four cationic epoxy systems were chosen for initial evaluation. The following resins were formulated and exposed to target doses of 5, 10 and 15 MRad. DPI-1 was obtained from Applied Poleramic and Fe(II) AcAc was synthesized at Adherent Technologies. As mentioned earlier, transition metal catalysts such as Fe(II) AcAc are often used to effect carbon-carbon and carbon-oxygen-carbon bond formation.

- EPON ® 826 with 2% (w/w) Cyracure ™ 6974 (826/6874)
- EPON ® 826 with 2% (w/w) Cyracure ™ 6974 and 0.5% (w/w) Fe (II) AcAc (826/6974/AcAc)
- CAT-B standard commercial formulation
- CAT-B with 0.5% (w/w) Fe(II) AcAc (CAT-B/AcAc).

Exposed samples were analyzed using differential scanning calorimetry (DSC). Residual cure exotherms were monitored for all samples and in cases where the resins appeared to have fully polymerized, glass transition temperatures (T_gs) were determined if possible.

In the case of the EPON ® 826/Cyracure 6974 formulations, it was found that complete cure could be obtained with a very low dose of e-beam radiation. Residual cure exotherms were indistinguishable on the DSC thermograms for all irradiated samples. CAT-B also exhibited a high degree of cure, in excess of 90% completion at both 10 MRad and 15 MRad dose; the degree of cure obtained using a 5 MRad radiation dose was not readily determined due to the complexity of the DSC thermogram. The glass transition temperatures (T_gs) of both resin systems were high, around 210-215°C for the 826/6974 system and approximately 230°C for the CAT-B system. These T_gs are in good agreement with those reported in Refs. 8-10.

In contrast, neither of the two systems containing Fe(II) AcAc cured completely, even at higher radiation doses. In fact, none of the 826/6974 samples with Fe(II) AcAc system cured to hardness; they were all in the form of viscous liquids. The CAT-B samples with Fe(II) AcAc, however, did cure to hardness; T_gs of the CAT-B/AcAc samples were similar to those observed for the standard CAT-B formulation.

The Fe(II) AcAc added to two of the formulations appears to interfere with cationic initiation in those formulations. It is probable that the acetyl acetonate catalysts, which are active in other polymerizations to promote carbon-oxygen-carbon bonding, act here to intercept the cation that initiates chain polymerization. Therefore, the use of these catalysts was discontinued for the remainder of the work with these cationically-initiated epoxy systems.

Final Resin Evaluation

A final set of resin formulations was then selected for evaluation with the purpose of evaluating the effects of several variables on e-beam curing of cationic epoxies. These resin formulations were:

- EPON ® 826 with 2% Cyracure ™ 6974 (826/6974)

- EPON ® 826 with 2% DPI-1 (826/DPI-1)
- EPON ® 828 with 2% Cyracure ™ 6974 (828/6974)
- EPON ® 828 with 2% DPI-1 (828/DPI-1)
- CAT-B base resin (supplied w/ no initiators) with 2% Cyracure ™ 6974 (CAT-Base/6974)
- CAT-B base resin with 2% DPI-1 (CAT-Base/DPI-1)
- EPON ® 826 with 2% DPI-1, filled with 15% (w/w) cabosil (826/DPI-1/cab)
- EPON ® 828 with 2% Cyracure ™ 6974 and 15% (w/w) cabosil (828/6974/cab)
- EPON ® 828 with 2% DPI-1 and 15% (w/w) cabosil (828/DPI-1/cab)
- CAT-B base with 2% Cyracure™ 6974 and 15% (w/w) cabosil (CAT-Base/6974/cab)
- CAT-B base with 2% Cyracure™ 6974 and 3% (w/w) carbon black (CAT-Base/6974/CB).

Variables evaluated were resin viscosity, radiation dose, and filler effects. Glass transition temperatures and residual cure exotherms were determined using DSC, as described previously. Flexural strengths of the cured resin samples were determined using the three-point flex test as outlined in ASTM D790.

Results of the testing for the unfilled resin samples are summarized in Tables V and VI. The results given in Tables V and VI are discussed in the following sections.

Viscosity Effects

EPON® 826 and 828 epoxy resins have similar chemical structures, but different molecular weights of the resin material; 826 is a much lower viscosity resin than is 828. When the 6974 initiator is used, it appears that there is little difference in the curability of the resins based on viscosity considerations alone. T_gs are in the range expected for these systems when a cationic polymerization mechanism is used (see EPON ® product literature 826 or 828 cured with BF_3-monoethylamine). The CAT-Base, however, is a much more viscous resin than either of the two EPON ® resins evaluated. When the 6974 initiator was used, both the 5 MRad and 10 MRad samples showed significant residual cure exotherms; degrees of cure were 83% and 95%, respectively. Only the 15 MRad sample showed no residual cure exotherm.

Table V. Thermal Data for Cationic-Cured Epoxy Systems with Cyracure ™ 6974 Initiator

Sample (Dose [MRad])	T_g (°C)	Exo. Onset (°C)	ΔH (J/g)	% Cure
826/6974 control	--	357.72	422.58	--
826/6974 (5)	~212			
826/6974 (10)	~215			
826/6974 (15)	~210			
828/6974 control	--	368.2	534.17	--
828/6974 (5)	206.56			
828/6974 (10)	212.42			
CAT-Base/6974 control	--	310.1	456.64	--
CAT-Base/6974 (5)	211.95	296.11	77.5	83.03
CAT-Base/6974 (10)	212.69	295.44	22.13	95.2
CAT-Base/6974 (15)	201.82			

Use of the DPI-1 initiator results in an incomplete cure for the 828 system dosed at 5 MRad; cure was complete for this system at 10 MRad. Both the 826/DPI-1 and CAT-Base/DPI-1 systems exhibited complete cure at both 5 MRad and 10 MRad. Slightly lower T_gs were noted for the DPI-1 initiated EPON ® systems. In contrast, T_gs for the CAT-Base/DPI-1 system appear to be largely in agreement with those observed for the CAT-Base/6974 systems.

Based on these data, it appears that resin viscosity may have a small effect on e-beam initiated polymerizations in these epoxy systems. The effect is somewhat more significant when the 6974 initiator is used.

Table VI. Thermal Data for Cationic-Cured Epoxy Systems with DPI-1 Initiator

Sample (Dose [MRad])	T_g (°C)	Exo. Onset (°C)	ΔH (J/g)	% Cure
826/DPI-1 control	--	214.95	445.26	--
826/DPI-1 (5)	187.8			
826/DPI-1 (10)	175.37			
828/DPI-1 control	--	215.62	448.102	--
828/DPI-1 (5)	174.74	80.75	46.973	89.5
828/DPI-1 (10)	173.67			
828/DPI-1 (15)	170.69			
CAT-Base/DPI-1 control	--	173.68	391.397	--
CAT-Base/DPI-1 (5)	221.02			
CAT-Base/DPI-1 (10)	198.82			

Radiation Dose Effects

At first glance, it appears that, in order to ensure full cure of the resin system, it would be advisable to choose a higher radiation dose. However, the case is not that simple. Table VII shows glass transition temperatures, flexural strength, and flexural modulus data for all resins evaluated.

Table VII. Glass Transitions and Mechanical Data for Cationic Epoxy Systems

Sample	Dose (MRad)	T_g (°C)	Flexural Strength (psi)	Flexural Modulus (psi)
828/6974	5	206.56		405888
828/6974	10	212.42	21540	363552
CAT-Base/6974	5	211.95	13756	1118356
CAT- Base/6974	15	201.82	15582	447605
828/DPI-1	5	174.74	15623	353143
828/DPI-1	10		5284	225181
828/DPI-1	15	170.69	7527	325184
CAT-Base/DPI-1	5	221.02	4515	231991
CAT-Base/DPI-1	10	198.82	8416	194334

The data given in Table VII indicate that the resins cured at higher dose have lower moduli and lower T_gs than the resins cured at the lower doses. This is despite the fact that some of the lower dose samples did not exhibit complete cure. This trend is particularly obvious in cases where DPI-1 is used as the initiator. Note that there is a 50% drop in flexural strength between the 828/DPI-1 samples cured at 5 MRad and 15 MRad. Likewise, there is a 23°C drop in the T_g for the CAT-Base/DPI-1 samples cured at 5 MRad and 10 MRad.

We believe that the origin of this trend lies primarily in the initiator chemistry, although the resin chemistry itself may also be a factor. Degradation of properties appears to be more significant for the CAT-Base formulations than for the 828 formulations. Figure 44 shows the degradation mechanisms for the two general types of initiators under investigation here.

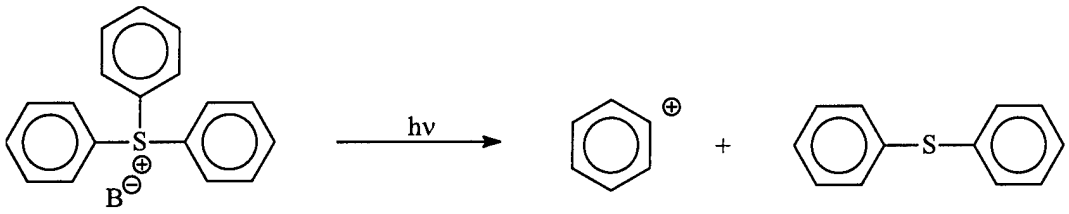

(a)

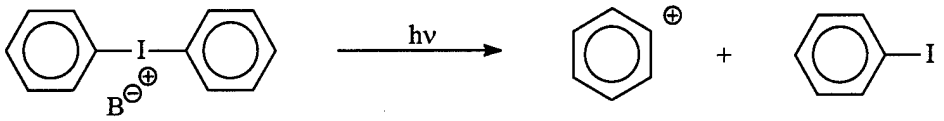

(b)

Figure 44. Radiation-induced dissociation of (a) triaryl sulfonium salt initiators, such as Cyracure™ 6974 and (b) diaryl iodonium salt initiators, such as DPI-1

The degradation products from these two materials may have a significant effect when it comes to considering radiation damage in these epoxy systems. In the case of the 6974 initiator, a triaryl sulfonium salt, one of the by-products is a diaryl sulfide, which may be expected to act as a radiation *stabilizer* in the cured system (see Appendix A for a discussion of stabilization). In contrast, the DPI-1 initiator is a diaryl *iodonium* salt. The by-product of concern here is an iodobenzene-like compound, which is unlikely to protect the cured system from radiation damage. Additionally, this by-product (iodobenzene) is a liquid that will plasticize the system (leading to the observed decrease in T_g) and could lead to significant (and undesirable) outgassing in the final products.

Filler Effects

The final variable to be evaluated was the effect of fillers on e-beam cure. Two fillers were tested: cabosil, a silica filler and carbon black. Cabosil was loaded into the resin at a concentration of 15% (w/w), whereas carbon black could only be loaded to a concentration of 3% (w/w). All samples showed a high degree of cure; residual cure exotherms were virtually undetectable using DSC. All samples were then tested for flexural strength and modulus as described previously.

Samples filled with cabosil showed a decrease in both flexural strength and flexural modulus relative to unfilled samples. In the case of carbon black, only one sample was able to undergo mechanical testing, the others broke before testing could take place. This sample showed a dramatic increase in modulus, as expected. The strength, however, showed a dramatic decrease; around 50% of the strength was lost relative to the unfilled resin.

It may be that the filler is interacting with the cationic initiation by surface termination or neutralization of the ion. Adsorbed water on the filler could intercept the propagating or initiating cation to form a hydroxyl termination. Interfacial considerations (*e.g.*, adhesion) may also have a significant effect.

Composite Fabrication and Characterization

Details of the experimental procedures for composite fabrication and testing are given in Appendix D. The panel with the resin formulation containing Fe(II) AcAc was a bit sticky to the touch, whereas the other panels were smooth and appeared well cured. This qualitative observation is consistent with the results discussed above for the resin plaques. That is, the resin formulations containing Fe(II) AcAc in addition to another cationic initiator did not polymerize as completely as the comparable material without Fe(II) AcAc. It is probable that the acetyl acetonate catalysts, which are active in other polymerizations to promote carbon-oxygen-carbon bonding, act here to intercept the cation, which initiates chain polymerization.

Difficulties were encountered throughout the composite curing studies with pressure application during the e-beam exposures. The first set of unidirectional 10 cm x 10 cm plates did not consolidate because the tolerances between the pressure application plates and the mold recepticals were too tight, causing the pressure plates to hang up. The resulting composite plates were too porous to test. Subsequent 10 cm x 10 cm plates were fabricated with smaller pressure plates, which alievated the uneven pressure application problem. Results from the unidirectional screening tests and quasi-isotropic fabrication trials are given in the following sections.

Unidirectional Screening Tests

Three variations on matrix resin formulation including subambient cure (-20°C) were included in the screening tests. The 10 x 10 cm composites fabricated were of general good quality; however, they were not as well consolidated as the thermally cured composite and were of lower fiber volume fraction. An attempt to cure a 20 x 20 cm plate without a pressure plate resulted in a uneven consolidation across the composite surface. The 20 x 20 cm plates using the thin aluminum pressure plates did not consolidate fully in the center, rather, the pressure plates bent causing a

gradient in thickness from the edges to the center of the composite laminates. Characterization data for the unidirectional laminates is given in Table VIII.

Table VIII. Characterization Data for Unidirectional Composites

Composite Matrix/Cure	Appearance	Fiber Volume, %	% Void Volume	T_g,, °C	% Cure
828/6974[1] 23°C	Generally good Some surface voids	50	< 2	191.5	100
828/DPI[1] ATI-9305E 23°C	Generally good Poorly consolidated	37	<2	180	100
828/DPI[1] 23°C	Generally good Some dry surface areas	53	< 2	NO[3]	100
828/6974[2] 23°C	Wavy surface Poorly consolidated	30	5-10	NO	100
828/6974[2] -20°C	Tapered from edges to center,	48	2-5	194.6	100
828/BF_3-MEA 188°C	Smooth, flat, and well consolidated	55	< 1	NO	66

1. 10x10 cm.
2. 20x20 cm.
3. Not observed.

The data given in Table VIII show that the composites cured with the electron beam, including the subambient cured laminate, displayed 100% cure. Curiously, the thermally cured laminate showed a residual exotherm indicating that cure was not complete. Four hours at 188°C should be adequate to fully cure that system. Future use of that chemistry should require a free standing post cure. The data in Table VIII also show that the e-beam cured laminates are generally low in fiber volume due to problems with pressure application during cure. It is recommended that future fabrication efforts use a stiffer pressure application plate to solve the consolidation problems.

Mechanical test data for the composites listed in Table I are given in Figures 45 through 49. The three data sets shown on the left side of the graphs correspond to the 10 x 10 cm plates, while the two sets on the right correspond to the 20 x 20 cm plates with the thermally cured data in the center.

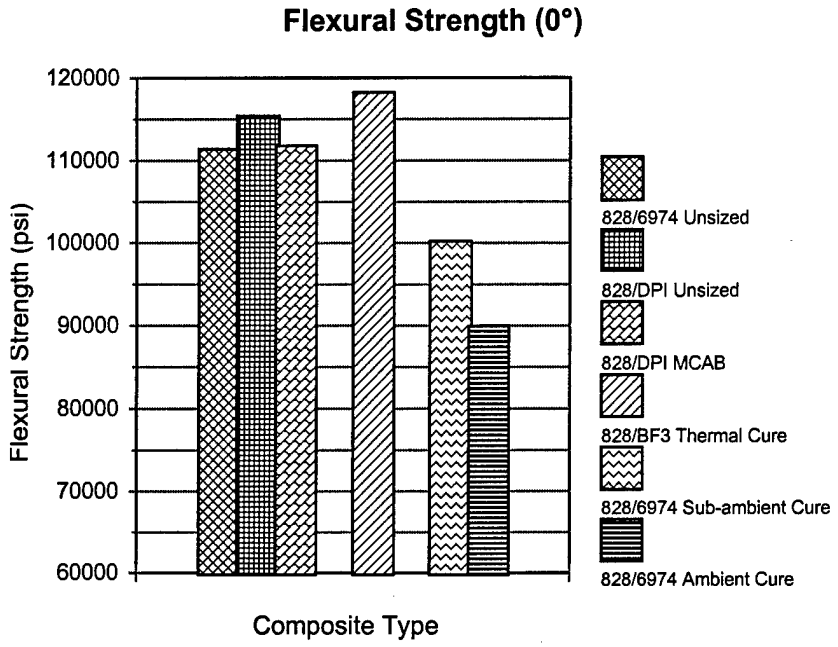

Figure 45. Longitudinal flexural strength of e-beam cured composites

The longitudinal flexural strenth data given in *Figure 45* show that the e-beam cured laminates at ambient temperature are equivalent to the thermally cured composite and that the subambient cured laminate shows an approximately 10% lower strength. The effect of the high void content and low fiber volume fraction of the 20 x 20 cm ambient cured plate is evident in its overall lower tensile strength (20%).

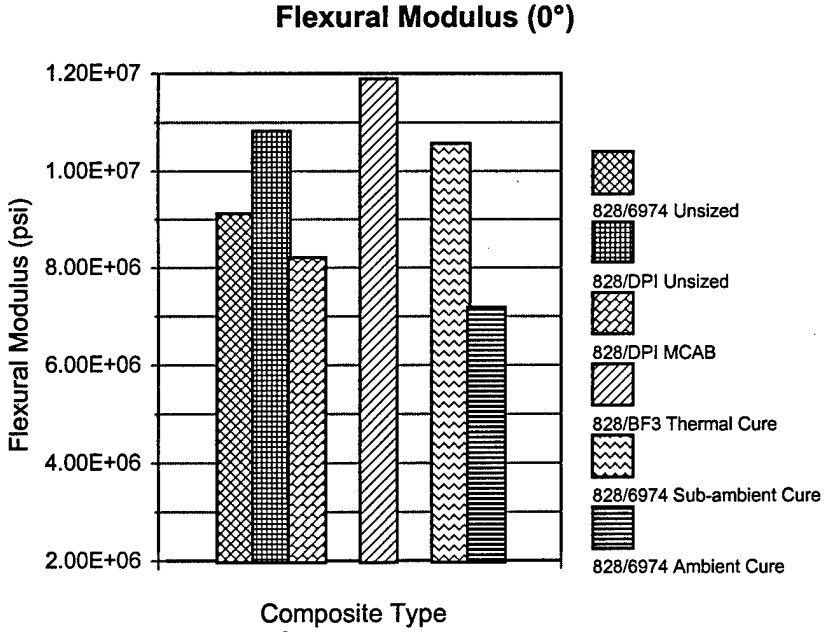

Figure 46. Longitudinal flexural modulus of e-beam cured composites

The longitudinal flexural moduli given in Figure 46 show the expected dependence on fiber volume fraction with the e-beam cured plates lower than the thermally cured composite. It is encouraging to note that the subambient cured composite modulus is only about 10% less than the thermally cured composite.

The short beam shear results given in Figure 47 show that the DPI cured composites are equivalent to that seen with the thermally cured laminate. The subambient laminate shear strength is only 4% below the thermally cured laminate. The cause of the low shear strength for the 10 x 10 cm 828/6974 matrix laminate is unknown.

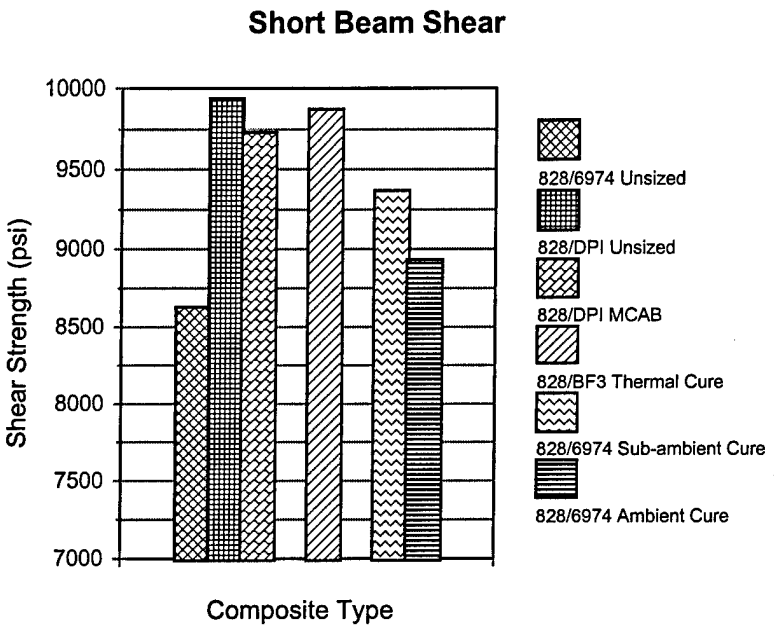

Figure 47. Short beam shear strengths of e-beam cured laminates

Transverse flexural strengths and moduli given in Figures 48 and 49 show much higher values for the thermally cured laminate compared to the e-beam cured composites. That is expected from the higher fiber volume fraction and superior quality produced by the hot press molding technique. The e-beam cured laminate with the reactive finish does show superior strength compared to the other e-beam cured materials. That improvement may be due to superior bonding at the interface or to better surface quality. Additional work is needed to determine the value of the reactive finish for e-beam cured composites.

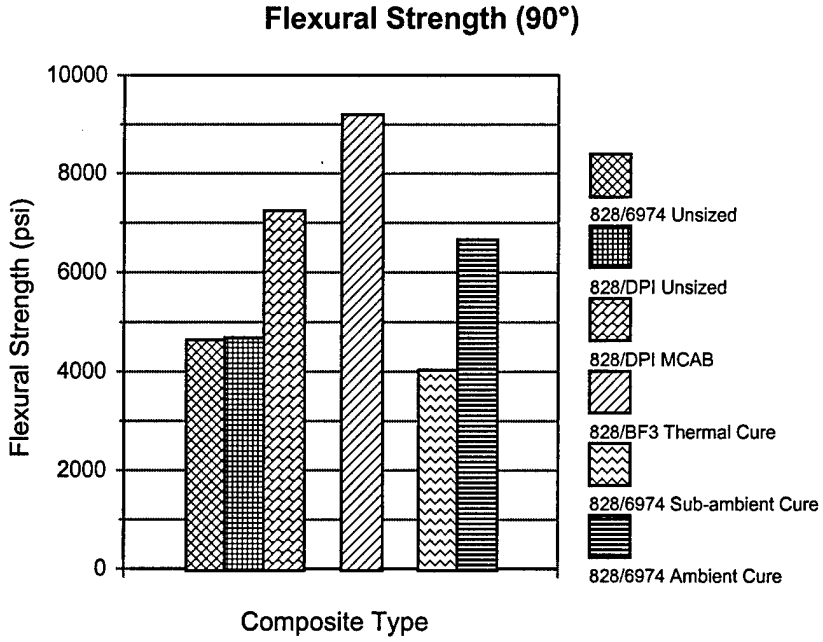

Figure 48. Transverse flexural strength of e-beam cured composites

In general, the unidirectional composite data show that, when optimized, e-beam curing should provide composites with equivalent or better properties than thermal curing. Subambient curing in particular should provide substantial benefits in terms of lower residual stresses and zero stress temperature nearer to operating temperature for space applications. Based on the data given in Figures 45 through 49 and Table VIII, the 828/6974 matrix system was chosen for use with the quasi-isotropic laminates discussed in the following section.

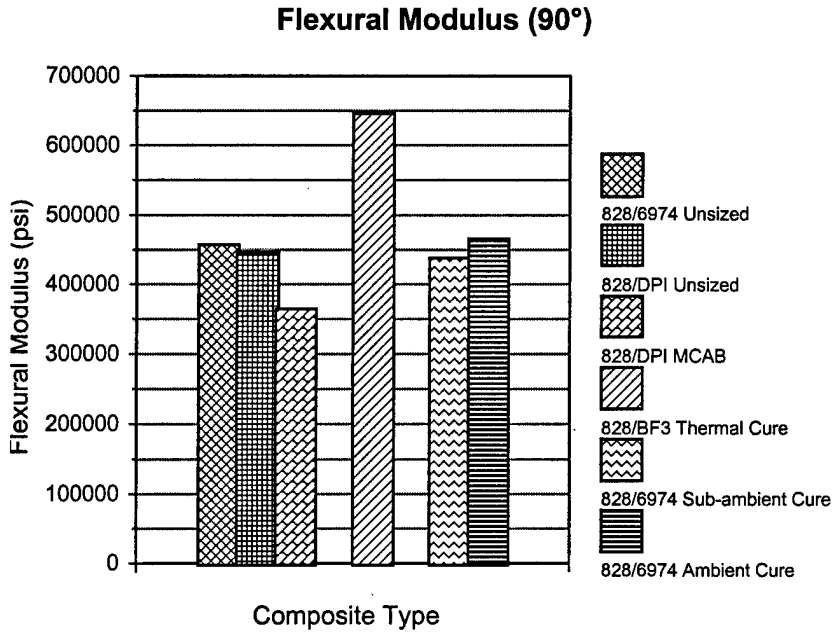

Figure 49. Transverse flexural modulus of e-beam cured composites

Quasi-isotropic Composite Characterization

Three different cure temperatures were examined with the quasi-isotropic $[90/+45/-45/0]_{2s}$ laminates, one ambient and two subambient. Characterization data for the quasi-isotropic laminates is given in Table IX.

Table IX. Characterization Data for Quasi-isotropic Composites

Cure Temperature	Appearance	Fiber Volume, %	% Void Volume	$T_{g,}$ °C	% Cure
23°C	Tapered Some surface voids	50	< 2	187.7	100
-20°C	Tapered Some surface voids	50	< 2	192.3	100
< -30°C	Tapered Some surface voids	50	< 2	193.8	100
-20°C*	Tapered Some surface voids	50	< 2	189.6	100
*one-half of < -30°C laminate.					

The thermal characterization data given in Table IX show that all the e-beam cured quasi-isotropic composites were fully cured with T_gs near 190°C. The laminates were of generally good quality except for some surface voids due to the poor consolidation. Mechanical property data for the quasi-isotropic composites is given in Figures 50 through 52.

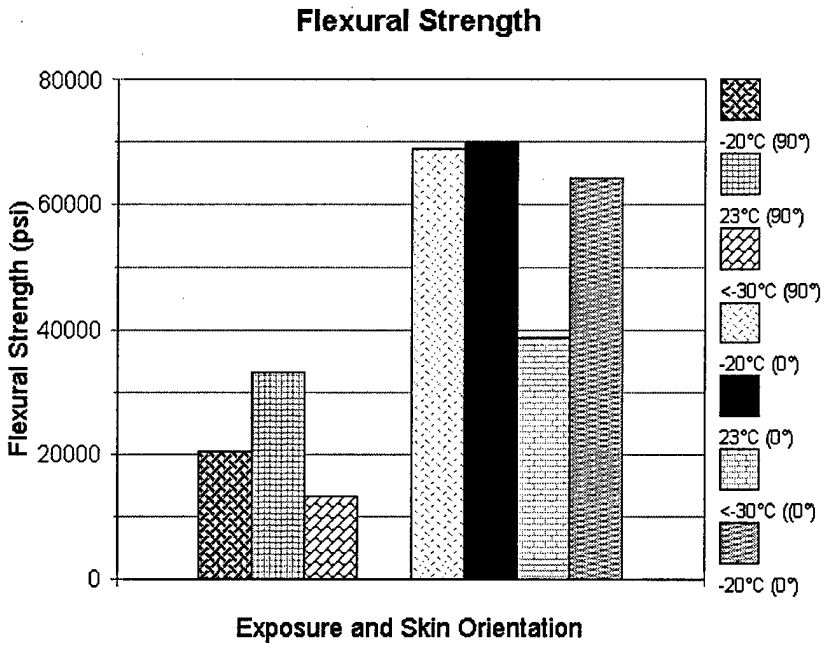

Figure 50. Flexural strength of quasi-isotropic e-beam cured composites

The flexural strength and moduli data given in Figure 50 and Figure 51 show that the ambient and –20°C cured laminates are essentially equivalent while the laminate cured below -30°C has lower properties despite showing a high T_g. The flexure data also show a high degree of dependence on the orientation of the outer ply, which is expected.

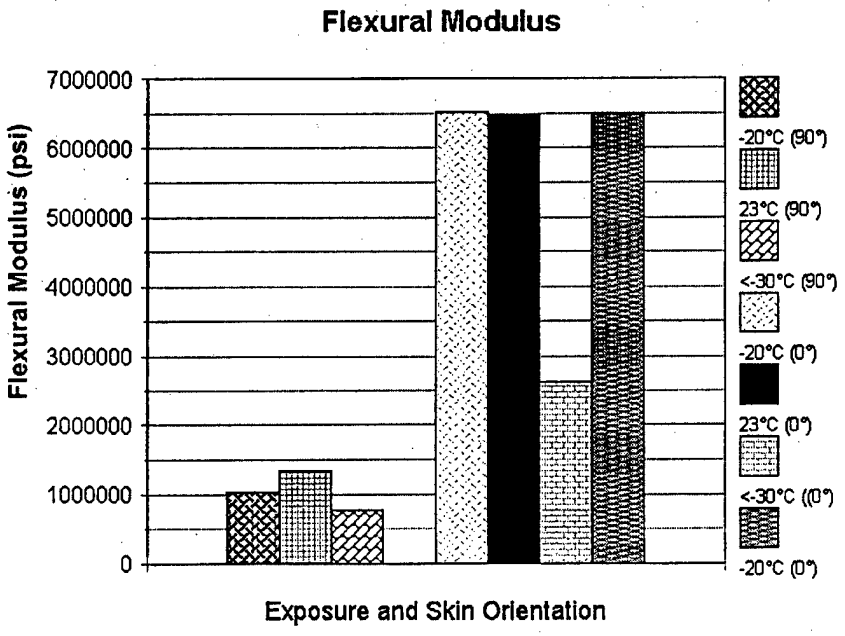

Figure 51. Flexural modulus of quasi-isotropic e-beam cured composites

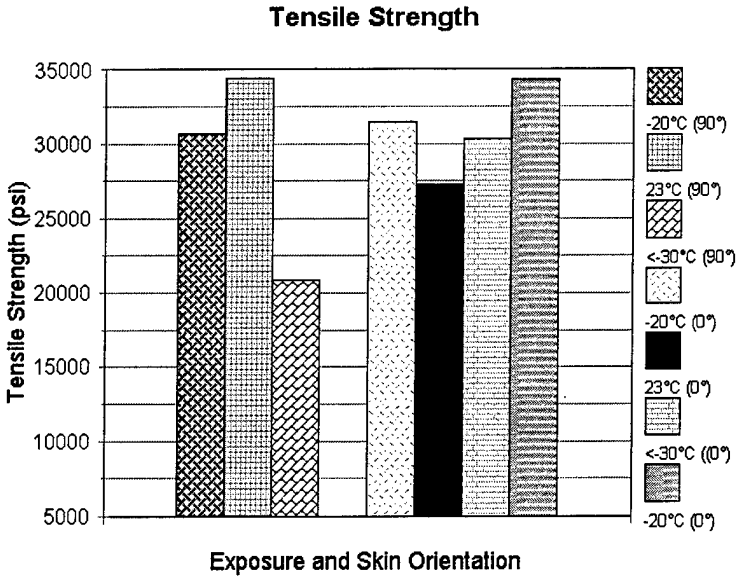

Figure 52. Tensile strength of of quasi-isotropic *e-beam cured composites*

Tensile strength data for the quasi-isotropic laminates is given in Figure 52. The tensile strength data do not show a large dependence on outer ply orientation except for the case when the outer ply of the laminate cured <-30°C is oriented at 90°. This may be indicative of surface defects, which would also influence the flexural data to a greater degree than the tensile strengths when the outer ply is oriented at 0°. With the outer ply at 0°, the strengths of the composite cured at <-30°C are equivalent to those cured at higher temperatures. The stiffness data obtained in the tensile tests were only relative values. The relative stiffness data did show that equivalent stiffness was obtained at low temperatures and room temperature in the quasi-isotropic laminates.

CONCLUSIONS AND RECOMMENDATIONS

The following section summarizes the results of our e-beam polymerization experiments and the conclusions that can be drawn from this work. We will discuss each pertinent system separately and highlight the conclusions for that system. Where our results differ from previous experimentation, we will attempt to derive information from these differences, and our experimentation, to provide guidance for resin development. In some cases, this work has suggested that certain structures are not suitable for e-beam (or UV) polymerization.

Cyanate Esters

The experiments performed here have clearly shown that the primary reaction of the cyanate ester moiety is dissociation into the component ions followed by recombination of these ions to give both the initial resin and the rearranged isocyanate. This dissociation serves to dissipate the radiation deposited energy without productive reaction. This reaction was confirmed by both infrared analysis and the observation that the resulting isocyanate reacted further following

irradiation with traces of water in the material or from the atmosphere to form the urethane group. We have assumed that this isomerization takes place from an excited vibrational state produced from the electronic excitation as it reverts to the ground state (by fluorescence or internal conversion).

In this resin, other reactions have occurred that were not investigated once the cyanate rearrangement was identified and shown to subvert any polymerization.

Several sensitizers and/or catalysts were used in an attempt to induce polymerization but failed to produce the desired result. The triplet sensitizers did appear to effectively concentrate the energy for reaction, but only resulted in higher yield of isomerization to isocyanate. The catalysts tried, iron (II) and Mn(II) AcAc, were ineffective. Attempts to induce polymerization with cationic initiators were without success.

These results suggest that the cyanate esters are unlikely to be polymerizable by either ionizing radiation or UV as a result of energy dissipation by the competing isomerization. They also suggest that further studies should be conducted on structures where this isomerization cannot take place. Although cyanides, without the carbon-oxygen-carbon linkage, may not as easily undergo the heterolytic cleavage of the cyanates, they do have the possibility for a similar rearrangement to isocyanides. Because of the stronger bond to the aromatic ring, they may be polymerizable through excitation.

Early studies [23,24] of aliphatic cyanides showed homopolymerization of the cyanide moiety and little rearrangement to isocyanide although the polymer yield was very low. Poly(acrylonitrile) undergoes facile ring formation to poly(pyridine) by a chain reaction induced by gamma radiolysis and this reaction has been used by one of us as a radiation dosimeter (previous studies by L.A. Harrah). Thermally induced reaction of this polymer is used in industry to prepare carbon fibers. It is likely that the polymerization yield from neat poly(acrylonitrile) is mediated by the proximity of the nitrile groups in the polymer; it may be a topochemical reaction since poly(acrylonitrile) is highly crystalline. Certainly, the further dehydrogenation of the ladder like structure produced, to a polynuclear aromatic, promotes the polymerization.

Resins containing the cyanide linkage do not appear promising for either radiation or UV induced curing by direct excitation based on the reactions identified here. An indirect polymerization mediated by a catalyst cannot be ruled out from this work, but no such catalyst or initiator was identified. Benzonitrile-like resins may polymerize by direct excitation or by the proper initiator or radiation prepared catalyst. Examination of the UV spectrum of benzonitrile itself suggested (*vide infra*) that anionic initiation may result in polymer. An experiment with a radiation produced anionic initiator did not result in efficient polymerization of benzonitrile in this work but a small yield of solid material did result.

Acetylene Resins

An acetylene (in the form of propargyl) resin, Bisphenol-A bis(propargyl ether) was prepared for this study and both UV and e-beam polymerizations were attempted. Like the case of the cyanate resin discussed above, these studies identified a rearrangement reaction as the principal product of excitation induced reaction. This rearrangement reaction gave a product even less polymerizable than the initial terminal acetylene moiety, but one that had the ability to compete favorably for the deposited excitation energy with the parent compound.

This reaction, the dissociation of the C—H bond on the methylene group adjacent to the acetylene, served to dissipate the excitation without inducing polymerization. The product structure, allenyl ether of Bisphenol-A, is formed when the dissociated hydrogen atom recombines with the original acetylenyl radical or the rearranged allenyl form of the acetylene radical in the cage formed by the surroundings. The overall process of dissociation followed by recombination, serves to deactivate the excitation without productive resin curing. Both direct excitation and sensitized reaction gave similar results. Energy harvesting by sensitizer was demonstrated to be effective in this system as it was in the cyanate esters but did not lead to the desired product.

Acetylenes having no adjacent aliphatic C-H bonds should not undergo this energy degrading dissociation reaction and have the possibility for polymerization. We did investigate a bisacetylene resin formed from phenylacetylene by coupling two phenylacetylene molecules with a methylene bridge between the phenyl rings. We also examined phenylacetylene itself. Small amounts of poly(phenylacetylenes) were produced by both UV and e-beam excitation. The yield was not sufficient to make this polymerization practical.

Several alternative polymerization techniques were examined for the acetylene resins: radiation induced catalysis with transition metal catalysts, free radical initiation, cationic initiation and anionic initiation. None of these techniques produced significant amounts of polymerization although the transition metal catalyst (Fe(II) AcAc) did show evidence of polymerization by UV excitation as did the free radical initiation.

An examination of the UV absorption spectrum (Figure 53) of phenylacetylene suggested that an anionic initiator may be effective.

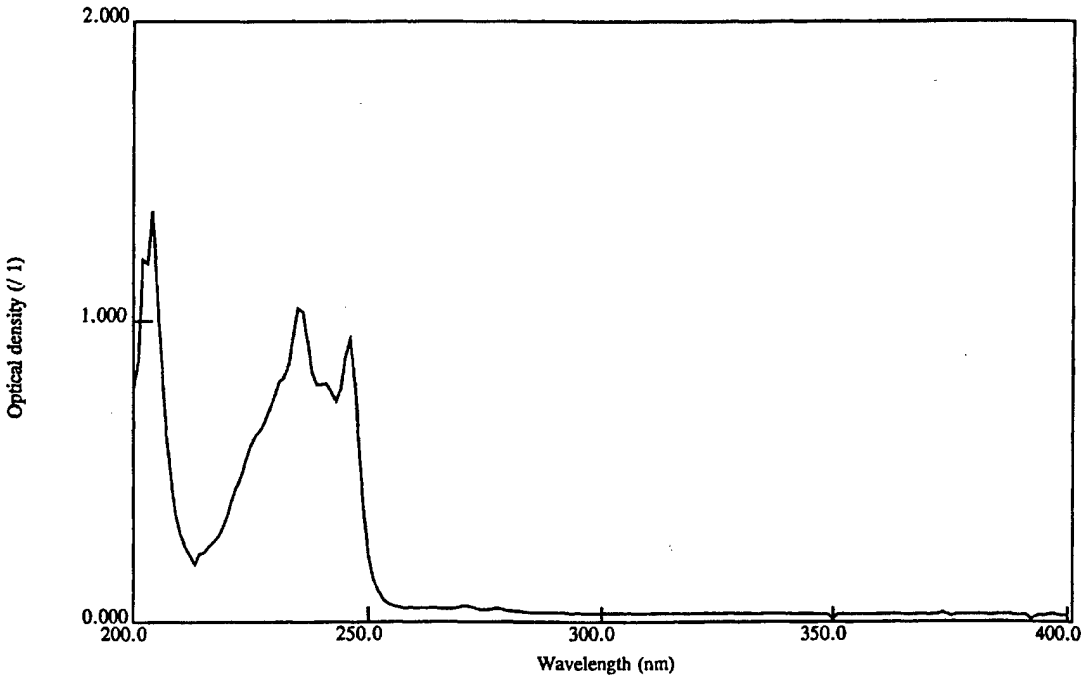

Figure 53. UV spectrum of phenylacetylene in methylcyclohexane

In the region from 200 to 400 nm, phenylacetylene has three bands, a weak band near 280 nm, a stronger band just below 250 nm and a band below 210 nm. The first of these is the first excited state of the benzene ring and shows the typical vibrational structure associated with this transition in monosubstituted benzenes. The second band is also structured and exhibits a splitting corresponding to a carbon-carbon vibration with intermediate strength between double and triplet bonding. This structure suggests that this excitation results from charge transfer from the pendant acetylene group to the ring (or from the ring to the acetylene, although ring to acetylene charge transfer is unlikely since the acetylene is more electron dense than the ring). The existence of this transition may imply a significant amount of charge transfer in the ground state from stabilization mixing of excited structures. The residual positive charge on the acetylene group should then encourage anionic initiation of acetylene polymerization. This observation provides guidance for tailoring structures for UV or e-beam polymerization.

Terminal acetylene groups do have an available, acidic C—H bond. This weak acid could serve to neutralize any strongly basic anionic initiator, converting it to acetylide, an inactive ion. Our attempts to polymerize the resins of this study with either cationic or anionic initiators were ineffective. In the cationic case, attack at the acetylene moiety was unlikely because of the like charges on the acetylene and the ion; terminal acetylenes neutralized the anionic initiator. It may be possible to initiate non-terminal acetylenes anionically. An attractive structure that should overcome the problems encountered in this investigation is the terminal phenylethynyl group attached to a high performance backbone polymer. Resins of

this type should be investigated using anionic initiators. It is not likely that ambient cure is possible with phenyl-ethynyl resins because they are inherently inflexible. Increasing the monomer flexibility while retaining the pertinent structural features of the phenyl-ethynyl is possible.

Other acetylenic related structures are possible that would have much more chain flexibility than the phenyl-ethynyl resins. Improved flexibility in both the initial resin and in intermediate polymers is necessary for rapid reaction, particularly at lower polymerization temperatures. These structures have chain-like segments with nearly zero rotational barriers that introduce flexibility during reaction. This chain rotational flexibility persists after the initial polymerization step. Although simple structures are higher melting than many resins, they are easily substituted to create randomness and inhibit crystallization; non-crystalline monomers should polymerize readily at or below ambient temperature. The initial polymerization step in these materials leaves a highly unsaturated network with the potential for highly dense crosslinking and a low permeability, very hard structure.

Cationic Epoxies

Three epoxy resins were investigated in this study for their radiation curing effectiveness using two different cationic initiators. EPON® 826, EPON® 828 (Shell) and an epoxy terminated novalac were examined under both UV and e-beam induced cure. The epoxy functionality undergoes homopolymerization when initiated with an acid cation. This homopolymerization is a living polymerization that is quite exothermic and continues in the absence of additional initiation until the living polymer chain ends are quenched by reaction with an ion capable of forming an inactive covalent bond on the chain. Termination is generally effected by an impurity such as water, which introduces a hydroxyl end group on the growing chain.

The chain extension reaction is very rapid and leads to polymer with relatively high T_g even when the resin is kept at ambient temperature during cure. The resulting cured epoxy has no volatile components except for those small quantities of impurities in the starting system and a small amount of initiator by-product.

Two initiator structures were examined: triaryl sulfonium hexafluoroantimonate (Cyracure ™ 6990 or 6974, Union Carbide) and diaryl iodonium hexafluoro-antimonate (DPI-1). These two initiator structures decompose into diphenyl sulfide or iodobenzene like species and the phenium cation upon exposure to UV or e-beam activation. The phenium cation is the initiator for epoxy polymerization. Each of these structures has been previously examined for use in UV or e-beam cure but their relative effectiveness differs. In this work, we attempted to determine the required dose for sufficient cure, the low temperature limit for effective cure, and the properties of the cured resin from these resins and initiators.

Cure doses have been previously reported to be in the vicinity of 15 MRad and this level was initially tried. Diaryl iodonium salts had been shown to give superior mechanical properties but cure at higher dose. In our study, this result was not confirmed.

We observed that the sulfonium salt initiator precursors gave initiation at lower dose than the iodonium salts *and* superior mechanical properties. The UV spectra of the two initiators examined are shown in Figure 54.

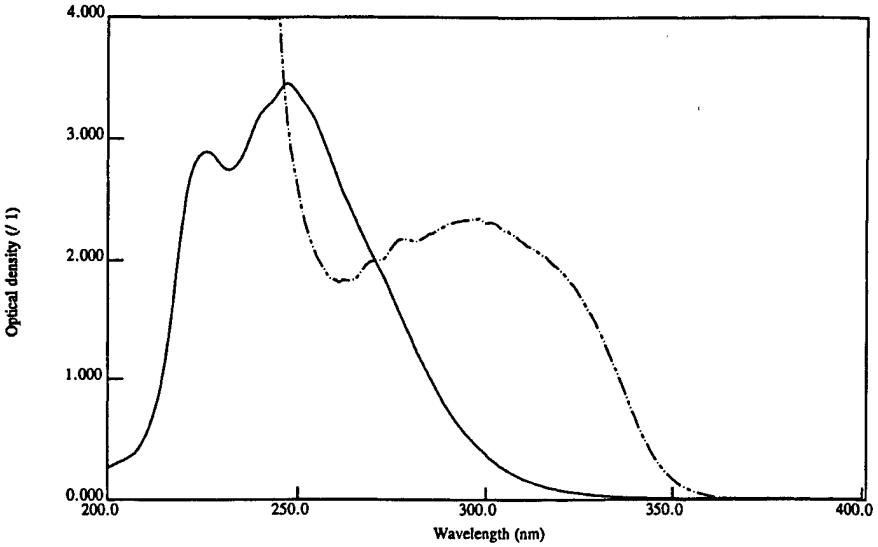

Figure 54. UV absorption spectrum of diphenyl iodonium hexafluoroantimonate in ethanol (solid line) and spectrum of triaryl sulfonium hexafluoroantimonate in ethanol (dashed line)

These spectra show that the aryl sulfonium salt absorbs at significantly longer wavelength than the iodonium salt and therefore is expected to better harvest the migrating excitation than the iodonium; it is expected to give higher yield of initiating cation. Since the resins used here all contain either mono, di or tri substituted benzene rings, they should all act as excellent donors for sulfonium decomposition (spectra not shown, see Appendix A). The iodonium salts absorb only very weakly in the fluorescence region of the resin moieties.

An additional advantage derived from using the aryl sulfonium salts is that the resulting diphenyl sulfide by-product of cation formation also absorbs in the region of resin fluorescence and can act as a stabilizer (Appendix A). In this work, we noted that the strength of the cured resins developed a maximum at cure doses of about 7-10 MRad and dropped below that maximum for higher initiation dose. Samples of resins initiated with the iodonium salt showed more strength reduction at the highest doses than did those initiated with sulfonium salt. Sulfonium salt initiation also gave more complete cure at lower dose. These are the results expected from the spectral data.

Our work indicates that the sulfonium salts are the preferred initiators for e-beam cure. They provide faster cure, lower dose for effective cure and the by-product of cation formation acts as a stabilizer for benzene ring containing resins.

In an attempt to effect cure at even lower dose, a catalyst known to accelerate polymerization in urethane polymerization was added to the resin-initiator formulations above. Fe(II) AcAc was added to the extent of 0.2% and the resins cured by e-beam exposure. In these experiments, inhibition, not acceleration occurred. These experiments were terminated due to their unfavorable result. We assume that the iron (II) catalyst intercepted the cation and acted as a chain terminator. This assumption was not verified.

Finally, subambient cures were attempted with the most promising system, EPON ® 828/Cyracure™ 6974 triaryl sulfonium hexafluoroantimonate (2%). While subambient temperature e-beam exposure was difficult in the Titan e-beam facility, we were able to maintain an exposure temperature of approximately 253 K in one exposure and 233 K in a second (±5 K) during the exposure by cooling the resin substrate with solid dry ice during exposure. For the upper temperature, only the lower surface was cooled; at the lower temperature, both surfaces were covered.

The 253 K exposures showed nearly complete cure at the exposure termination while that at 233 K appeared uncured. The sample exposed at lower temperature (233K) slowly cured after returning to ambient temperature (about 2-3 days were necessary to the no tack condition). These experiments seem to indicate that at the lower of these two temperatures, little dissociation of initiator precursor has occurred while with only a 10 K rise in temperature, sufficient cation was produced to nearly complete the cure. Here, if the resin mobility inhibited cure, we would have expected rapid cure of the colder sample upon reaching room temperature; that did not occur.

EPON® 828, a chain extended diglycidyl ether of Bisphenol-A initiated with triaryl sulfonium hexafluoroantimonate, appears to be a viable e-beam curing system. The epoxidized phenolic resin with the same initiator gave an acceptable cured product but was less radiation stable and cured at somewhat higher dose. Energy transport in these systems was shown to enhance the cure initiation as well as provide some radiation damage protection. A cure dose of 5-7 MRad was sufficient to afford good product. A somewhat lower dose may be useful during manufacture to cause part hardening. The required dose needs optimization for manufacturing design.

We did examine the influence of filler on cure for silica and carbon black fillers. Only a single fill level was tried for each filler to determine if these filler surfaces interfered with the initiation or polymerization. This study did indicate that both materials reduced cure, presumably by cation termination or initiator capture. Carbon black caused the greatest inhibition and indicates that the reinforcing fiber surface in a composite may cause similar results; however, the carbon filler has a

much higher surface area and would amplify any surface effect. A higher cure dose may be required in composites than in neat resin. This may be partly offset by the greater mean density of the reinforced material with the attendant increased dose to the resin in the presence of filler for a fixed exposure dose.

Unidirectional and quasi-isotropic composites fabricated with intermediate modulus carbon fiber and cationic curing epoxies showed mechanical properties equivalent to those of thermally cured composite systems, even when cured at reduced temperatures. All the composites displayed 100% cure and T_gs around 190°C for e-beam cures between 23°C and < -30°C. This shows that high performance composite space structures can be fabricated with stress-free temperatures < -30°C, which should improve dimensional stability in the space environment. Difficulties encountered with pressure application during this program should be alieviated by the use of stiffer pressure plates, possibly using honeycomb composite materials. Additional work is needed in optimizing matrix cure chemistry versus radiation dose, improving bonding at the fiber-matrix interface, producing well consolidated, low void composites at subambient temperatures, and controlling temperature during subambient cure.

REFERENCES

1. F. A. Bovey, "The Effects of Ionizing Radiation on Natural and Synthetic High Polymers," *Interscience*, New York, 1958.

2. A. Charlesby, *Atomic Radiation and Polymers*, Pergamon, New York, 1960.

3. A. Chapiro, *Radiation Chemistry of Polymeric Systems*, Interscience, New York, 1962.

4. R.F. Gould, ed., *Irradiation of Polymers*, ACS Advances in Chemistry Series No. 66, ACS, Washington, DC, 1967.

5. M. Dole, ed., *The Radiation Chemistry of Macromolecules*, Academic Press, New York, 1972, Vols. I & II.

6. (a) G. W. Meyer, S. J. Pak, Y. J. Lee, and J. E. McGrath, *Polymer,* 1995, *36*, 2303; (b) J. G. Smith, Jr., J. W. Connell, and P. M. Hergenrother, *Polymer,* 1997, *38*, 4657.

7. (a) D. Beziers and J. Denost, "Composite Curing: A New Process," *AIAA 89-2868,* American Institute of Aeronautics and Astronautics, Washington, DC (1989); (b) D. Beziers, *35th Intl. SAMPE Symp.,* 1990, *35*, 1220.

8. C. B. Saunders, V. J. Lopata, and W. Kremers, *38th Intl. SAMPE Symp.,* 1993, *38*, 1681.

9. C. J. Janke, G. F. Dorsey, S. J. Havens, and V. J. Lopata, *41st Intl. SAMPE Symp.*, 1996, *41*, 196.

10. V. J. Lopata, M. Chung, C. J. Janke, and S. J. Havens, *28th Intl. SAMPE Tech. Conf.*, 1996, 28, 901.

11. D. A. Shimp, and W. M. Craig, Jr., *34th Intl. SAMPE Symp.*, 1989, *34*, 1336.

12. D. A. Shimp and S. J. Ising, *35th Intl. SAMPE Symp.*, 1990, *35*, 1045.

13. T. Matsumoto, M. Mohri, and A. Nanjo, *35th Intl. SAMPE Symp.*, 1990, *35*, 1045.

14. C. Arnold, P. MacKenzie, V. Malhotra, D. Pearson, N. Chow, M. Hearn, and G. Robinson, *37th Intl. SAMPE Symp.*, 1992, *37*, 128.

15. S. Srinivasan, S.S. Joardar, D.B. Priddy, T.C. Ward, and J.E. McGrath, *39th Intl. SAMPE Symp.*, 1994, *39*, 60.

16. B.P. Rice, A.S. Crasto, and T.B. Tolle, *40th Intl. SAMPE Symp.*, 1995, *40*, 1672.

17. R.C. Romeo, *40th Intl. SAMPE Symp.*, 1995, *40*, 1672.

18. T. Förster, *Naturwiss,* 1946, *33*, 166.

19. I. B. Berlman, "Energy Transfer Parameters for Aromatic Compounds," Academic Press, NY, 1974, p. 22.

20. I. B. Berlman, *Handbook of Fluorescence Spectra of Aromatic Molecules, 2nd ed.*, Academic Press, NY, 1971, p. 220.

21. R. M. Silverstein, G. C. Gassler, and T. C. Morrill, *Spectrometric Identification of Organic Compounds, 4th Edition*; John Wiley and Sons, NY, 1981; Chapter 4.

22. L. A. Harrah, unpublished work.

23. T. D. Nevitt, R. E. Rondeau, L. A. Harrah, H. H. Barber, Jr., and J. Maniotes, *"Radiation Chemistry of Triple Bond Compounds: Part I, Acetonitrile and 2-Butyne,"* ASD-TR-65, Aeronautical Systems Division, US Air Force, 1965.

24. L. A. Harrah, R. E. Rondeau, S. Zakanycz, D. Hale, and D. Dunbar, *"Electron Spin Resonance Study of Gamma Irradiated Solid Acetonitrile,"* ASD-TDR-63-785, Aeronautical Systems Division, US Air Force, 1963.

25. D. L. Dexter, *J. Chem. Phys.*, 21, *836 (1953).*

APPENDIX A—ENERGY TRANSFER AND LOCALIZATION

Energy Transfer

A detailed theory of radiationless transfer of electronic excitation was developed by Förster [18] in terms of a resonant dipole-dipole interaction between the donor and acceptor molecules. In this theory, neighboring molecules with degenerate excitations are coupled to each other as well as to the radiation field. A transition event then has a possibility of either transferring to the neighbor or emitting a photon. The probability for transfer to the neighbor for this dipole-dipole interaction varies as the inverse 6th power of the molecular separation and directly as the probability that the two molecular states are degenerate in energy.

$$P_T=P_E/R^6 \qquad (A.1)$$

In condensed phases, the molecular excited states of molecules are affected by the nature of their environment and do not have the discrete nature of gas phase molecules. The excited state energy can vary with changes in the environment that alter the positional distribution of surrounding molecules or their kinetic energy. In a collection of molecules, many variations of the surroundings can occur. As a result of this environmental distribution, the excited states of a molecular specie are broadened and accidental degeneracies between even unlike molecules can and do occur. The probability distribution of energies encountered by a single specie in a condensed phase are reflected in the energy distribution of fluorescence from that specie. Absorption spectra of molecules also reflect this distributional fluctuation and are broadened. The energy transfer probability between molecules can then be estimated by comparing the overlap of the acceptor's absorption spectrum with the fluorescence of the donor. Equation A.2, below, gives the rate of energy transfer between donors and acceptors in condensed phases.

$$k_{d>a}=[\, A\cdot K^2/n^4\tau_0 R^6] \int f_d(\nu)\, \epsilon_a(\nu)\, d\nu / \nu^4 \qquad (A.2)$$

Where A is a collection of physical constants, $K_{d>a}$ is the rate constant for energy transfer to the acceptor, n is the refractive index of the solution, R is the donor-acceptor distance, τ is the radiative lifetime for donor fluorescence, $f_d(\nu)$ is the fluorescence distribution of the donor as a function of energy (ν), and $\epsilon_a(\nu)$ is the energy distribution of the extinction coefficient of the acceptor. K is an orientational function of the angle between the *transition dipole moments* of donor and acceptor. In solution, the orientational factor, K, and the molecular spacing, R, must be averaged over all possible values to define the rate of transfer. In crystalline solids, K usually has a single value and R needs only to be averaged over thermal excursions. In fluid solution, these quantities are random and R is related

to concentration. Förster and others have shown that in a randomly distributed system (isotropic solution) the following equation gives the transfer probability:

$$P_{d>a}=2x\ \mathrm{Exp}(x^2)\int_x \mathrm{Exp}(-t^2)\ dt = \pi^{1/2}\ \mathrm{Exp}(x^2)\ [1-\mathrm{erf}(x)] \qquad (A.3)$$

$$x=C/C_0 \qquad (A.4)$$

where erf(x) is the error function and C_0 is the acceptor concentration at which energy transfer and radiation are equally probable. This concentration may be calculated from the spectra from a value, R_0, the distance at which the rate of transfer equals the rate of fluorescence.

$$C_0 = (7.66 \times 10^{-8}/R_0)^3 \qquad (A.5)$$

The quantity C_0 is the critical energy transfer concentration and at that concentration, the transfer efficiency is 76%. At that concentration, the fluorescence from donor is reduced to 24% of its initial value and the lifetime of fluorescence is also reduced by that quantity. Note, the above equations do not distinguish between differing or like molecules, only the overlap between absorption and fluorescence determines the transfer probability. Generally, however, transfer between molecules of differing structure can be more rapid than between like species since the spectral overlap cane be greater.

The above analyses assume that the only near field interaction between molecules is dipole-dipole. Dexter [25] has treated higher order interactions and shown that they do not contribute significantly compared to the dipole-dipole. This interaction mechanism is appropriate for interactions between molecules in singlet excited states where this interaction is by far the strongest. Energy transfer between triplet states is much slower and may involve magnetic dipoles and electric quadrupole mediated transfer. These processes are slow compared with the dipolar interaction and generally ineffective in fluids. They show a much stronger inverse distance dependence and operate almost solely between nearest neighbors; they will not be treated here.

The calculations outlined above have been incorporated into our spectrometer control program and were performed for the experimental systems directly upon the observed spectra.

Excimers and Exciplexes

When molecules approach one another sufficiently closely that the energy transfer process outlined above can occur at rates comparable to molecular vibrations, the excitation can no longer be described as localized on one molecule, but is best considered as an excitation of the molecular pair. The very rapid transfer lowers the energy of the excitation by an amount related to the transfer rate and provides

an attractive force between the molecular pair. This attractive force (bonding) exists only for a pair with excitation and becomes repulsive upon decay of excitation. For such a closely bound pair, molecular interactions other than dipole-dipole may become important and increase the bonding to values greater than those predicted from the interaction considered in the first section, above. The excited state pairs are termed excimers (from excited state dimers) when formed from like molecules, or exciplexes if the two molecules are of different structures. Because other interactions beside the dipole-dipole come into play at the close distances, triplet excimers and exciplexes are also possible. Singlet excimers and exciplexes have been observed between acetylenic moieties and their existence provided motivation for this work.

Sensitizers

In this work we have used the term sensitizer to refer to molecular species that perform a catalyst-like function in inducing chemical reaction. These materials act as acceptors in energy transfer processes, and since they generally have the lowest excitations of the system, act as energy traps. When energy migrates to the sensitizer molecule, it level is lowered sufficiently that the probability for transfer to its neighbors is lowered to an insignificant value. Sensitizers differ from stabilizers in that the resulting excitation can initiate a chemical reaction, or other desired change in the host material (resin or solvent). In this study, the sensitizer was designed to harvest the energy deposited in the host (resin) and provide activation of chemical reaction in the acetylenic or cyanate group of the host by forming a reactive triplet electronic state at the reactive linkage of the resin. This was accomplished through intersystem crossing in the sensitizer, followed by exciplex-like association with the host.

Energy transfer from host to host followed by transfer to sensitizer was utilized to harvest the randomly deposited excitation and concentrate it into chemical reaction rather than random damage.

Stabilizers

There are several types of stabilizers: oxidation inhibitors, spectral masking agents, sacrificial stabilizers, and damage inhibitors. This last type of stabilizer has nearly the same properties as the sensitizers described above. It harvests deposited energy by energy transfer processes to an excitation of the stabilizer molecule. The only difference between this type of stabilizer and the sensitizer is the result of this excitation; the stabilizer molecule is designed to decay very rapidly to its ground state without inducing chemical reaction. One realization of this behavior is to incorporate a specie that has high fluorescence quantum yield and thus fluoresces to give light rather than damage.

A second type of material, related to the sensitizers used in this study, undergoes internal isomerization in the excited state, which, when it decays to the ground state, reverts to its initial structure. The isomerization energy in the excited state degrades the excitation to a level where further chemical reaction is not possible. Decay from the excited state of the isomerized specie mat be either by fluorescence, phosphorescence, or emission of phonons (thermal decay). The decay is thus broken up into three steps, isomerization, de-excitation, and reversion, each of which is small compared to the energy required to induce chemical change in the host.

Oxidation inhibitors are materials that intercept the intermediates in thermoxidative reactions and shorten the chain nature of oxidations. They are sacrificial inhibitors in that they are used up in the inhibition process and delay the onset of rapid oxidation.

Masking stabilizers are used chiefly to prevent UV (or visible light) damage to the substrate material by very strongly absorbing the UV light and preventing its penetration. Ideally they are stable toward UV degradation by the existence of processes like fluorescence or the isomerization scheme described above. In some cases, they may undergo sacrificial degradation but ensure that only this surface layer is affected.

Initiators

Initiators differ from sensitizers in that they do not behave catalytically. Instead, they undergo chemical change to produce a specie that initiates the desired chemical reaction, usually a polymerization by chain reaction. The chemically produced specie becomes incorporated onto the growing chain as a chain terminator.

To be efficient in initiating chain reactions, they, like the sensitizers described above, should harvest deposited energy from the host but utilize this energy to change to their active form. Furthermore, they are generally only effective for chain polymerization since they are destroyed in a one to one correspondence to chain initiation.

Common initiators are materials that release: a strongly acidic specie upon excitation (cationic initiators), a strong base (anionic initiators), and those materials that decay to free radicals. Reactive unsaturated moieties may be initiated by any of these initiators but the reaction rates for each type of initiator vary greatly. The appropriate initiating specie depends upon the structure of the host molecule, particularly those segments of its structure that may react adversely with the initiator. For example, molecules that contain weak acid functionality cannot be initiated effectively with anionic initiators, neutralization occurs. Free radical initiators react only slowly with non-activated unsaturation, hydrocarbon-like unsaturation.

Intersystem Crossing

Molecular systems, like atoms, can exist in more than a single system of excited states. These excited states are characterized according to the resultant contained angular momentum of the electrons spins. Normal ground states of molecules have their bonding electrons arranged in pairs with the spin angular momenta of the electrons in the pair, opposed. In excited states, the electrons are no longer completely paired and their total spin angular momentum can be either like the ground state, zero or differ from the ground state by one unit of electron spin. Higher lying electronic excitations may exhibit a spin angular moment of greater than one but these are not normally encountered for excitations below the ionization potential and will not be further discussed here. With a resultant angular momentum greater than zero, a magnetic dipole moment exists that can take n orientations in a magnetic field:

$$n=2S+1 \qquad \text{(A.6)}$$

where n is the number of available orientations in a magnetic field, each with a distinct energy, and S is the total spin angular momentum of the molecule in its excited state. In the absence of a magnetic the n states are still distinct but all n states have the same energy; they are degenerate! In an isolated molecule, the interaction between states with differing angular momenta is strictly forbidden due to a requirement for conservation of spin angular momentum. Thus an isolated molecule can exist in a state of the same angular momentum as the lowest energy, ground state or can be in a configuration differing from the ground state spin angular momentum by one unit of spin angular momentum (or two or three units, see comment above regarding the existence of higher states). The electron configuration with zero spin is referred to as a singlet configuration and all excitations with this configuration are referred to as the "singlet manifold." Spin configurations with spin angular momentum of one have three degenerate levels and belong to the "triplet manifold" of excitations.

While interaction between these states is forbidden for isolated molecules, particularly in condensed systems, it can occur mediated by collisions between molecules or by interaction with electric and magnetic fields, either produced in the surroundings or by transient fluctuations in the molecule itself. Generally, the probability for intersystem interaction (crossing from one manifold to another) is much less probable than decay of excitation. Phosphorescence, the decay of the lowest triplet to the ground state with emission of light has a probability of 10^{-7} to $10^{-9}$of that for fluorescence. Phosphorescence lifetimes are typically seconds long while fluorescence occurs in nanoseconds.

The production of triplet states in condensed systems is termed intersystem crossing.

Internal Conversion

Internal conversion is the intramolecular process where the electronic excitation is degraded from a higher level of excitation to a lower within a multiplicity manifold of states, by converting the electronic energy, at least partially, into molecular vibrational excitation. In most molecules, the higher vibrational states of lower electronic excitations overlap the energy range of higher electronic excited states. If exact coincidence of levels is not achieved, no interaction can occur; in most cases, transition between these levels without the emission of a photon, is forbidden; energy must be conserved in transition.

In condensed phases with their rapid intermolecular collisions, the excitations are broadened and *accidental* degeneracy of levels becomes possible. This accidental degeneracy allows internal conversion to highly excited vibrational levels of lower electronic excited states. The change in vibrational excitation is still a forbidden transition if a quantum level change of greater than one is required but where rapid collisions are occurring, at least a part of the vibrational energy change required is expended in non-quantized translational kinetic energy providing an allowed pathway. Generally, the rate of internal conversion is inversely related to the energy level separation so that conversion between excited states is rapid. Degradation to the electronically unexcited ground state is generally slower than between higher excited states since the energy spacing is usually greater. It does however, give the higher vibrational excitation. If the vibrational excitation produced is concentrated in a single bond, reaction or dissociation may occur.

Heavy Atom Effect

In molecules with heavy atoms, those species that have high nuclear charge, the high electric fields near these atoms cause strong field fluctuations during normal vibrational and rotational motions of the molecule. These fields tend to reduce the distinction between electron spin angular momentum and other angular momenta (electron orbital, molecular rotation and nuclear spin) within the molecule. This results in higher probability for intersystem crossing rates and is termed the heavy atom effect. Typically, atoms with greater "Z" can cause the intersystem crossing rates to be competitive with processes within the singlet manifold.

APPENDIX B—CALCULATION OF DOSE GENERATED BY E-BEAM IRRADIATION

X-Ray Dose Calculation Worksheet

A spreadsheet was designed to aid in the estimation of x-ray dosage during the Titan tests. The worksheet has several key input parameters that include beam parameters, material properties, and geometrical parameters of the beam. Once the parameters are entered into the worksheet, the deposited energy and RADs per pass are calculated. A plot of the beam current density is also generated as part of the worksheet to give the user a profile of several beam passes.

Beam Parameters. There are several beam parameters that must be input by the user: first are the basic operating parameters, which include, beam energy, beam current, pulse repetition rate, and pulse width. Finally, the transition speed, speed at which the beam passes over the sample is input.

From this information, a RAD multiplier is calculated, which takes into account the movement of the beam across the sample. It is assumed that the repetition rate of the beam provides several pulses per beam diameter.

Gassuian Parameters. Two pieces of information are needed for the beam profile calculations, beam radius measured at FWHM and beam spacing. Both of these parameters are determined from actual profile measurements and will be illustrated in the next section.

Material Properties. Material properties encompasses several parameters about the material such as thickness and density. Once key parameter is the stopping power. This parameter is determined from the beam energy and the uses of the "Tables of Energy Losses and Ranges of Electrons and Positrons" by Martin J. Berger and Stephen M. Seltzer.

After all of the above information is input into the worksheet, the RADs per pass is calculated and the beam profile is given (Figure B-1).

Worksheet Verification and Calibration

The worksheet was verified and adjusted from data taken at Titan. The first data-set to be used was the data taken on 8-7-97. This was a simple run at the typical beam parameters shown in the worksheet. The beam was translated across the sample, which was 4.75 in. below the beam pipe, and was then shifted 1.3 in.

The data is shown in Figure B-2. The optical density was converted into Mrads with the help of the calibration curve given in Figure B-3. After the conversion was

done, it was determined that the peak amplitude of the absorbed radiation was 4.5 Mrads for one pass and 8 Mrads for two passes. The inconsistency in measurements was most likely due to the calibration curve for the dosimeter material.

This beam profile was then normalized and plotted against the calculated profile from the worksheet. The beam spacing and beam FWHM was adjusted to obtain a reasonable match between the measured and calculated results. The actual beam spacing turned out to be 1.25 in. per pass and the beam width at 4.75 in. is 0.66 in. An overlay of the calculated and measured data is shown in Figure B-4.

A comparison was also made to the data taken on 9-23-97. The beam parameters were the same. The beam spacing was reduced to 0.354 in. The beam was passed 3 times for each shot before translating. The worksheet in Figure B-5 shows the dose expected for a single pass of 10.45 Mrads, for 3 passes that equates to 31.2 Mrads. This is much higher than the measured dose of 23 Mrads (Figure B-6). The discrepancy again shows a much higher calculated dose than measured dose. This was true for the case of the data taken of 8-7-97 as well. Two passes did not double the dose. However, to first order the numbers appear to be right and the profile look correct.

Beam Paramters				Gaussian Parameters	
Beam Energy	14	MeV	Beam Radius FWHM	0.33	inches
Total Beam Current	0.180	A	Beam Spacing	1.25	inches
Pulse Repetition Rate	35	Hz			
Pulse Width	5.5	us			
Beam Speed	0.83	cm/s		0.354	
RAD multiplier	70.7	multiplier due to rep-rate and speed (assumes many pulse per beam dia.)			
Material Properties					
Density	1.2	g / cm^3			
Stopping Power	2.3	MeV-cm^2 / g			
Sample Thickness	0.3	cm			
Peak Current Density	0.040775	A / cm^2			
Flat Current Density	0.040838	A / cm^2	taken from graph		
Electron Flux	2.55E+17	e / s-cm^2			
Energy deposited / e	0.828	MeV / e			
Total Energy Deposoted	33813.7	J / (cm^2-s)			
Energy per Pulse	0.185975	J / cm^2			
Rads per pulse	0.05166	MR/pulse			
RAD Scaling Factor	70.69	taken from above			
Rads per pass	3.65	MR/pass	Scaled LAB	4.82	MR/pass

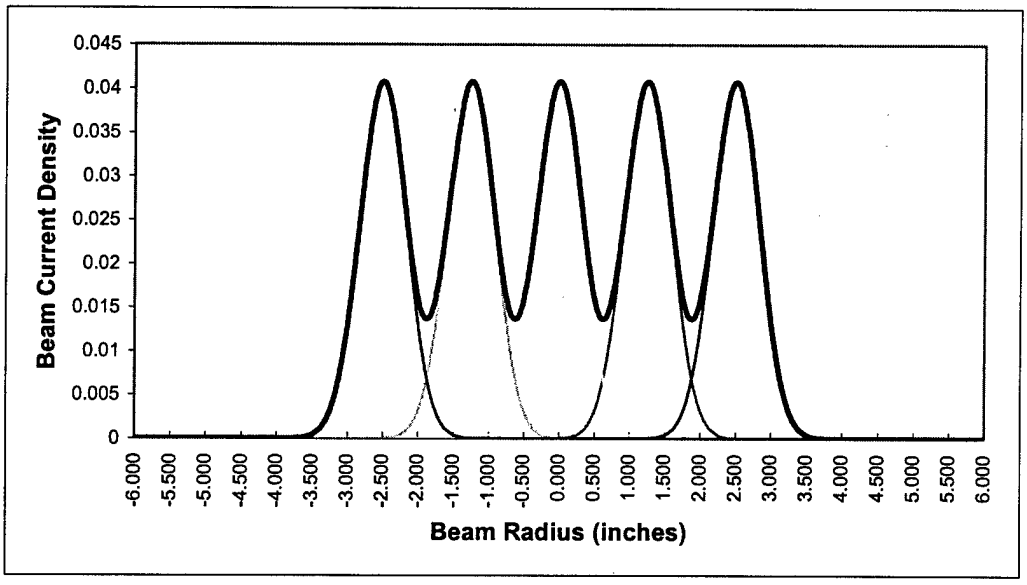

Figure B-1. Spreadsheet for calculating dose and beam profile for 8-7-97 data

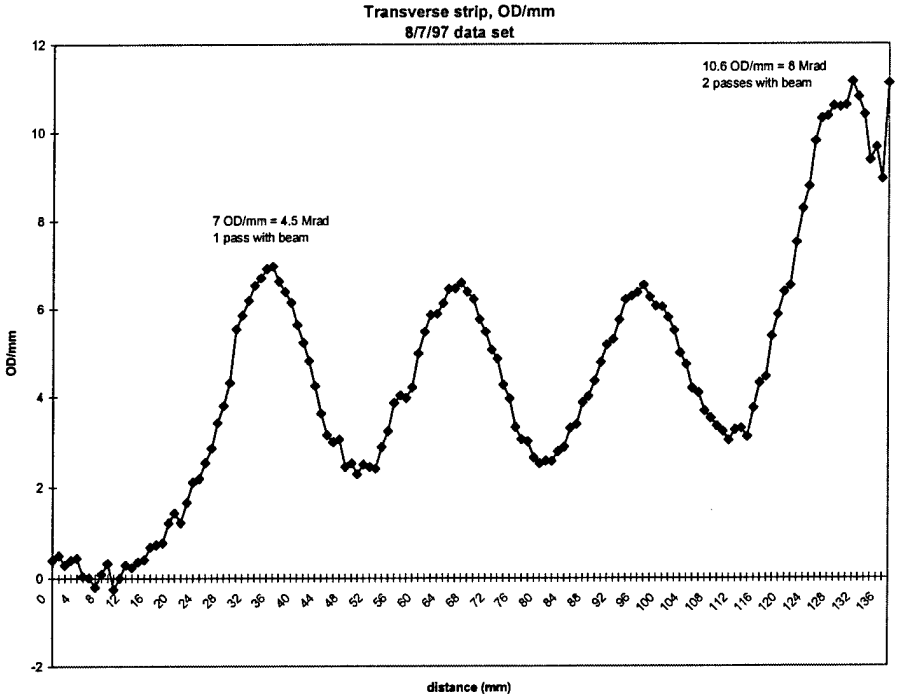

Figure B-2. Measured dose for tests conducted on 8-7-97

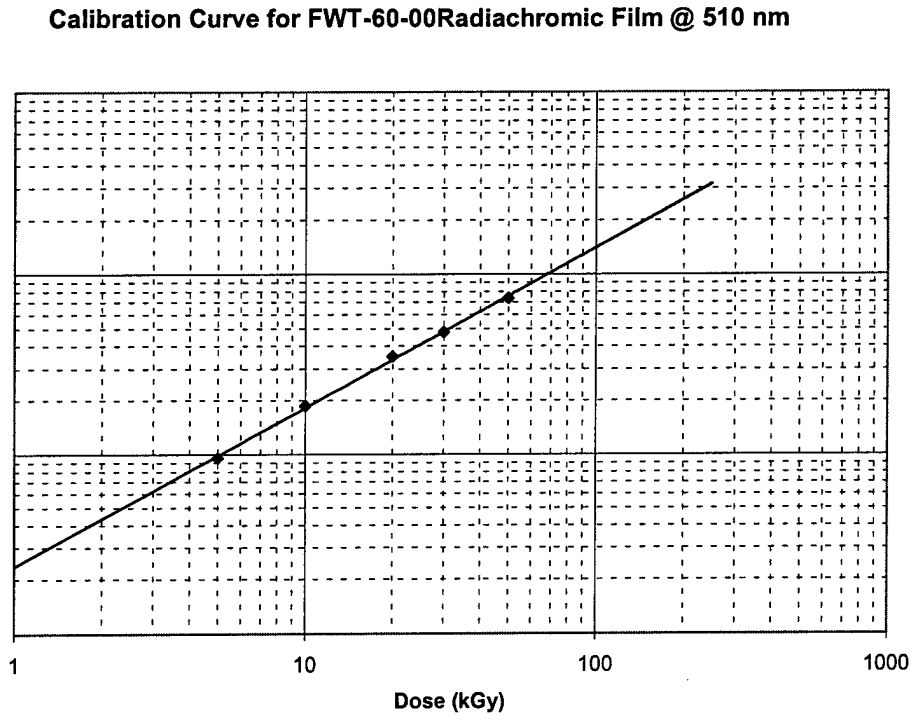

Figure B-3. FWT-60-00 dose calibration curve

FIT TO LAB DATA 8-7-97

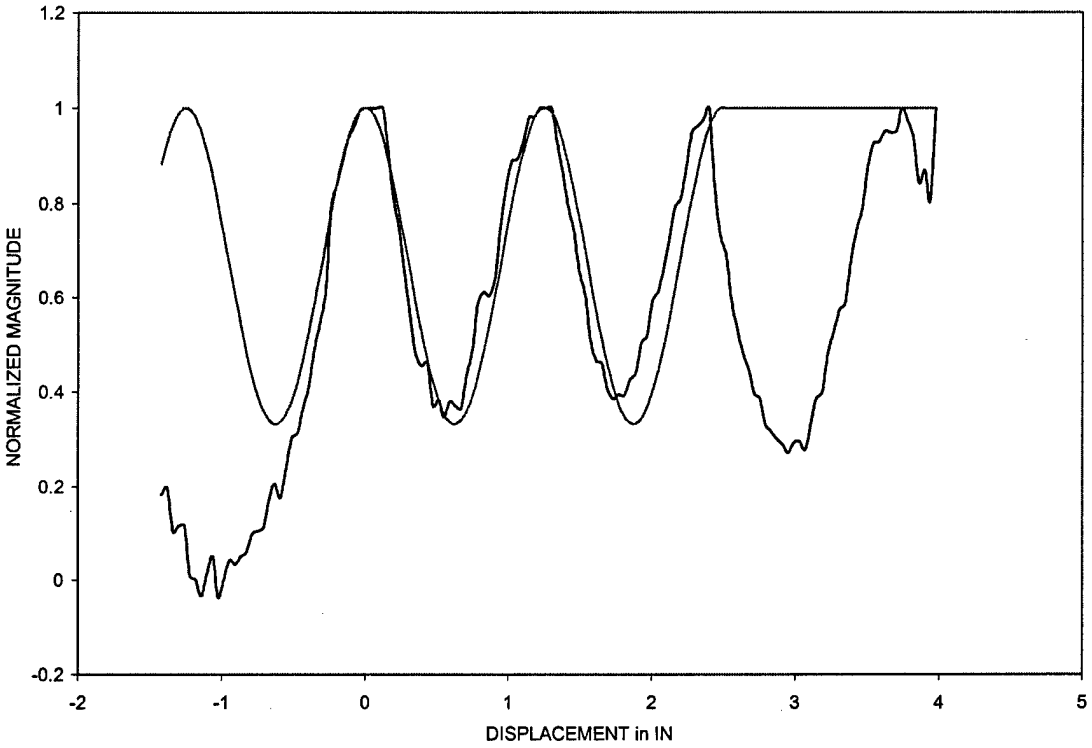

Figure B-4. Overlay of calculated and measured dose

Beam Paramters				Gaussian Parameters	
Beam Energy	14	MeV	Beam Radius FWHM	0.33	inches
Total Beam Current	0.180	A	Beam Spacing	0.354	inches
Pulse Repetition Rate	35	Hz			
Pulse Width	5.5	us			
Beam Speed	0.83	cm/s			
RAD multiplier	70.7	multiplier due to rep-rate and speed (assumes many pulse per beam dia.)			
Material Properties					
Density	1.2	g / cm^3			
Stopping Power	2.3	MeV-cm^2 / g			
Sample Thickness	0.3	cm			
Peak Current Density	0.040775	A / cm^2			
Flat Current Density	0.094811	A / cm^2	taken from graph		
Electron Flux	5.93E+17	e / s-cm^2			
Energy deposited / e	0.828	MeV / e			
Total Energy Deposoted	78503.68	J / (cm^2-s)			
Energy per Pulse	0.43177	J / cm^2			
Rads per pulse	0.119936	MR/pulse			
RAD Scaling Factor	70.69	taken from above			
Rads per pass	8.48	MR/pass	**Scaled LAB**	**10.45**	**MR/pass**

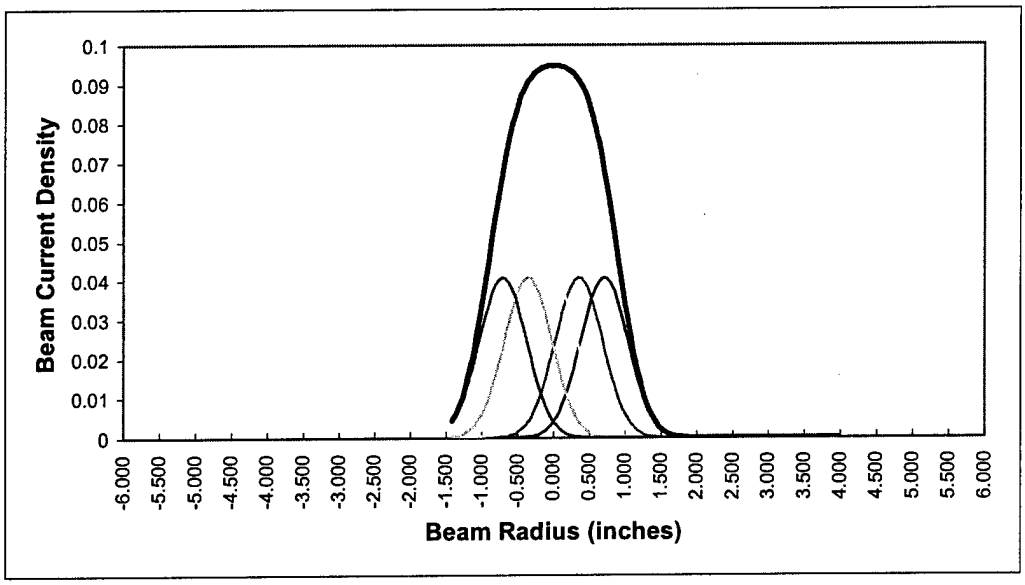

Figure B-5. Worksheet for 9-23-97 data

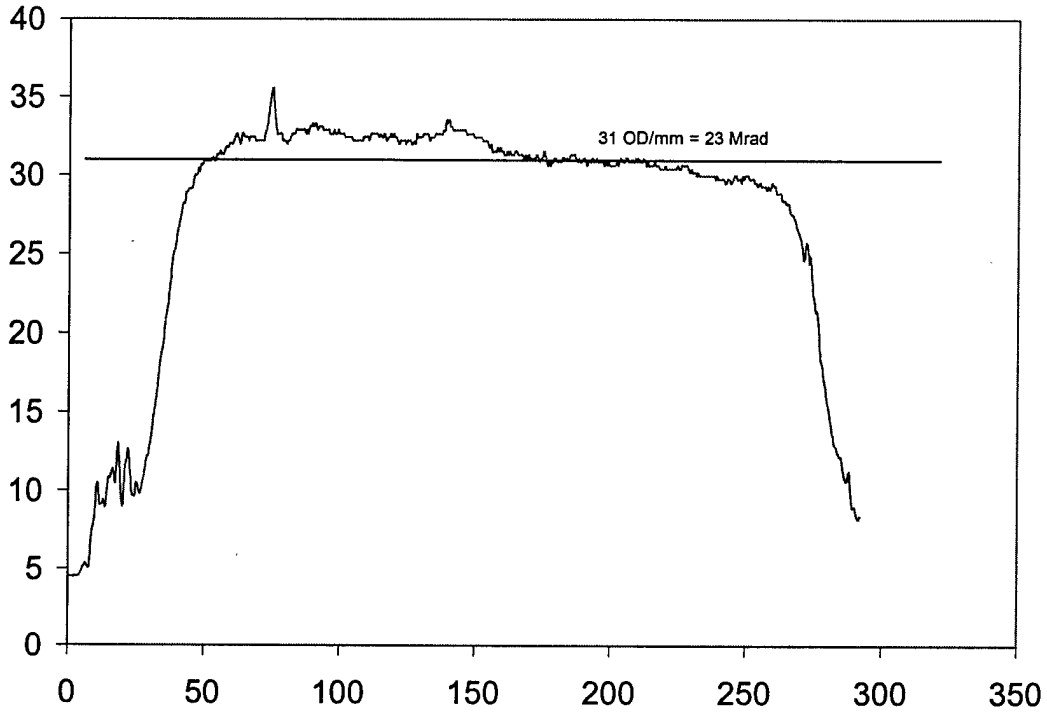

Figure B-6. Measured dose for 9-23-97 tests

APPENDIX C—EXPERIMENTAL METHODS

Synthesis and Characterization

Synthetic Methods

Examples of the synthetic methods used for propargyl-functionalized resin and sensitizer preparations are outlined below. Parent compounds used included various hydroxyl-functionalized materials, pyridine-derived materials and aniline-derived materials. Aniline-derived starting materials were purified by sublimation before use; all other parent materials were used as received. Examples of synthetic procedures are given for use of Bisphenol-A as the parent compound. Similar procedures apply to all other hydroxyl- and amine-functionalized parent compounds.

Preparation of Sodium Salt of Bisphenol-A

A solution of 2.025 mol sodium hydroxide (NaOH) in 500 ml water was prepared and deaireated with flowing nitrogen. To this solution was added 1 mol of Bisphenol-A. The mixture was then heated to 70-90°C and maintained at this temperature for 4 hours. The solution was then cooled to <5°C and the crystals recovered by suction filtration.

Preparation of Propargyl Derivatized Resin

Method A, Bisphenol-A sodium salt + propargyl bromide in toluene

A suspension of 0.02 mol Bisphenol-A sodium salt in 200 ml toluene was prepared. To this suspension, 4.5 ml of an 80% propargyl bromide solution in toluene was added, dropwise. The reaction was stirred for 4 hours after which the reaction mixture was filtered to remove the sodium bromide coproduct.

Method B, Bisphenol-A + propargyl bromide in toluene with triethylamine

To 100 ml toluene in a round bottom flask was added 0.039 mol Bisphenol-A followed by 0.078 mol propargyl bromide, 80%(w/v) in toluene. To the resulting white slurry was added 0.078 mol triethylamine. The reaction was stirred at room temperature for one hour and then heated to 70°C for 1.5 hours. Toluene was then removed by rotary evaporation. The resulting sticky material was washed with water to remove any water-soluble by-products, after which the water layer was decanted and the remaining material was dried under vacuum at room temperature overnight.

Method C, Bisphenol-A sodium salt + propargyl bromide in methyl isobutyl ketone

To a mixture of 0.02 mol Bisphenol-A sodium salt in 25 ml methyl isobutyl ketone was added 0.04 mol propargyl bromide, 80% (w/v) in toluene. The reaction mixture was then heated at 60-80°C for 18 hours. The reaction solution was then extracted with water followed by extraction with 5% aqueous sodium carbonate. The solvent was then evaporated from the organic layer and the material dried at elevated temperature under vacuum overnight.

Organic Williamson synthesis in acetonitrile

To a solution of 0.025 mol Bisphenol-A in 25 ml acetonitrile was added 0.075 mol propargyl bromide and 0.075 mol sodium carbonate. The reaction flask was then equipped with condenser and temperature control and heated to 70°C for 4 hours. The reaction mixture was then hot filtered and the acetonitrile evaporated from the filtrate. The resulting material was dissolved in methyl isobutyl ketone and extracted several times with 5% aqueous sodium carbonate. The solvent was then removed from the organic layer to yield the product that was dried under vacuum at elevated temperature overnight.

Organic Williamson Synthesis in N,N-dimethylacetamide

To a stirred suspension of 0.04 mol Bisphenol-A sodium salt in approximately 25 ml N,N-dimethylacetamide (DMAc) was added 0.1 mol propargyl chloride. The reaction mixture was then heated at 75°C for 18 hours. The reaction mixture was then poured into water to precipitated the product, which was collected by suction filtration and washed with additional water. The product was dried at ~ 50°C under vacuum for 20 hours.

This general method can also be used for preparations from the starting hydroxyl-functionalized parent compounds.

To a mixture of 0.012 mol Bisphenol-A and 0.024 mol potassium carbonate in 10 ml DMAc was added, with good stirring, 0.03 mol propargyl chloride. The reaction was then heated at 75°C for 18 hours. The product was precipitated in water, isolated by suction filtration and washed with additional water followed by drying at 50 - 60°C under vacuum overnight.

Synthesis of Brominated Propargyl Resin

In a 250 ml three-necked reaction flask equipped with a condenser, nitrogen inlet, and a rubber septum, a suspension consisting of 10 g (0.044 mol) Bisphenol-A and approximately 0.1 g (3.4 mmol) iron (III) bromide in 100 ml nitrobenzene was prepared. Over a period of 30 min., 7.5 g (0.047 mol) liquid bromine was added to the suspension using a hypodermic syringe. During the addition, hydrogen bromide was evolved and the suspended solid dissolved in the solvent. The quantity of

bromine used was sufficient to result in the substitution of one atom of bromine onto each molecule of Bisphenol-A.

After stirring under nitrogen purge for 2 hours to remove the majority of the dissolved hydrogen bromide, 0.1 mol propargyl chloride and 0.15 mol potassium carbonate were then added. This mixture was heated to 100°C overnight to form the propargyl resin.

The mixture containing the raw product was then cooled and 1 g decolorizing charcoal added. The mixture was filtered and the resin precipitated with methanol. The resulting resin was liquid and this second phase was removed from the methanol-nitrobenzene mixture using a separatory funnel. After drying overnight, some crystallization had occurred but the raw product remained quite colored. To further purify the product, the semi-liquid mixture was redissolved in toluene and again treated with decolorizing charcoal, followed by filtration to remove the charcoal. This solution remained quite dark after treatment. However, the resin remaining after toluene evaporation was yellow but crystalline. The expected structure was verified by infrared spectroscopy.

Bis(ethynyl) endcapped Resin Material

A method used for the preparation of Resole phenolic resins was used. Equimolar amounts of ethynylbenzene and formaldehyde (as paraformaldehyde) were combined in a round bottom flask with an excess of 10% sulfuric acid in water. This mixture was refluxed with stirring for 24 hours, cooled and the two-phase mixture separated. During the reflux, the solid paraformaldehyde dissolved in the aqueous phase and reaction with the ethynylbenzene occurred. The aqueous phase was discarded. The organic phase was dried and analyzed by FTIR spectroscopy. This product was not evaluated using UV photolysis, but was used instead in e-beam irradiation experiments.

Characterization Techniques

Fourier Transform Infrared (FTIR) Spectroscopy

All materials were characterized using FTIR spectroscopy. Spectra were collected using a Mattson Cygnus 100 FTIR spectrometer at a resolution of 4 cm^{-1}. Samples were prepared as resin melts between KBr windows. The following spectral regions were of particular interest: 2200-1950 cm^{-1} (acetylenic C≡≡C stretch) for propargyl-functionalized materials and 2500-2200 cm^{-1} (C≡≡N stretch) for cyanate materials.

Ultraviolet/Visible (UV/VIS) and Fluorescence Spectroscopy

All spectra were obtained using our combined UV/Visible spectrophotometer in either the absorption mode or fluorescence mode. This instrument was designed to operate at low light levels for examination of photosensitive materials. It uses

photon counting detection in both absorption and fluorescence. Samples were examined in short path cells (2mm) at ambient temperature. Methyl cyclohexane and 2-propanol solutions were used to provide transparency in the 200-400 nanometer region. Fluorescence spectra were excited using a deuterium lamp source that gives a near continuum from <200 nm to 400 nm.

Photophysical calculations to determine fluorescence lifetimes and energy transfer parameters were carried out with the spectrometer control program. These spectral calculations are incorporated in the spectral display functions of that program.

Nuclear Magnetic Resonance (NMR) Spectroscopy

Proton (^1H) and carbon-13 (^{13}C) NMR spectra were collected using a Bruker AC250 Fourier Transform NMR Spectrometer. Samples analyzed were dissolved in deuterated chloroform for analysis. Chemical shifts are reported in parts per million (δ) downfield from tetramethylsilane.

Resin Exposures and Characterization

Resin Formulation for UV Screening and E-Beam Exposures

Resin samples were prepared for UV or E-Beam cure by mixing the resin with the desired amount of sensitizer. Resins were heated as necessary to induce flow before the addition of sensitizer. Heating was continued as needed until all sensitizer dissolved into the resin.

UV Cure Procedure

Small amounts of the resin/sensitizer mixtures were placed into aluminum weighing dishes. These dishes were then placed inside plastic bags that were purged with nitrogen and sealed. The samples were irradiated for 20 minutes using a 3 kW mercury arc lamp in an aluminized box.

E-Beam Exposure Methods

Resin samples were placed into 5 cm x 5 cm x 5 mm wells machined into a 1-cm thick polyethylene block. Resins were slightly heated as needed to induce sufficient flow for pouring. An aluminum support frame was then placed around the mold to prevent warping. A Kapton polyimide sheet was then used to cover the entire mod assembly for the purpose of preventing premature reaction induced by ambient UV light.

The covered mold was then placed on a graphite beam stop and sufficient wood blocks to give a spacing of 9.5 cm between the beam pipe exit and the surface of the mold. The beam was positioned at the edge of the first column of sample wells by moving the mold assembly on a translation table.

The filled mold was then subjected to e-beam irradiation using the beam parameters specified in the E-Beam Exposure Experimental Plan section of this report. The number of passes per strip and translation distances between strips were calculated for the desired dose magnitude and uniformity. See above-mentioned E-beam Exposure Experimental Plan and Appendix B for more detailed discussions.

Nylon-based radiochromic film supplied by Far West Technology was used in determination of the actual dose received by the samples. Strips of film were placed along the entire width of the mold, on top of the Kapton UV-shielding films The films were analyzed at Adherent Technologies using UV/VIS absorbance spectroscopy. Comparison of the measured absorbance at a wavelength of 510 nm with calibration data supplied by Far West Technology allowed the determination of the actual radiation dose received by the samples. Dose uniformity could also be determined.

Characterization of Unexposed and Exposed Resin Formulations

Fourier Transform Infrared (FTIR) Spectroscopy

The following spectral regions were of particular interest: 2200-1950 cm^{-1} (acetylenic C≡≡C stretch) for propargyl-functionalized materials and 2500-2200 cm^{-1} (C≡≡N stretch) for cyanate materials.

All materials subjected to either UV or e-beam irradiation were analyzed using FTIR spectroscopy. Spectra were collected using a Mattson Cygnus 100 FTIR spectrometer at a resolution of 4 cm^{-1}. Methylene chloride solutions (~ 10%(w/v)) of the resin/sensitizer mixtures, both unexposed and partially cured were used. Solution experiments were chosen here for the purpose of avoiding all complications in data analysis that might arise as a result of resin crystallization. The following spectral regions related to polymerizable functionalities were integrated: 3334-3201 cm^{-1} (acetylenic C—H stretch), 2333-2200 cm^{-1} (C≡≡N stretch), and 2150-2092 cm^{-1} (acetylenic C≡≡C stretch). The following bands were integrated for use as "internal standards": 3018-2777 cm^{-1} (aliphatic C—H stretch), and 1536-1467 cm^{-1} or 1529-1452 cm^{-1} (aromatic C=C stretch).

Nuclear Magnetic Resonance (NMR) Spectroscopy

Proton (^{1}H) and carbon-13 (^{13}C) NMR spectra were collected using a Bruker AC250 Fourier Transform NMR Spectrometer. Samples analyzed were dissolved in deuterated chloroform for analysis. Chemical shifts are reported in parts per million (δ) downfield from tetramethylsilane.

UV Spectroscopy

UV absorption spectra were collected over the range from 200 to 400 nm (2000-4000Å) to assist in the interpretation of chemical changes indicated in the infrared solution spectra. These were obtained in dilute solution in either methyl cyclohexane or 2-propanol contained in a 2-mm pathlength cell.

Differential Scanning Calorimetry (DSC)

Samples of exposed resins were analyzed using a Perkin-Elmer DSC-4 Differential Scanning Calorimeter at a heating rate of 10°C/min in a nitrogen atmosphere. Melting points, glass transition temperatures, and cure exotherms were determined as applicable. Uncured resins were polymerized in the DSC chamber to determine a baseline cure exotherm.

APPENDIX D—COMPOSITES FABRICATION

Prepreg Fabrication

All prepregs manufactured used Hercules IM7 carbon fibers as a starting materials. Some prepregs starting with IM7 fiber were finished using a reactive coupling agent developed by Adherent Technologies. Table D-I represents the types of prepregs fabricated.

Table D-I. Prepreg Types

Prepreg 1a: Epon 828 resin with 2% (w/w) Cyracure 6974; Fiber IM7 unsized
Prepreg 1b: Epon 828 resin with 2% (w/w) Cyracure 6974; Fiber IM7, ATI-9305E finish
Prepreg 2a: Epon 828 resin with 2% (w/w) DPI-1; Fiber IM7, unsized
Prepreg 2b: Epon 828 resin with 2% (w/w) DPI-1; Fiber IM7, ATI-9305E finish
Prepreg 3a: Cat B resin with 2% (w/w) Cyracure 6974; Fiber IM7 unsized
Prepreg 3b: Cat B resin with 2% (w/w) Cyracure 6974; Fiber IM7, ATI-9305E finish
Prepreg 4a: Aliphatic Epoxy resin with 2% (w/w) Cyracure 6974; Fiber IM7 unsized
Prepreg 5: Epon 828 resin with 2 % (w/w) BF3 Monoethylamine; Fiber, IM7-W-12K

For these prepregs IM7 fiber was dispensed from a tensioned fiber delivery rack onto a 45.7-cm diameter drum winder. The fiber feeder spool to the drum winder was weighed before and after winding to establish the amount of carbon used in making the prepreg. Fiber was wrapped over a polyethylene backing sheet at 6.3 wraps per cm.

Since some of the resins used are UV sensitive, mixing and resin application were performed in reduced lighting with low UV emissions. Prepregs were impregnated with their respective resin/initiators using a natural bristle brush. All mixed resin was applied to the drum winder. Residual resin adhering to the mixing container

was weighed to determine the amount of resin applied to each prepreg. For all prepregs manufactured the average resin content was 50 weight percent.

For prepregs with reactive finish, a roller wetting bath technique shown in Figure D-1 was used. Details of the finish can be found in Reference 1.

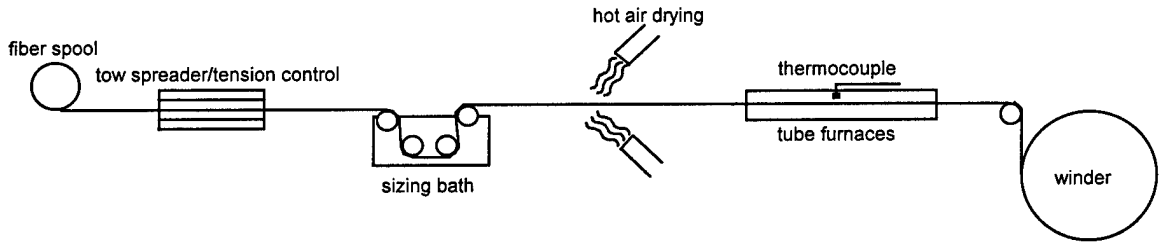

Figure D-1. Finish application set up

ATI-9305E coupling agent was added to the unsized IM7 fiber using 0.1 weight percent coupling agent along with a 1.0 weight percent Epon 828 epoxy resin carrier from an acetone solution. Processing temperature for the tube furnace was set at 215 degrees centigrade. Residence time in the furnace was adjusted so that the fibers exiting were dry to the touch, this was typically 76 cm/min. Finish pickup was determined to be 0.80% by weight. Enough material was run to complete the fabrication of all prepregs to ensure uniformity in finish application.

All prepregs with finish or without were rotated on the drum winder for 10-15 minutes after the resin was applied to ensure even resin application to the fiber.

Prepregs after impregnation were cut from the drum winder and stored in a closed polyethylene bag in a freezer until needed for composite panel layups.

Composite Layup

Composite plates were processed by electron beam and vacuum bagged press molding techniques. Table D-II shows the six types of composite plates that were fabricated.

Table D-II. Composite Layups for E-beam Cure

Plates 1-8: 8 plies unidirectional, prepregs 1a,1b, 2a,2b, 3a,3b, 4a,4b; size 10 x 10 cm
Plate 9: 8 plies unidirectional prepreg 1a, ambient cure; size 25 x 25cm
Plate 10: 8 plies unidirectional prepreg 1a, sub-ambient cure; size 25 x 25cm
Plate 11: 8 plies quasi-isotropic prepreg 1a, ambient cure; size 25 x 25 cm
Plate 12: 8 plies quasi-isotropic prepreg 1a, sub-ambient cure; size 25 x 25 cm
Plate 13: 8 plies unidirectional prepreg 5a, press mold cure; size 10 x 10 cm

Due to the very tacky nature of the uncured resins in the prepreg a freezing technique using dry ice was used to remove the polyethylene backing and cover sheets from all the prepregs. Individual sheets of prepreg were placed on a dry ice block and allowed to thoroughly freeze. The backing sheets then could be easily removed. Between each ply, after the backing sheets had been removed a heat gun was used to warm the prepreg up to room temperature and drive off any residual moisture. After the 8 plies of prepreg had been compiled they were placed in another polyethylene bag and put into a freezer for storage until needed for the curing operation.

Layups for the quasi-isotropic composite plates were performed in the same manner as above, but the ply orientation pattern had the sequence [90° +45° –45° 0° 0° –45° +45° 90°].

For electron beam cured plates, the compiled 8 ply prepregs were removed from the freezer and allowed to thaw to room temperature in their respective polyethylene bags. The 10 x 10 cm prepregs were placed in a 1.27 cm thick 30 x 30 cm polyethylene mold that had 4 rectangular depressions machined into its surface to a depth of 67mm. The prepregs where then covered with a 64mm thick rectangular polycarbonate plate which acted as a pressure intensifier during the cure. This array was then placed in a ridged aluminum frame and the total assembly was vacuum bagged. As in the case of the resin plaques, a Kapton sheet was placed over the mold to prevent premature UV-initiated polymerization of the resin.

For the larger 25 x 25 cm prepregs the eight plies of unidirectional and quasi-isotropic layups were placed between two sheets of mold released 16.5mm aluminum. In all four corners next to the prepreg were placed 7.6 mm stops and the whole assembly was vacuum bagged.

Composite Cure

The smaller 10 x 10 cm composite plates were held under vacuum along with external cooling from a dry ice/ethylene glycol chilling plate during the electron beam cure. Each composite plate was irradiated to a dose of 15 MR. After exposure the array was dismantled and the composite plates removed for specimen preparation for mechanical and optical testing.

On the larger 25 x 25 cm composite plates, a cooling box consisting of high density foam filled with crushed dry ice was used for the sub-ambient e-beam exposures. The vacuum bagged composite array was placed on the top of the dry ice box and allowed to chill down to a cure temperature of approximately –20°C. One quasi-isotropic plate was exposed with dry ice above and below the layup to reach a cure temperature of approximately -30°C. After cure, these plates were de-molded and the composite plates prepared for mechanical and optical testing.

The thermal composite plate used the prepreg described in Table D-I. The 8 plies of prepreg were removed from the freezer and allowed to thaw in the polyethylene bag before use. The prepreg stack was placed inside a picture frame stop that had a thickness of 35.6 mm. Then 2 sheets of 1.56-mm aluminum plate were placed on either side of the prepreg and stop. The entire assembly was then vacuum bagged and placed in a Pasadena Hydraulics, Inc., heated platen press equipped with Micristaar controller. Figure D-2 shows the vacuum bagged tool ready for cure.

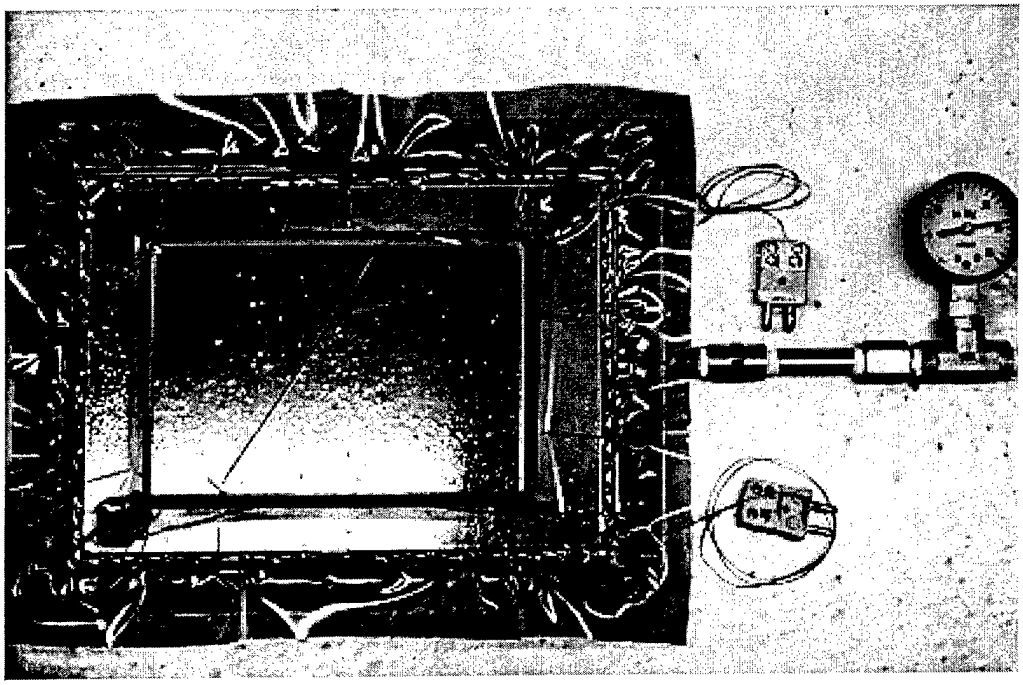

Figure D-2. Press molding tool

With vacuum applied, the composite plate was processed as shown in Figure D-3.

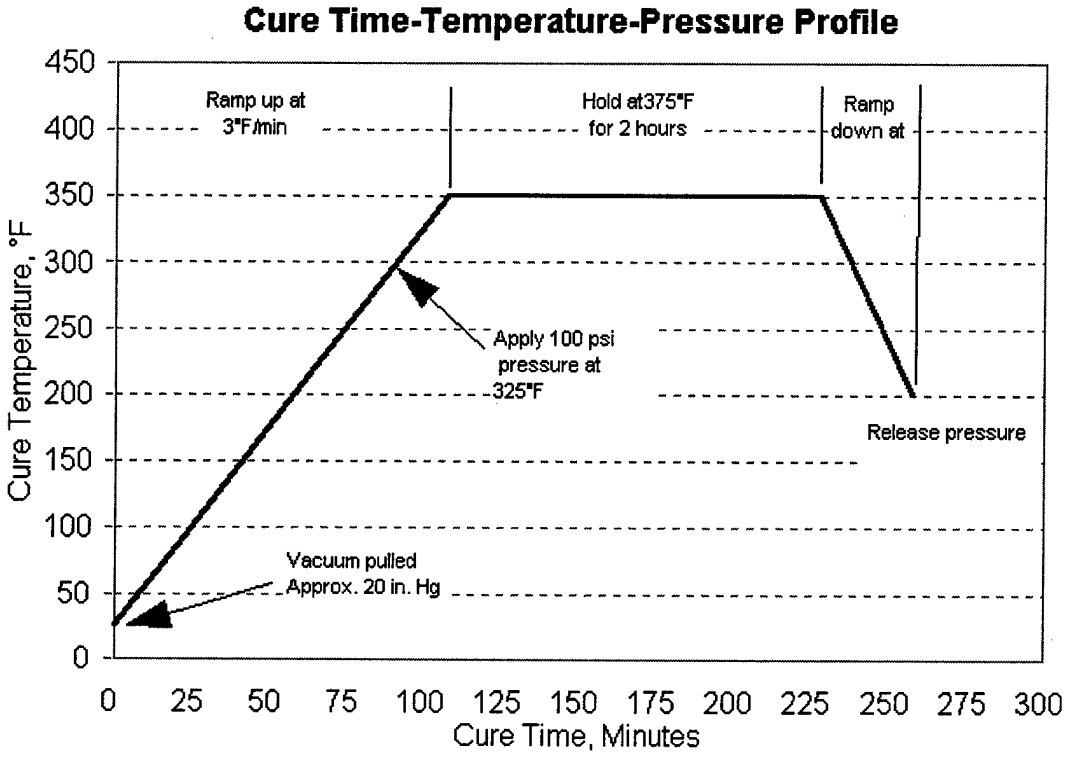

Figure D-3. Press molding cure cycle

After the cure cycle was completed the composite plate was de-molded and the composite plate prepared for mechanical and optical testing.

Mechanical Testing

All composite plates were machined with a diamond water saw to dimensions to be used for testing. The three point bend flexure tests were performed in accordance with ASTM D790-84a using an Instron Model 1101 mechanical testing machine. The fixed crosshead of the mechanical tester was fitted with an Instron 752 tension/compression load cell with a 1000 lb capacity. An instron Model M933227 chart recorder was connected to the load cell to record load in pounds force and sample deflection in inches up to the point of rupture. For the 0° flexure samples the loading rate was set at 0.127 cm per minute and the chart recorder was set at 1.27cm per minute giving a chart scale factor of 0.1. The support span, L, was set at 4.572 cm, and the nominal sample depth, d, was 0.254 cm, giving a L/d ratio of approximately 18. For the 90° flexure samples, the loading rate was set at 0.0508 cm/min., and the chart recorder was set at 0.508 cm/min. The support span was 2.032 cm and the nominal sample depth was again 0.254, giving an L/d ratio of approximately 8.

Optical Evaluation

Representative sections of cured composite plates were cast into optical mounts using an epoxy resin. Samples were polished to a 1-micron diamond surface finish. These samples were evaluated using an optical microscope at 125 and 250 X.

References

1. R. E. Allred and J. K. Sutter, "Fiber Finish for Improving Thermo-Oxidative Stability of Polyimide Matrix Composites," *Proc. 42nd Intl. SAMPE Symp. and Exhib.*, Anaheim, CA, May 1997, pp. 1291-1305.

DISTRIBUTION LIST

AUL/LSE **Bldg 1405 - 600 Chennault Circle** **Maxwell AFB, AL 36112-6424**	**1 cy**
DTIC/OCP **8725 John J. Kingman Rd, Suite 0944** **Ft Belvoir, VA 22060-6218**	**2 cys**
AFSAA/SAI **1580 Air Force Pentagon** **Washington, DC 20330-1580**	**1 cy**
AFRL/PSOTL **Kirtland AFB, NM 87117-5776**	**2 cys**
AFRL/PSOTH **Kirtland AFB, NM 87117-5776**	**1 cy**
AFRL/MLBC (E. Shinn, F. Abrams) **2941 P St., Ste 1** **Wright-Patterson AFB, OH 45433-7750**	**2 cys**
Adherent Technologies, Inc. **9621 Camino del Sol NE** **Albuquerque, NM 87111**	**1 cy**
Official Record Copy **AFRL/VSDV (Capt R. Pittman)** **Kirtland AFB, NM 87117-5776**	**3 cys**